



Universidade do Estado do Rio de Janeiro

Centro de Tecnologia e Ciências

Instituto de Química

André Luis Moreira Nahes

Heat exchanger network retrofit optimization with heat exchanger design

Rio de Janeiro

2024

André Luis Moreira Nahes

Heat exchanger network retrofit optimization with heat exchanger design

Tese apresentada, como requisito parcial para a obtenção do grau de Doutor, ao Programa de Pós-Graduação em Engenharia Química, da Universidade do Estado do Rio de Janeiro.

Área de concentração: Processos Químicos, Petróleo e Meio Ambiente.

Orientador: Prof. Dr. André Luiz Hemerly Costa

Prof. Dr. Miguel Jorge Bagajewicz

Rio de Janeiro

2024

CATALOGAÇÃO NA FONTE
UERJ / REDE SIRIUS / BIBLIOTECA CTC/Q

N153 Nahes, André Luis Moreira

Heat exchanger network retrofit optimization with heat exchanger design. – 2024.
194 f.

Orientador (a): André Luiz Hemerly Costa
Miguel Jorge Bagajewicz

Tese (Doutorado) – Universidade do Estado do Rio de Janeiro.
Instituto de Química.

1. Permutadores térmicos – Teses. 2. Calor – Transmissão - Teses. I.
Costa, André Luiz Hemerly. II. Bagajewicz, Miguel Jorge. III.
Universidade do Estado do Rio de Janeiro. Instituto de Química. IV.
Título.

CDU 536.24

Autorizo, apenas para fins acadêmicos e científicos, a reprodução total ou parcial desta dissertação, desde que citada a fonte.

André Luis Moreira Nahes

Assinatura

29/04/25

Data

André Luis Moreira Nahes

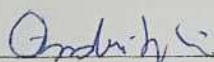
André Luis Moreira Nahes

**Heat exchanger network retrofit optimization
with heat exchanger design**

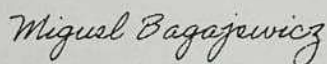
Tese apresentada, como requisito parcial para obtenção do grau de Doutor, ao Programa de Pós-Graduação em Engenharia Química, da Universidade do Estado do Rio de Janeiro. Área de concentração: Processos químicos, petróleo e meio-ambiente.

Aprovada em 26 de dezembro de 2024.

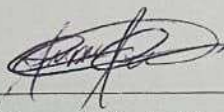
Banca examinadora:



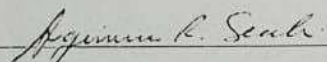
Prof. Dr. André Luiz Hemerly Costa (Orientador)
Instituto de Química – UERJ



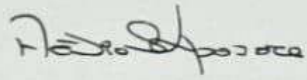
Prof. Dr. Miguel Jorge Bagajewicz
University of Oklahoma



Prof. Dr. André Luis Alberton
Instituto de Química – UERJ



Prof. Dr. Argimiro Resende Secchi
PEQ – UFRJ



Fábio dos Santos Liporace

Petrobras

Rio de janeiro

2024

AGRADECIMENTOS

Aos meus pais, Mauro Nahes Filho e Varinia Moreira da Silva, à minha irmã Maria Alice Moreira Nahes, por todo amor e carinho dedicado durante toda a minha vida.

Ao meu orientador, André Luiz Hemerly Costa, pela sua grande dedicação, atenção e paciência durante todos os anos da minha formação acadêmica.

Ao meu orientador, Miguel Jorge Bagajewicz, pelo seu suporte e grande experiência profissional para o desenvolvimento desta pesquisa.

Dedico este trabalho à Coordenação de Aperfeiçoamento de Pessoal de Nível Superior (CAPES), cujo apoio foi fundamental para a realização desta pesquisa e para minha formação acadêmica.

Para todos os meus professores da graduação e pós-graduação, que desempenharam um papel importante na minha vida profissional e pessoal.

Para meu querido professor André Alberton, que foi fundamental para meu desenvolvimento, para o professor Argimiro Secchi e Fábio Liporace por aceitarem o convite para fazer parte dessa Banca Examinadora.

RESUMO

NAHES, André Luis Moreira. *Otimização do Retrofit de Redes de Trocadores de Calor com Projeto de Trocadores de Calor*. 2024. 194 f. Tese (Doutorado em Engenharia Química) – Instituto de Química, Universidade do Estado do Rio de Janeiro, Rio de Janeiro, 2024.

Redes de trocadores de calor (HEN) são estruturas que promovem a transferência de calor entre correntes quentes e frias de processo, com o objetivo de reduzir o consumo de utilidades. Uma das aplicações de HEN de grande relevância industrial é o retrofit de redes existentes, situação na qual realiza-se um investimento em uma rede já existente para intensificar a recuperação de calor. Comparado com o problema de projeto de uma nova HEN, o problema de retrofit é significativamente mais complexo uma vez que se deve incorporar as características de uma rede já em operação. Do ponto de vista matemático, este é um problema com uma drástica explosão combinatorial e com relevantes não linearidades, apresentando problemas de convergência, múltiplos ótimos locais e elevado esforço computacional. Por conta disso, os trabalhos existentes na literatura estão repletos de simplificações, especialmente os cálculos envolvendo trocadores de calor da rede. Uma modelagem mais detalhada do projeto de novos trocadores e do retrofit de trocadores existentes não só leva a soluções mais lucrativas, mas também a soluções mais realistas uma vez que a modificação do serviço de trocadores existentes deve levar em conta uma série de questões práticas operacionais. Esta tese apresenta uma metodologia de retrofit de redes, baseada em enumeração, que é robusta, lida de maneira eficiente com todas as não linearidades do problema, incorporando um cálculo detalhado dos trocadores da rede.

Palavras-chave: retrofit de redes de trocadores de calor; retrofit de trocadores de calor; otimização; enumeração; *set trimming*.

ABSTRACT

NAHES, André Luis Moreira. *Heat Exchanger Network Retrofit Optimization With Heat Exchanger Design*. 2024. 194 f. Tese (Doutorado em Engenharia Química) – Instituto de Química, Universidade do Estado do Rio de Janeiro, Rio de Janeiro, 2024.

Heat exchanger networks (HENs) are structures that promote heat transfer between hot and cold process streams, with the goal of reducing utility consumption. One highly relevant industrial application of HENs is the retrofit of existing networks, in which an investment is made in an already operational network to intensify heat recovery. Compared to the design of a new HEN, the retrofit problem is significantly more complex, as it must incorporate the characteristics of an existing operating network. From a mathematical standpoint, this is a problem with a drastic combinatorial explosion and significant nonlinearities, leading to convergence issues, multiple local optima, and high computational effort. As a result, existing works in the literature are full of simplifications, especially in the calculations involving the network's heat exchangers. A more detailed modeling of both the design of new exchangers and the retrofit of existing ones not only leads to more profitable solutions but also to more realistic ones, since modifications to the service of existing exchangers must take into account a series of practical operational issues. This thesis presents a robust network retrofit methodology that efficiently handles all the nonlinearities of the problem, incorporating detailed calculations for the exchangers in the network.

Keywords: heat exchanger network retrofit; heat exchanger retrofit; optimization; enumeration set trimming.

FIGURE LIST

Figure 1.1 – Existing network in the illustrative example.....	12
Figure 1.2 – Energy loop of the existing HEN in the illustrative example	13
Figure 1.3 – Existing network with different heat distribution	13
Figure 1.4 – Utility path of the existing network	14
Figure 1.5 – Existing HEN with different utility consumption.....	14
Figure 1.6 – Composite curve of the illustrative example.....	16
Figure 1.7 – HEN retrofit with new cooler.....	17
Figure 2.1 – Existing HEN	28
Figure 2.2 – Existing HEN with a resequencing	28
Figure 2.3 – Existing HEN with a repiping	29
Figure 2.4 – Existing HEN with a new match.....	29
Figure 2.5 – Cash flow of a traditional retrofit problem	30
Figure 2.6 – Phased project HEN retrofit.....	31
Figure 2.7 – Existing HEN A	33
Figure 2.8 – NPV and Investment cost plot for a phased HEN retrofit.....	34
Figure 2.9 – Cash flow representation of multiple HEN retrofit.....	36
Figure 2.10 – Existing HEN B	36
Figure 2.11 – NPV plot for multiple HEN retrofit	37
Figure 2.12 – NPV plot for multiple financial sources	39
Figure 2.13 – Strauss plot.....	40
Figure 2.14 – Original HEN proposed by Saboo <i>et al.</i> (1986).....	43
Figure 2.15 – Retrofit solution proposed by Pan <i>et al.</i> (2013).....	44
Figure 2.16 – Utility consumption with constant and predictive fouling factor	47
Figure 3.1 – Alternatives of insertion of a HEX in series with the existing one.....	64
Figure 3.2 – Temperature x Enthalpy diagrams	66
Figure 3.3 – New unit in parallel.....	67
Figure 3.4 – Typical temperature control in an energy integration HEX.....	71
Figure 3.5 – Profiles for using by-pass to reduce heat load	73
Figure 3.6 – Profiles for plugging tubes to reduce heat load.....	74
Figure 4.1 – Crude oil preheating train existing HEN.....	109
Figure 4.2 – Example 1: Retrofitted HEN.....	112
Figure 4.3 – Example 2: Existing HEN.....	114

Figure 4.4 – Example 2: Retrofitted HEN.....	117
Figure 5.1 – HEN retrofit procedure	130
Figure 5.2 – Flowchart of the incremental enumeration	134
Figure 5.3 – Example Based on Yee and Grossmann (1987) - Existing HEN.....	137
Figure 5.4 – Example Based on Yee and Grossmann (1987) - Retrofit solution.....	138
Figure 5.5 – Example Based on Saboo <i>et al.</i> (1986) – Existing HEN	139
Figure 5.6 – Example Based on Saboo <i>et al.</i> (1986) – Retrofit solution.....	141
Figure 5.7 – Example 3: Existing HEN.....	143
Figure 5.8 – Example 3: Retrofit solution	145
Figure 5.9 – Example 4: Existing HEN.....	149
Figure 5.10 – Example 4: Retrofit solution	151
Figure 8.1 – Set Trimming application to the STHE.....	168
Figure 8.2 – HEN retrofit of Example 3 using the simplified approach	184
Figure 8.3 – HEN retrofit of Example 4 using the simplified approach	189

TABLE LIST

Table 1.1 – Existing network stream data in the illustrative example.....	12
Table 1.2 – Existing network HEX data in the illustrative example	12
Table 1.3 – Existing HEN with new heat distribution in the illustrative example	15
Table 1.4 – Existing HEN with topological modification	17
Table 2.1 – HEX 5 details	44
Table 3.1 – Geometry of existing HEXs subjected to heat load reduction	72
Table 3.2 – STHE search space	76
Table 3.3 – GPHE search space.....	76
Table 3.4 – Tube insert search space	77
Table 3.5 – Plate dimensions from an industrial supplier	77
Table 3.6 – Economic parameters	77
Table 3.7 – Streams physical properties	78
Table 3.8 – Retrofit task	78
Table 3.9 – Existing HEXs	79
Table 3.10 – Existing 1: Existing HEX performance	79
Table 3.11 – Example 1: Optimal solution of each alternative	79
Table 3.12 – Example 2: Existing HEX performance	80
Table 3.13 – Example 2: Optimal solution of each alternative	81
Table 3.14 – Example 3: Existing HEX performance	81
Table 3.15 – Example 3: Optimal solution of each alternative	82
Table 3.16 – Comparison with traditional approach	83
Table 4.1 – STHE search space	106
Table 4.2 – GPHE search space.....	107
Table 4.3 – Tube insert search space	107
Table 4.4 – Plate dimensions from and industrial supplier	107
Table 4.5 – Economic parameters	108
Table 4.6 – Example 1: Streams data	109
Table 4.7 – Example 1: HEX information in the existing HEN.....	110
Table 4.8 – Example 1: Design variables of the existing HEXs	111
Table 4.9 – Example 1: HEX information in the retrofitted HEN	112
Table 4.10 – Example 1: Design variables of the HEX retrofit solution.....	113
Table 4.11 – Example 2: Streams data	114

Table 4.12 – Example 2: HEX information in the existing HEN.....	115
Table 4.13 – Example 2: Geometric variables of existing HEXs.....	116
Table 4.14 – Example 2: HEX information of the retrofitted solution.....	117
Table 4.15 – Example 2: Design variables of the GPHE added to the HEN.....	118
Table 4.16 – Example 2: HEX information of the STHE added to the network.....	118
Table 4.17 – Comparison with the traditional approach	120
Table 5.1 – Example Based on Yee and Grossmann (1987) - Streams data	136
Table 5.2 – Example Based on Yee and Grossmann (1987) - Information of existing HEX in the original HEN.....	137
Table 5.3 – Example Based on Yee and Grossmann (1987) - Information of existing HEX in retrofit solution	138
Table 5.4 – Example Based on Yee and Grossmann (1987) - Solution comparison with previous work in literature.....	138
Table 5.5 – Example Based on Saboo <i>et al.</i> (1986) - Streams data.....	139
Table 5.6 – Example Based on Saboo <i>et al.</i> (1986) - Information of existing HEX in the original HEN	139
Table 5.7 – Example Based on Saboo <i>et al.</i> (1986) - Information of existing HEX in retrofit solution	142
Table 5.8 – Example Based on Saboo <i>et al.</i> (1986) - Solution comparison.....	142
Table 5.9 – Example 3: Streams data	144
Table 5.10 – Example 3: HEX information of the existing HEN.....	144
Table 5.11 – Example 3: HEX information in the retrofitted HEN	146
Table 5.12 – Example 3: Details solution of retrofitted HEXs	146
Table 5.13 – Example 3: Detailed solution of new matches	147
Table 5.14 – Example 3: Comparison between different approaches in example 3	148
Table 5.15 – Example 4: Streams data	149
Table 5.16 – Example 4: HEX information of the existing HEN.....	150
Table 5.17 – Example 4: HEX information in the retrofitted HEN	151
Table 5.18 – Example 4: Details solution of HEX retrofit.....	152
Table 5.19 – Example 4: Detailed solution of new matches	152
Table 5.20 – Example 4: Comparison between different approaches in example 3	153
Table 8.1 – STHE search space in Set Trimming example.....	167
Table 8.2 – Hot stream data of example 1	171
Table 8.3 – Cold stream data of example 1	172

Table 8.4 – Coolers details of example 1	173
Table 8.5 – Hex information in the retrofitted HEN of example 1	174
Table 8.6 – Geometric variables of the HEX retrofit solution of example 1	175
Table 8.7 – Streams data of example 2.....	176
Table 8.8 – Coolers details of example 2	177
Table 8.9 – Hex information in the retrofitted HEN of example 2	178
Table 8.10 – Geometric variables of the HEX retrofit involving STHE of example 2.....	179
Table 8.11 – Geometric variables of the HEX retrofit involving GPHE of example 2.....	180
Table 8.12 – Hot stream data of example 1	181
Table 8.13 – Cold stream data of example 1	182
Table 8.14 – Coolers details of example 1	183
Table 8.15 – HEX information of the HEN retrofit solution of Example 3	185
Table 8.16 – HEX details of the HEN retrofit solution of Example 3	186
Table 8.17 –HEX details of new matches of HEN retrofit solution of Example 3	187
Table 8.18 –Streams Data of Example 4	187
Table 8.19 –Coolers details of Example 4.....	188
Table 8.20 –HEX information of the HEX retrofit solution of Example 4.....	189
Table 8.21 – HEX details of HEN retrofit solution involving STHE of Example 4.....	190
Table 8.22 – HEX details of the HEN retrofit solution involving GPHE of Example 4....	191
Table 8.23 – HEX details of new matches of HEN retrofit solution of example 4.....	192

SUMMARY

	INTRODUCTION	7
1.	HEN RETROFIT	8
2	A ROADMAP FOR HEAT EXCHANGER NETWORK RETROFIT: CHALLENGES AHEAD	21
2.1	Introduction	21
2.2	<u>Hen Retrofit Problem</u>	26
2.2.1	<u>Alternative interventions on existing HEN in retrofit problems</u>	27
2.3	Cash Flow in HEN Retrofit Problems	30
2.3.1	<u>Project size limitations</u>	31
2.3.2	<u>Prased retrofit</u>	31
2.3.3	<u>Portfolio selection problem</u>	34
2.3.4	<u>Multiple Financial Sources</u>	38
2.3.5	<u>Risk Analysis</u>	39
2.4.	Design of Heat Exchangers in Retrofit Problems	41
2.5.	Fouling	45
2.6.	Layout	48
2.7.	Pressure Drop	49
2.8.	Challenges of considering these advancements	50
2.9.	Conclusions	52
3.	A NOVEL PROCEDURE FOR HEAT EXCHANGER RETROFIT CONSIDERING MULTIPLE INTERVENTION ALTERNATIVES	54
3.1.	Introduction	54
3.2.	Problem Statement	57
3.3.	HEX retrofit – Heat Load Increase	59
3.3.1.	<u>Desig problem and optimization of a new unit</u>	60
3.3.2	<u>Insertion of a new HEX in series</u>	64
3.3.3	<u>Insertion of a new HEX in parallel</u>	67
3.3.4	<u>Insertion of intensification devices in the existing HEX</u>	68
3.3.5	<u>Complete procedure</u>	69
3.4	HEX Retrofit – Heat Load Reduction	70
3.4.1	<u>Heat Load reduction by stream by-pass</u>	72
3.4.2	<u>Heat load reduction by plugging tubes</u>	74

3.5	Results	75
3.5.1	<u>Example 1</u>	79
3.5.2	<u>Example 2</u>	80
3.5.3	<u>Example 3</u>	81
3.5.4	<u>Comparison with the traditional approach</u>	82
3.6	Conclusions	84
4.	HEN RETROFIT WITH DETAILED HEX DESIGN – PART 1: HEAT LOAD MODIFICATIONS	88
4.1	Introduction	88
4.2	Problem Statement	92
4.3	HEN Retrofit Procedure	94
4.3.1	<u>HEX retrofit</u>	95
4.3.2	<u>MSTR HEN retrofit</u>	99
4.3.3	<u>Non MSTR HEN retrofit</u>	102
4.4	Results	106
4.4.1	<u>Example 1</u>	108
4.4.2	<u>Example 2</u>	113
4.4.3	<u>Comparison with the traditional approach</u>	119
4.5	Conclusion	121
5.	HEN RETROFIT WITH DETAILED HEX DESIGN – PART 2: TOPOLOGICAL MODIFICATIONS	125
5.1	Introduction	125
5.2	HEN Retrofit Procedure	130
5.2.1	<u>Topological modifications model</u>	131
5.3	Results	135
5.3.1	<u>Comparison with previous results from the literature with simplified HEX evaluation</u>	136
5.3.2	<u>Comparison with previous results based on heat load modifications only</u>	142
5.4	Conclusion	154
	FINAL CONCLUSION	157
	REFERENCES	161
	APPENDIX A – Set Trimming application	167
	APPENDIX B – HEN retrofit without topological modifications results	171
	APPENDIX C – HEN retrofit with topological modifications results	181

APPENDIX D – Articles published during the thesis development	193
--	------------

INTRODUCTION

Heat exchanger network (HEN) is a well-known problem and has been researched intensively over the last 40 - 50 years (Chang *et al*, 2019). There are some reasons associated with the interested in HEN, such as the depletion of the energy resources, the increasing in environmental concerns and the energy prices (Sreepathi and Rangaiah, 2014).

Because the design of new plants (grassroot problem) has become scarce nowadays, the modification of existing plants towards their improvement (retrofit problem) is much more often than the grassroot problem.

There are different methodologies in literature that address the HEN retrofit, especially the Mathematical Programming and Pinch Technology. Despite the significant effort in developing good techniques for solving the HEN problem, there are some aspects not addressed yet, or treated in a simplified form. One of the main difficulties is the complexity associated with the problem, regarding with the non-convexity, its combinatorial nature and non-linearity of the model, which leads to several issues such as local optimal solution, convergence problems and large computational effort. Thus, the approaches used in the literature usually use some simplifications to be able to solve the problem.

This thesis presents a novel procedure to address the HEN retrofit optimization, based on an Enumeration procedure, which aims to overcome important limitations and simplifications presented in the traditional approaches.

Section 1 introduces the HEN retrofit problem as it is typically addressed and discussed in classical literature. Section 2 provides a deeper conceptual discussion of the problem, highlighting fundamental aspects not yet explored in the literature. Section 3 details the heat exchanger (HEX) retrofit problem, along with an innovative proposal for an optimization procedure for HEX retrofits. Subsequently, Sections 4 and 5 present the proposed HEN retrofit procedures, without and with topological modifications, respectively. Chapters 2 through 5 are written in the format of scientific articles, narrating the entire development of this thesis in chronological order. In addition, due to the structure of this thesis, each chapter (including chapter 1) have its own nomenclature and references.

1. HEN RETROFIT

Heat exchanger networks are structures formed by the interconnection of heat exchangers that enable heat transfer between hot and cold process streams, thereby reducing energy consumption from utilities. One practical application of HENs is network retrofit, which involves investing in the existing network to enhance heat recovery. This opportunity of saving money with the decrease of energy consumption can be justified by the increase of the energy price, a poorly executed network synthesis, changes in the streams data, etc. (Smith, 2005).

One way to enhance heat recovery in existing networks is by redistributing energy from utility exchangers to integration exchangers without altering the structural connections of the HEXs within the network. This type of retrofit, where the original matches of the network remain preserved (i.e., the streams in each HEX are not altered, nor are new matches added), is known as HEN retrofit without topological modifications. This approach is discussed in foundational books (Smith, 2005; Kemp, 2007) and has been explored in the literature more recently (Wang *et al.*, 2012; Pan *et al.*, 2013; Pan *et al.*, 2016; Pan *et al.*, 2018).

In this case, heat recovery is increased through utility paths, which are paths in the HEN that connect a heater to a cooler via network HEXs, allowing energy redistribution from utilities to integration exchangers (Kemp, 2007). Note that the redistribution of energy in the network alters the heat load, the LMTD, the inlet and outlet temperatures of the streams feeding a HEX, and potentially the flow rates and correction factor.

These modifications represent one of the sources of investment costs in the retrofit problem, as they may lead to a new heat transfer scenario that the existing HEXs cannot accommodate. Consequently, interventions in the existing HEXs become necessary to ensure they can meet the new thermal service requirements, which involves the HEX retrofit problem.

There are essentially two ways to increase the heat transfer capacity of existing HEXs. One approach is to add more heat transfer area, which is typically achieved by installing a new HEX aligned with the existing one. The calculation of the new heat transfer area (A_{new}) is performed in nearly all studies in the literature using Equation 1 below:

$$A_{new} = \max\left(\frac{Q}{U_{LMTD}} - A_{ex}; 0\right) \quad (1.1)$$

where Q is the heat load, U is the overall heat transfer coefficient and A_{ex} is the heat transfer area of the existing HEX. The increase in heat recovery usually involves narrowing the LMTD and increasing the heat duty of some exchangers in the network. Generally, the more energy is recovered, the more pronounced these effects become. Thus, as seen in Equation 1, as heat recovery increases, there is typically a greater need to add heat transfer area to existing HEXs. This directly impacts the rise in capital investment costs, since the cost associated with a new HEX is directly related to its heat transfer area, which is generally expressed by Equation 1.2 below:

$$IC_{HEX} = CF + a A_{new}^b \quad (1.2)$$

where CF is a fixed cost, a and b are cost parameters. This discussion highlights the inherent trade-off in the problem between cost savings from improved energy efficiency and the associated investment costs.

Another approach to increasing the heat transfer capacity of existing HEXs is the installation of enhancement devices, such as twisted tapes, coil-wires, finned tubes, and others. Recently, this capacity enhancement strategy has been gaining increasing attention in the literature (Sreepath and Rangaiah, 2014), primarily due to its potential to boost heat transfer without requiring modifications to the heat transfer area of the existing exchangers. This is generally achieved because these devices primarily act by increasing the heat transfer coefficients. The topic of heat exchanger retrofitting will be discussed in much greater detail throughout this thesis.

Another possible pathway in a HEN involves energy loops, which correspond to a closed path identified along heat exchangers and streams of a network, starting and returning to the same point. An energy loop allows for redistributing heat among the HEXs that are part of it without altering the network's utility consumption. Although it does not change utility consumption, energy loops are crucial because, as previously discussed, changes in the heat duty of HEXs (also affecting stream temperatures and other related factors) directly influence investment costs.

While achieving significant energy recovery and proposing effective HEN retrofit solutions is possible, reducing utility consumption without topological modifications has its limitations. This limitation arises because, from a structural perspective, no modifications are

made, thereby preserving the existing network characteristics as well as the matches associated with energy recovery bottlenecks. These energy bottlenecks, identified by Asante and Zhu (1996) and referred to as Pinch Matches, are specific matches that constrain utility consumption reduction without violating thermodynamic principles. For example, such violations occur when a hot stream reaches a temperature lower than that of a cold stream, or vice versa.

Additionally, another aspect that does not directly restrict heat recovery but may hinder utility consumption reduction is the presence of inefficient matches, often associated with criss-cross matches, as discussed by Linnhoff and Flowers (1977). These matches involve heat transfer arrangements that inefficiently utilize the driving force between hot and cold streams, leading to a heat transfer area requirement greater than the theoretical minimum. Consequently, while they do not prevent heat recovery, they can impose practical limitations by making recovery economically unfeasible due to significantly increased investment costs.

Thus, retrofitting HENs without topological modifications has a limited capacity to recover heat, while making changes to the network topology can be an appealing intervention as it enables overcoming Pinch Matches as well as criss-cross Matches. These topological modifications involve altering an existing match or introducing a new one into the network (Smith, 2005), including the following:

- i) Resequencing: it moves a unit to a new location, preserving the streams in the original match.
- ii) Repiping: the streams involved in the match do not need to be the same as the original one, where one or both streams can be different.
- iii) Inserting a new match: an entirely new match is added in the HEN.

Most studies in the literature focus on topological modifications, which introduce a significant level of complexity due to the severe combinatorial explosion caused by the numerous possible alterations in the network topology. As a result, identifying the optimal modifications becomes exceedingly challenging when considering the existing network's characteristics and accurately evaluating the trade-off between cost savings and investment expenses. This challenge is particularly pronounced for industrial-scale problems, which typically involve a considerable number of process streams and HEX.

Another critical aspect is the operationalization and practical implementation of these modifications. As discussed in several studies (Wang *et al.*, 2012; Pan *et al.*, 2013; Pan *et al.*, 2018), implementing such modifications entails complex mechanical and civil engineering work, which, in industrial practice, is often met with skepticism. Among the three

modifications mentioned above, resequencing and adding a new match are generally more accepted, whereas repiping is rarely implemented. Thus, for these reasons recently there is a tendency to approach the HEN retrofit problem without considering topological modifications.

Thus, the retrofit problem involves proposing interventions in the network, leading to energy and temperature redistribution among the HEX, with the ultimate goal of reducing utility consumption. Each intervention and a given energy redistribution are associated with an investment cost required for implementation, which counterbalances the potential cost savings. The objective function of the retrofit problem can be expressed as the Net Present Value (NPV), as shown in Equation 1.3 below:

$$NPV = \sum_t \frac{CF_t}{(1+i)^t} - IC \quad (1.3)$$

where CF_t is the cash flow in time t , i is the interesting rate and IC the investment cost, which involves the cost associated with topological modifications, adding new areas and intensifying existing HEX. The cash flow is evaluated as:

$$CF = C_{HU}(E_{HU}^{old} - E_{HU}) + C_{CU}(E_{CU}^{old} - E_{CU}) \quad (1.4)$$

where C_{HU} and C_{CU} are the energy cost of hot and cold utility in $\$/(\text{kW}\cdot\text{y})$, respectively. In addition, E_{HU}^{old} and E_{CU}^{old} are the hot and cold utility consumption in the original HEN, E_{HU} and E_{CU} the new consumption.

In order to exemplify a HEN retrofit problem, consider a hypothetical existing network presented in Figure 1.1, associated with the streams data and basic data of the existing HEX (for simplification, consider only countercurrent shell-and-tube heat exchangers) displayed in Tables 1.1 and 1.2, respectively. In addition, consider that the cost of hot (C_{HU}) and cold (C_{CU}) utility are, respectively, 55 $\$/\text{kW}\cdot\text{y}$ and 6 $\$/\text{kW}\cdot\text{y}$, the project time horizon is 10 years, the interest rate is 10% and the cost of additional area is given by Equation 1.5 below:

$$IC_{HEX} = 10000 + 560 A_{new} \quad (1.5)$$

Table 1.1: Existing network stream data in the illustrative example

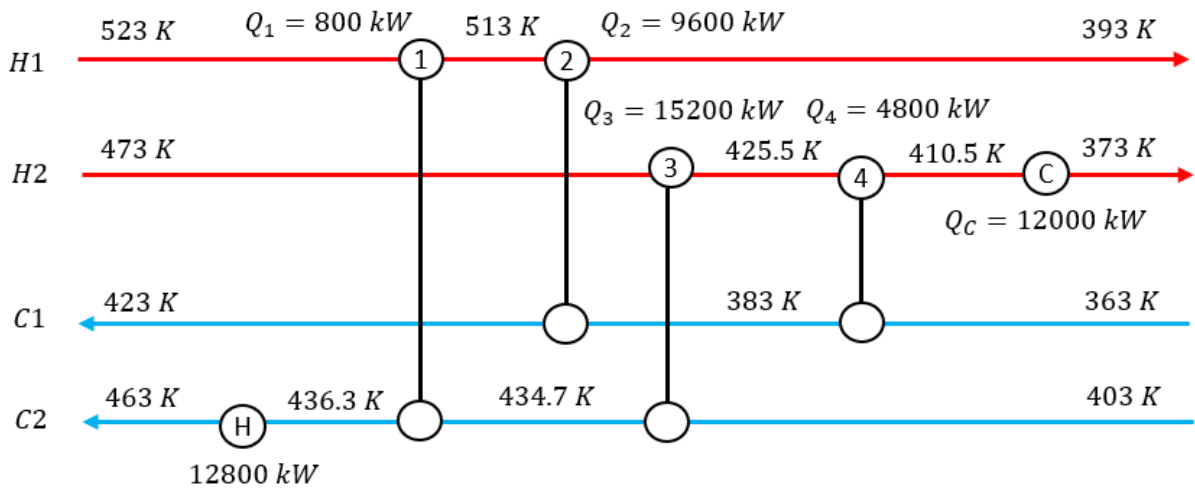
Stream	$F C_p$ (kW/K)	T_{in} (K)	T_{out} (K)
H1	80	523	393
H2	320	473	373
C1	240	363	423
C2	480	403	463
HU	-	493	493
CU	-	305	315

Source: Author's own work, 2024.

Table 1.2: Existing network HEX data in the illustrative example

HEX	Q (kW)	U (kW·m ⁻² ·K ⁻¹)	$LMTD$ (K)	Area (m ²)
1	800	0.2	82.43	48.53
2	9600	0.3	36.41	878.88
3	15200	0.45	29.70	1,137.30
4	4800	0.24	44.95	444.94
H	12800	0.6	41.94	508.66
C	12000	0.5	80.97	296.41

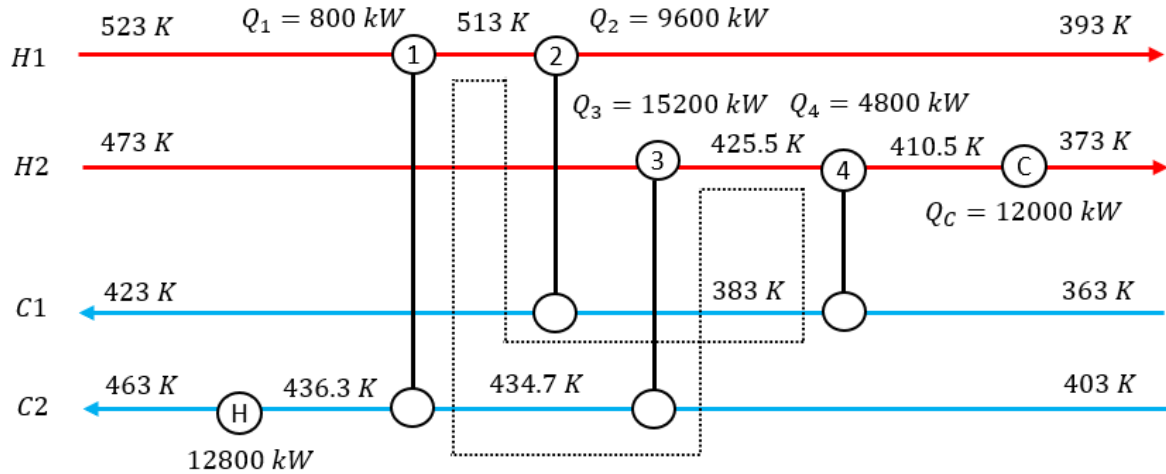
Source: Author's own work, 2024.

Figure 1.1: Existing network in the illustrative example

Source: Author's own work, 2024.

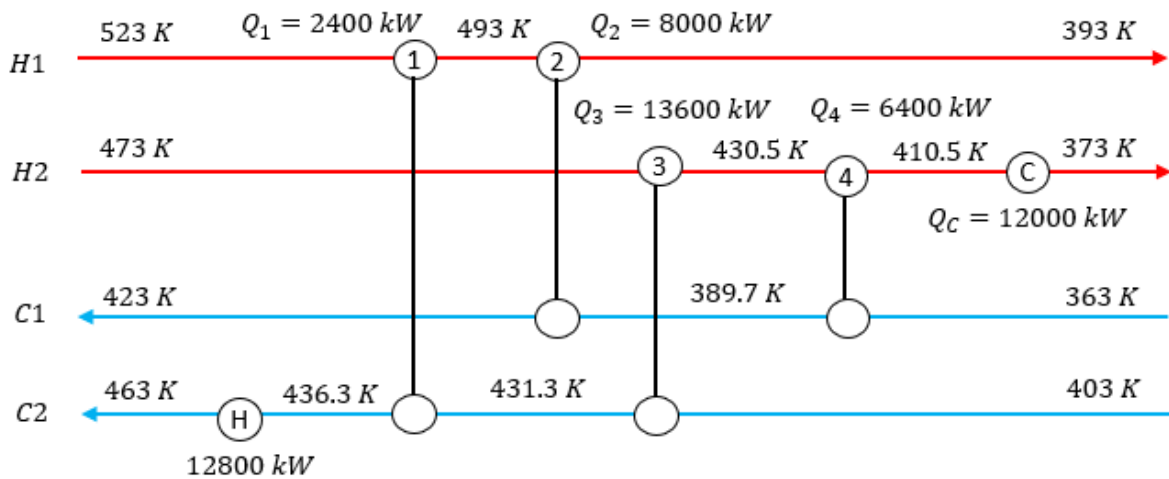
The existing HEN have a consumption of 12800 kW of hot utility and 12000 kW of cold utility. The HEN presented in Figure 1.1 contains one energy loop involving HEXs 1, 2, 3 and 4 as illustrated in Figure 1.2. In order to illustrate the energy loop feature, Figure 1.3 shows a different heat distribution inside the loop, without altering the utility consumption.

Figure 1.2: Energy loop of the existing HEN in the illustrative example



Source: Author's own work, 2024.

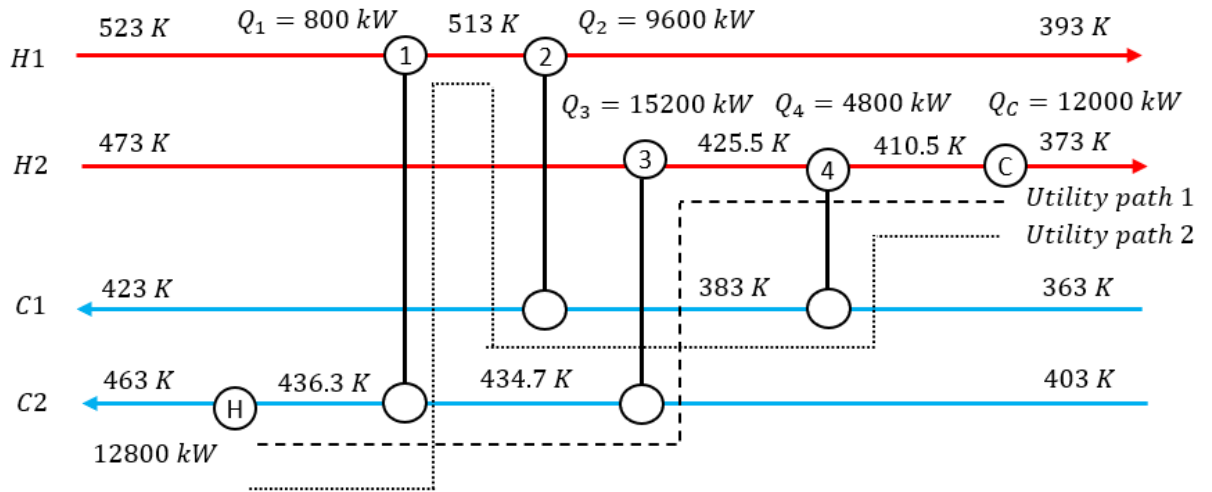
Figure 1.3: Existing network with different heat distribution



Source: Author's own work, 2024.

There are two different utility paths in the HEN, as depicted in Figure 1.4. For example, beside the cooler and heater, for the utility path 2, the heat duty of HEXs 1, 2 and 4 changes, and for utility path 1 only the HEX 3. Figure 5 illustrates a new utility consumption, using the utility path 1, which maximizes the energy recovery of the HEN for a minimum approach temperature (ΔT_{min}) equal to 10 K.

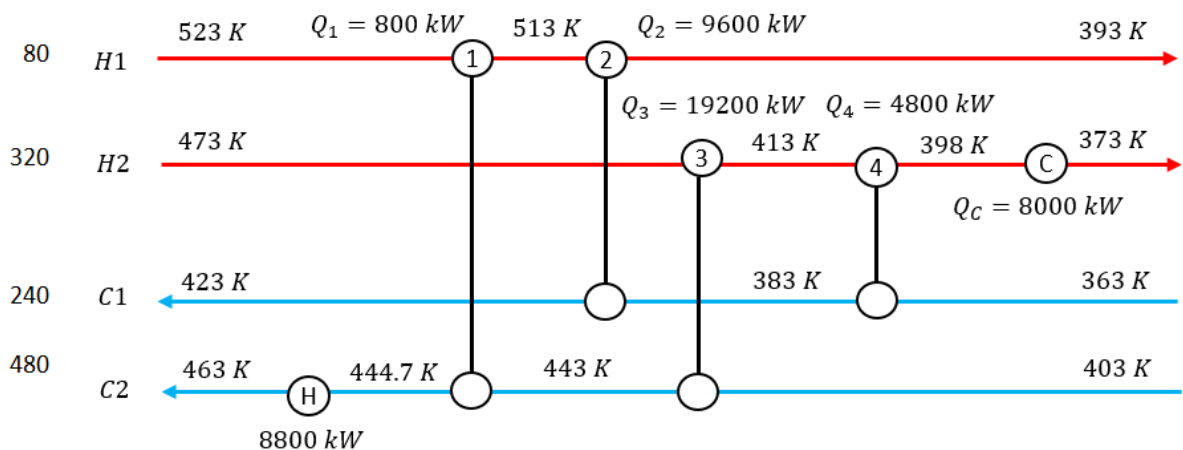
Figure 1.4: Utility path of the existing network



Source: Author’s own work, 2024.

Note that the cold side of HEX 3 reached a temperature difference of 10 K, and any additional of energy recovery would violate the ΔT_{min} of 10 K (which can be also defined as the Pinch Match, according to Asante and Zhu, 1996). The comparison between Figures 1.3 and 1.5 shows an increase of 4000 kW of the heat recovery, requiring an increase of the heat duty of the HEX 3 in the same amount, without changing the heat load of the other ones. Table 1.3 shows the required area for each existing HEX for the new service:

Figure 1.5: Existing HEN with different utility consumption



Source: Author’s own work, 2024.

Table 1.3: Existing HEN with new heat distribution in the illustrative example

HEX	Q (kW)	U (kW·m ⁻² ·K ⁻¹)	$LMTD$ (K)	$Area$ (m ²)	$Required\ area$ (m ²)
1	800	0.2	74.07	48.53	54.00
2	9600	0.3	36.41	878.88	878.88
3	19200	0.45	18.20	1,137.30	2,344.32
4	4800	0.24	32.43	444.94	616.71
H	8800	0.6	38.44	508.66	381.55
C	8000	0.5	75.25	296.41	212.62

Source: Author's own work, 2024.

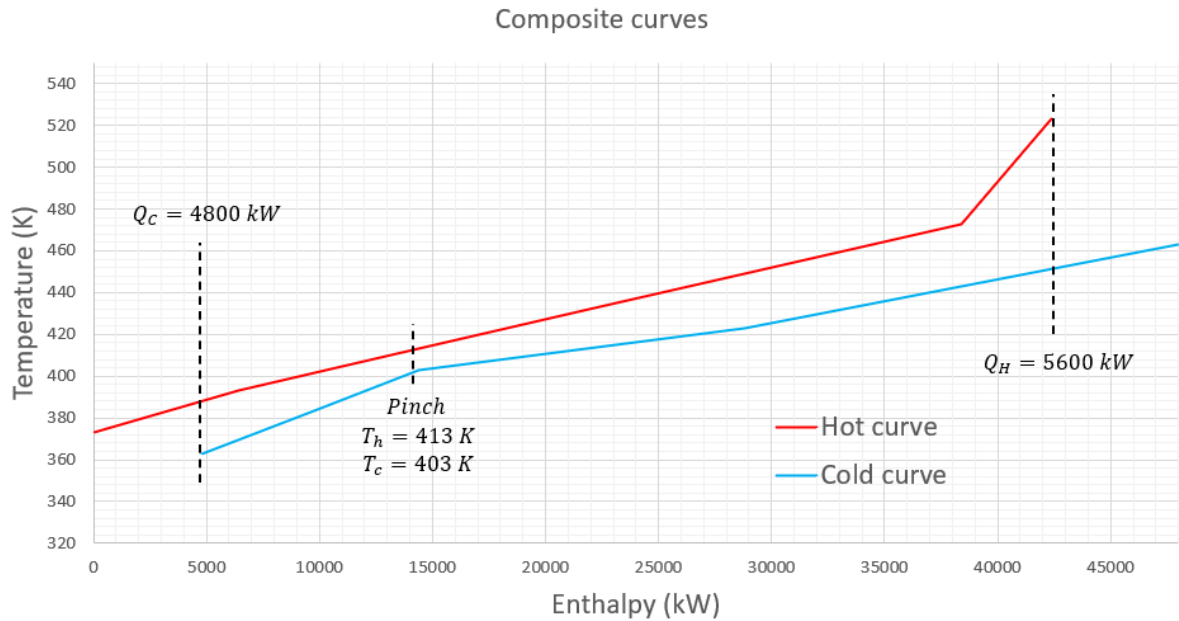
Table 1.3 shows that the existing HEX 3 cannot supply the entire new service, due to the increase of the heat load and the reduction of the LMTD. In addition, although the heat duty of HEXs 1 and 4 are unchanged, an additional area is required due to the reduction of the LMTD.

If Equation 1.1 is used, the additional area in the illustrative example would be 5.47 m² for HEX 1, 1207 m² for HEX 3 and 171.77 m² for HEX 4. The investment cost can be evaluated using Equation 1.2, giving a value of 805,186 \$, and the cash flow, evaluated with Equation 4, is equal to 244,000 \$/y. The NPV of the retrofit is equivalent to 631,133 \$, which shows that the proposal HEN retrofit worths.

Although significant energy recovery can be attained in the HEN presented in Figure 5, no more recovery can be attained without violating the ΔT_{min} of 10 K. In order to analyze the potential energy recovery, the Pinch Analyses can be used as an important tool. Figure 6 illustrates the composite curves of the example for a ΔT_{min} of 10 K.

Figure 1.6 shows that the minimum energy consumption of the cold utility is 4800 kW and for the hot utility is 5600 kW, revealing that more energy can be recovered in the network. However, as already discussed, no more energy can be recovered in the HEN without violating the ΔT_{min} , which means that a topological modification is required, if it is decided to recover more energy.

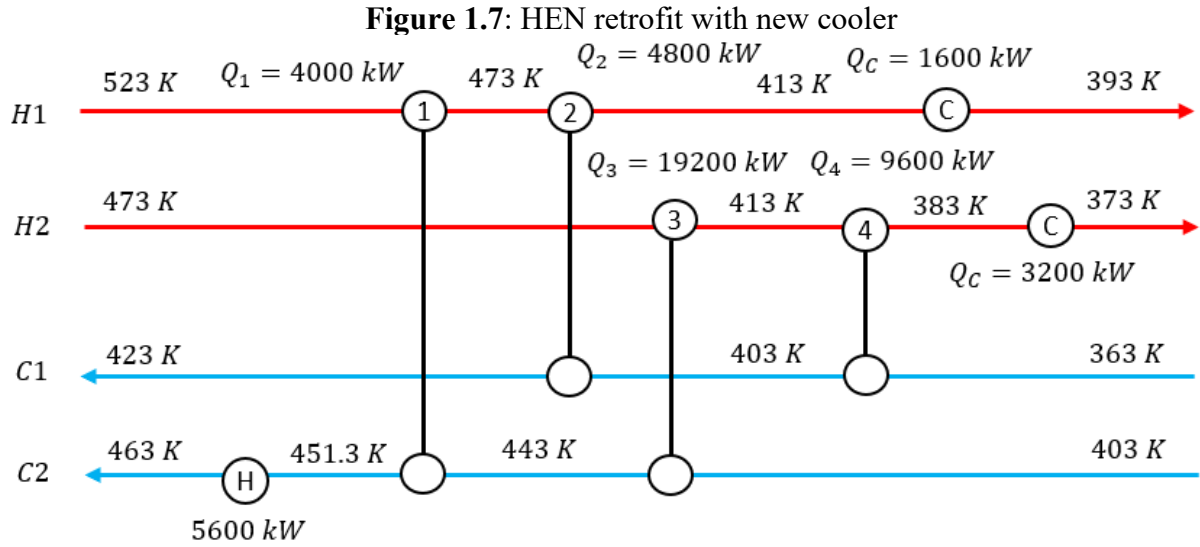
A possible way to guide the decision of which type of modification should be performed is to identify the cross-pinch unit in the HEN. The temperature pinch of the problem is 413 K for the hot stream and 403 K for the cold stream (see Figure 1.6). Since the problem involves a small number of streams, it is not difficult to see in Figure 1.5 that HEX 2 violate the pinch, because stream H1 goes from 513 K to 393 K and C2 from 383 K to 423 K.

Figure 1.6: Composite curve of the illustrative example.

Source: Author's own work, 2024.

Figure 1.7 illustrates one proposal to overcome the cross-pinch match, where adding a new cooler in stream H1 and shifting heat in order to attain the minimum utility consumption. Table 1.4 shows the required area for each existing HEX for the new service and the design of the new cooler.

For the case presented in Figure 1.7 and Table 1.4, an investment cost of 2,245,263 \$ and a uniform cash flow of 439,200 \$/y is obtained, which gives an NPV of 412,209 \$. Although this enterprise is also profitable, gives a NPV smaller than the first case where no HEX is added, illustrating that maximizing the energy recovery do not guarantee the best return.



Source: Author's own work, 2024.

Table 1.4: Existing HEN with topological modification

HEX	Q (kW)	U (kW·m ⁻² ·K ⁻¹)	$LMTD$ (K)	$Area$ (m ²)	$Required\ area$ (m ²)
1	4000	0.2	47.85	48.53	417.97
2	4800	0.3	24.85	878.88	643.86
3	19200	0.45	18.20	1,137.30	2344.32
4	9600	0.24	14.43	444.94	2772.00
H	5600	0.6	35.53	508.66	262.69
C (H1)	1600	0.5	92.91	-	34.44
C (H2)	3200	0.5	68.00	296.41	94.12

Source: Author's own work, 2024.

Even if the hypothetical example explored above is significant simple, several points can be highlighted in order to explore the complexity of the HEN retrofit:

- For a given structure (where the HEXs, coolers and heater are already selected), the utility consumption varies between the current one (the original value) and the minimum value (limited by a given ΔT_{min}). The curve of NPV with the utility consumption is not monotone neither smooth. Therefore, the identification of the best energy recovery of a given structure is significantly difficult.
- For a given structure, it is possible to exist different utility paths and energy loops that increase the possibility of different solutions associated with different distribution of heat loads, consequently with different investment costs.
- The HEN retrofit example explored is all based on a given ΔT_{min} , where different values lead to different solutions.

- The retrofit of a single HEX, as will be explored in Section 3, is not a trivial task since there are different ways to increase area (installing different types of HEX – shell and tube heat exchangers (STHE) or gasketed-plate heat exchangers (GPHE), for example – which can be alignment in series or in parallel, using heat intensification devices).
- The identification of problematic matches, like cross-pinch units, can be significant difficulty. In addition, the selection of which type of topological modification and how it is installed is not trivial.

Therefore, it is important to realize that performing the HEN retrofit based on grid diagrams and human decisions is a complex challenge to explore all the combinations and details presented in the problem.

Another typical approach to addressing the problem involves using mathematical formulations followed by optimization, with Mathematical Programming being the predominant procedure in the literature. Numerous studies are available on this topic (a detailed literature review will be presented in subsequent chapters of this thesis). However, the retrofit of HENs is characterized by significant nonlinearities, nonconvexities, and large dimensionality due to the multitude of intervention alternatives. The problem's size increases dramatically with the network's complexity, making its application to industrial-scale problems exceedingly challenging.

Consequently, as discussed by several authors (Yee and Grossman, 1991; Ma *et al.*, 2000; Pan *et al.*, 2013; Pan *et al.*, 2018), the application of Mathematical Programming faces numerous challenges, including convergence difficulties, issues with local optimality, the need for good initialization strategies, and high computational effort. The cumulative effect of these challenges results in difficulties in applying these methods to industrial-scale problems and significantly undermines the quality of the solutions obtained—if a viable solution is achieved at all, as highlighted by Pan *et al.* (2013).

It is evident, therefore, that the HEN retrofit problem poses numerous challenges. Accordingly, as will be presented later, various studies in the literature have sought to propose solution procedures to address these difficulties. However, limited attention has been given to discussing the limitations and assumptions typically adopted in these approaches and their practical implications. Moreover, there is a lack of conceptual reflection on how the HEN retrofit problem aligns with the realities of industrial practice.

One of the objectives of this dissertation, addressed in Chapter 2, is to reflect on how the HEN retrofit problem can be framed from the perspective of industrial practice.

Furthermore, we will explore in greater detail several gaps that remain unexplored in the literature, arguing that these omissions contribute to a significant disconnect between the solutions proposed by the scientific community and their practical implementation.

In addition, we will examine the impact of common simplifications in the literature, particularly the simplified retrofit of individual heat exchangers. Finally, we will discuss the challenges of incorporating these critical aspects into classical approaches from the literature, which, from our perspective, are essential to addressing the HEN retrofit problem comprehensively.

In Chapter 3, we delve deeper into the problem of HEX retrofit. Various aspects and alternative methods for increasing the heat transfer capacity of an HEX are presented, along with their respective effects—an area that remains underexplored in the literature. Additionally, we propose an innovative procedure that integrates all the discussed alternatives, incorporating a precise thermofluid-dynamic modeling of the equipment using well-established models from the literature. This approach is robust, efficient, and free from convergence issues, which is critical for addressing the HEN retrofit problem effectively.

Chapters 4 and 5 build upon these advancements by presenting a comprehensive HEN retrofit methodology that fully integrates the detailed HEX calculations developed in Chapter 3. This integration is performed simultaneously with the HEN retrofit optimization process. In Chapter 4, we detail the procedure for retrofitting HENs without topological changes, while Chapter 5 introduces an enumeration-based methodology to tackle retrofits involving topological modifications.

The results presented in each chapter highlight the significant advantages of incorporating the proposed advancements, demonstrated through comparisons with the classical approaches predominant in the literature. Furthermore, as will be shown, the proposed procedure does not suffer from convergence issues or require variable initialization, as it efficiently handles all nonlinearities inherent to the problem. The optimization is performed using a global optimization method, ensuring a reliable and high-quality solution. Unlike existing methods, particularly those based on Mathematical Programming, our approach delivers solutions that are both practical and trustworthy.

It is worth reiterating that Chapters 2 through 5 have been written in the format of scientific articles, although they have not yet been published.

ACRONYMS AND ABBREVIATIONS

HEN	Heat exchanger network
HEX	Heat exchanger
LMTD	Logarithmic mean temperature difference
NPV	Net present Value

NOMENCLATURE

a	Parameter of capital cost	\$/m ²
A_{new}	Additional area	m ²
A_{ex}	Area of existing HEX	m ²
b	Parameter of capital cost	Dimensionless
C_{HU}	Cost of hot utility	\$/kW·y
C_{CU}	Cost of cold utility	\$/kW·y
CF	Fixed cost	\$
CF_t	Cash inflow in time t	\$/y
\widehat{E}_{CU}^{old}	Cold utility consumption of the original HEX	kW
\widehat{E}_{HU}^{old}	Hot utility consumption of the original HEX	kW
E_{CU}	Cold utility consumption	kW
E_{HU}	Hot utility consumption	kW
FCp	Heat capacity flow rate	kW/K
\hat{i}	Interest rate	%
IC_{HEX}	Investment cost associated with a new HEX	\$
Q	Heat load	kW
T_{in}	Inlet temperature	K
T_{out}	Outlet temperature	K
U	Overall heat transfer coefficient	kW·m ⁻² ·K ⁻¹

2. A ROADMAP FOR HEAT EXCHANGER NETWORK RETROFIT: CHALLENGES AHEAD

2.1. Introduction

Due to rising energy costs, the increasing scarcity of energy resources, and growing concerns over environmental issues, energy integration has garnered significant attention from process industries, leading to a substantial rise in publications in international journals (Sreepathi and Rangaiah, 2014). Although the number of publications on retrofit problems is smaller compared to those addressing grassroots design, the focus on HEN retrofitting has increased in recent years, primarily because the focus switch to the increase of energy efficiency in existing plants, instead of capacity increase associated with new projects.

Similarly to the HEN synthesis, the approaches to solving HEN retrofit problems can be categorized into three main groups: Pinch Technology-based methods, Mathematical Programming approaches, and Metaheuristic techniques.

In the realm of Pinch Technology, the pioneering work was proposed by Tjoe and Linnhoff (1986), which extended the tool originally developed for synthesis problems to address HEN retrofitting. Modifications to the network are guided by the concept of area efficiency, which evaluates the ratio between the actual network area and the minimum area required, considering vertical heat transfer (Kemp, 2007).

However, extending this tool to retrofit problems is not straightforward. The HEN retrofit involves a significant number of possible modifications and requires the incorporation of existing network characteristics into the procedure, which is a complex task. Consequently, several works following Tjoe and Linnhoff (1986) introduced new tools to address these challenges.

Reisen *et al.* (1995) introduced Path Analysis, which helps identify the critical parts of the existing network that require modification. This method also facilitates the generation of subnetworks, making it easier to apply Pinch Technology. Lakshmanan and Bañares-Alcántara (1996) proposed a new diagram called the Retrofit Thermodynamic Diagram, which aids in visualizing the driving forces within the existing network and overcoming violations of pinch rules and crisscross matches. Varbanov and Klemes (2000) addressed the difficulty in identifying matches that create bottlenecks in energy recovery within the

network. They presented heuristics to ease the identification of these bottlenecks. Nordman and Berntsson (2001) developed new composite curves to incorporate the characteristics of the existing network into the analysis.

In the last decade, noteworthy contributions include the work of Li and Chang (2012), who proposed a systematic procedure to overcome matches that transfer heat across the pinch. Their method involves splitting the thermal load of such matches and redistributing it among other heat exchangers in the network. Gadalla (2015) introduced the Streams Plot, a graphical tool that can be divided into different regions to help identify matches in the existing network that exchange heat across the Pinch. This visualization aids in identifying inefficiencies and provides a clear basis for targeted modifications in the retrofit process.

On the other hand, Mathematical Programming-based approaches aim to optimize HEN retrofitting through fully automated procedures. Ciric and Floudas (1989) proposed a two-stage method: a MILP model to identify topological modifications in the network, followed by a NLP model to optimize the proposed network. Subsequently, Ciric and Floudas (1990) presented a simultaneous approach using a unified MINLP model, addressing the limitations of the decomposition method used in their earlier work. Yee and Grossmann (1991) introduced a prescreening stage to assess the potential gains of network retrofitting. After this initial analysis, a MINLP model was employed to carry out the retrofitting process. Briones and Kokossis (1999) developed a screening stage to identify existing matches suitable for modification while preserving others deemed adequate. The proposed changes focus on improving the network by modifying inefficient matches.

In another approach, Ma *et al.* (2000) proposed a linearized model to generate an initial estimate for a MINLP model, which is subsequently refined in later stages. Sorsak and Kravanja (2004) extended these methodologies by incorporating models that allow for the inclusion of different heat exchanger types during the retrofit process. Nguyen *et al.* (2010), developed a single-stage MILP model. By dividing the network into distinct temperature intervals, the LMTD in each interval is known, the model eliminates the nonlinearity of area calculations.

Addressing the enhancement of existing heat exchangers, Pan *et al.* (2012) proposed a network retrofit strategy that increases the heat exchangers heat load using intensification devices. To handle the problem nonlinearities, they introduced an iterative procedure that solves a series of MILP problems repeatedly. Wang *et al.* (2012) highlighted the drastic simplifications in previous studies, particularly the assumptions of constant and known heat transfer coefficients and the disregard for pressure drop calculations. By focusing on

intensification devices, Wang *et al.* (2012) proposed a set of heuristics to determine appropriate interventions in the network. Then, a detailed calculations of the heat exchangers is performed, explicitly considering their geometries to provide a more accurate and practical solution.

Pan *et al.* (2013) expanded the discussion on heat exchanger intensification by highlighting that, beyond enhancing heat transfer coefficients, intensification also reduces fouling propensity. To address this, a fouling model was integrated into the formulation, enabling the evaluation of the required downtime for cleaning each heat exchanger. The solution procedure remained consistent with that of Pan *et al.* (2012), relying on successive MILP iterations to navigate the problem nonlinearities effectively. Building on these advancements,

Pan *et al.* (2018) introduced a methodology that incorporates detailed heat exchanger calculations directly into the retrofit formulation. In this approach, LMTD and its correction factor (F) are accurately computed, while convective heat transfer coefficients and pressure drops are determined using correlations related to the specific geometry of existing heat exchangers. The focus of Pan *et al.* (2018) remained on intensification devices, and to address the inherent nonlinearities, an iterative procedure was implemented. This procedure utilized Taylor series expansions truncated to the first term to obtain a linearized model. Angsutorn *et al.* (2021) discussed the difficulty of modifying existing heat exchangers and the existing network topology. Thus, they proposed a HEN retrofit approach addressing only new heat exchangers without increasing heat transfer area of existing HEX.

Although fewer papers explored metaheuristic programming to HEN retrofit, there are some interesting previous attempts. These approaches also involves the utilization of a Mathematical Programming tool (therefore, this set of approaches could be also classified as Hybrid Methods, but this term is limited in the current text to the simultaneous utilization of Pinch Technology and Mathematical based methods).

Athier *et al.* (1998) proposed a two-stage procedure. The first one, or master problem, addresses the topological modification using a Simulated Annealing procedure (SA). The second one optimizes the required area of the modified network obtained from the master problem, using a NLP model. Later, Bochenek *et al.* (2006) formulated a single multivariable problem using a structural matrix instead of superstructures, and solved the problem in two levels. The first one addresses the topological modification using a Genetic Algorithm (GA), and the second one is used to obtain the split ratio and areas.

Rezaei and Shafiei (2009) discussed the difficulty of GA to handle continuous variables. Therefore, in order to address this limitation, it was proposed to couple the GA with a NLP and ILP models to deal with the continuous variables of the HEN retrofit problem, such as, heat loads, temperatures, split ratios, etc. Soltani and Shafiei (2011) considered the pressure drop in the retrofit using an iterative algorithm coupling the GA (topological modification), a LP model (network evaluation) and a ILP model (network modification to maximize the profit, where the streams pressure drops are calculated between the LP and ILP runs).

Biyanto *et al.* (2016) proposed a GA method to solve the HEN retrofit based on enhancement tools. Stampfli *et al.* (2022) proposed a GA model for topological modification, followed by a differential evolution (DE) algorithm to optimize the heat loads. They proposed a parallelized procedure for the GA evaluation, where the DE is performed on each chromosome parallel on multiple cores.

Further discussions of different HEN retrofit approaches, up until 2014, can be found in the review article by Sreepathi and Rangaiah (2014).

Despite significant advancements in the literature, especially in recent years, fundamental challenges remain unaddressed in the context of HEN retrofitting. The analysis of these challenges indicates that there is a gap between how the problem is addressed in the literature and the needs of a methodology able to solve real problems. From a critical point-of-view, without addressing these neglected issues, the solutions proposed in the scientific community remain largely disconnected from industrial practice.

Reflecting on pinch-based approaches, nearly all methods attempt to address the same challenges: overcoming the combinatorial explosion of potential modifications and incorporating the characteristics of the existing network. However, even if a method successfully addresses these issues, additional unresolved challenges persist, such as the inability to adequately evaluate the trade-off between investment cost and energy recovery, and the reliance on the expertise of the designer to attain a satisfactory solution.

These shortcomings stem primarily from an inherited philosophy and conceptual framing borrowed directly from HEN synthesis. As this thesis will discuss, HEN retrofit introduces higher complexity both conceptually and practically. The inherent nature of intervening in an existing network—whose characteristics must be integrated into the formulation—demands a far more intricate approach than simply connecting streams through existing heat exchangers defined by surface area and an overall heat transfer coefficient.

Similarly, in the realm of mathematical programming approaches, the situation remains unchanged, albeit with different limitations. Numerical difficulties associated with nonlinearity, nonconvexity, and combinatorial explosion render the quality of solutions questionable—if solutions are obtained at all. Existing works largely attempt to circumvent these limitations, timidly and superficially incorporating some additional characteristics. Recent contributions from Pan and Smith’s group have introduced greater detail into formulations, focusing on networks without topological changes and exclusively on intensification devices. While these represent evident progress, as this thesis will argue, they still fail to address several critical aspects of the retrofit problem holistically.

Metaheuristic methods, on the other hand, possess the ability to overcome local optima and, compared to Mathematical Programming, handle numerical challenges associated with the nonlinearities of the problem more effectively. However, these methods are also associated with several limitations, particularly due to being penalized by the combinatorial explosion inherent to HEN retrofit problems. Additionally, they require fine-tuning of control parameters, involve high computational effort, do not guarantee global optimality and face significant challenges in qualifying the solutions obtained.

According to this scenario, this thesis aims to discuss and highlight various practical aspects of HEN retrofitting that remain unexplored in the literature. Our central objective is to establish a roadmap—a practical guide to help the scientific community converge toward solutions that hold real industrial applicability. At this stage, we do not aim to provide a comprehensive solution to all these problems. We are fully aware of the complexity underlying these issues, which limited previous approaches to address them. Nevertheless, our aim is to identify technological targets that need to be addressed to fulfill the significant gap between academic studies and industrial requirements. The importance of the issues discussed here are illustrated by several simplified retrofit examples. According these results, the solution of the retrofit problem can be considerably affected.

The rest of this chapter is organized as follows: Section 2 describes the HEN retrofit problem and the interventions employed in the existing HEN to increase the energy recovery, Section 3 presents cash flow issues that affect the retrofit problem and are not explored in the HEN retrofit literature; Section 4 demonstrates the need to include the design of heat exchangers (HEX) in the formulation of the retrofit problem;

2.2 HEN Retrofit Problem

Retrofit is a type of process design, which the objective is to modify an existing plant (differently from the grassroot problem, which is associated with the design of an entire new plant). There are different motivations to retrofit an existing system, such as to increase plant capacity, accommodate different feed or product specifications, reduce operating costs, improve safety or reduce environmental emissions (Smith, 2005). Because the retrofit involves the modification of an existing plant, it is desired to use most of the existing equipment, since changing it or purchasing new ones demands additional costs. However, at least one equipment is probably operating at, or close to, its maximum capacity, thus in retrofit design is common the necessity of purchasing new equipment (Smith, 2005).

For the specific case of heat exchanger network, the company has the opportunity of investing in the existing HEN to increase energy recovery and reduce utility consumption. The opportunity of saving money with the decrease of energy consumption in an existing HEN can be justified by different reasons, such as, the increase of energy prices, a poorly executed network synthesis, changes in the streams data, etc. (Smith, 2005). Therefore, a HEN retrofit project involves capital expenditures (CAPEX) that will modify the existing HEN, (e.g. HEX substitution, insertion of intensification devices, etc.) in order to attain a reduction of the operational expenditures (OPEX) after the intervention (i.e. the economic gain associated with the project corresponds to the reduction of the energy consumption attained through the retrofit).

From a financial perspective, the HEN retrofit problem is framed as a project in which the company may or may not invest, depending on its profitability and the comparison with other alternatives. Thus, unlike the synthesis of a new HEN, where the goal is to find the lowest-cost network for a given project, the retrofit problem must incorporate concepts from investment analysis in order to attain a solution associated with the largest value creation for the shareholders.

2.2.1. Alternative interventions on existing HEN in retrofit problems

Energy recovery increase can be attained without modifying the topology of the existing network, which means that all existing matches are preserved, and new matches are not added in the network. It can be executed exploring a utility path, which is a path connecting a heater to a cooler through heat exchangers. In this case, heat is distributed from utilities HEXs (heaters and coolers) to energy recovery HEXs, thus reducing the utility consumption.

An additional path that can be used is an energy loop, which is a closed path along different HEXs and streams of a network, leaving at a point and returning to this same point. Energy loops are paths where heat can be redistributed without changing the utility consumption. However, it can be important to the HEN retrofit because changing the heat distribution also changes the heat load and the inlet and outlet temperatures in each HEX, thus affecting the capital costs.

Therefore, HEN retrofits involve the increase the heat load of, at least, one HEX of the network. Thus, modifications to existing HEX are required, to increase the heat transfer duty in these units. It should be noted that due to the interconnected nature of a HEN, the retrofit solution may also demand the reduction of the heat load in other HEXs.

The most common approach adopted in the literature to represent the increase of a HEX heat load in the network is to add area to the existing unit, as shown below:

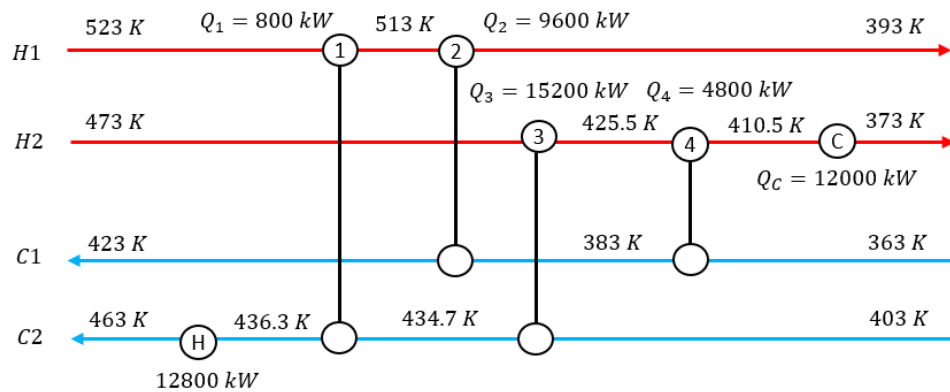
$$A_{new} = \max\left(\frac{Q}{U LMTD} - A_{ex}; 0\right) \quad (2.1)$$

Although widely used, this equation relies on several assumptions, which are usually far from the reality. According Eq. (2.1), the existing HEX and the new HEX to be added are both countercurrent HEXs. Additionally, the overall heat transfer coefficient of the new HEX is the same of the existing one. This latter assumption implies that the new unit is aligned in series with the existing one and it must have a similar geometry (for example, for shell-and-tube HEXs, the unique difference between the new and the existing units must be the tube length, because both HEXs have the same overall heat transfer coefficient).

In practice, the new HEX can be aligned in series or in parallel, it may have a different geometry, or even it may be associated with a different HEX type at all. The need of a more realistic representation of the increase of the heat load associated with an existing HEX in the retrofit problem will be addressed further.

Besides the increase of the heat load of existing HEXs, the retrofit may also involve other interventions, which demands the modification of the HEN topology. Suppose the following existing HEN present in Figure 2.1.:

Figure 2.1. Existing HEN.

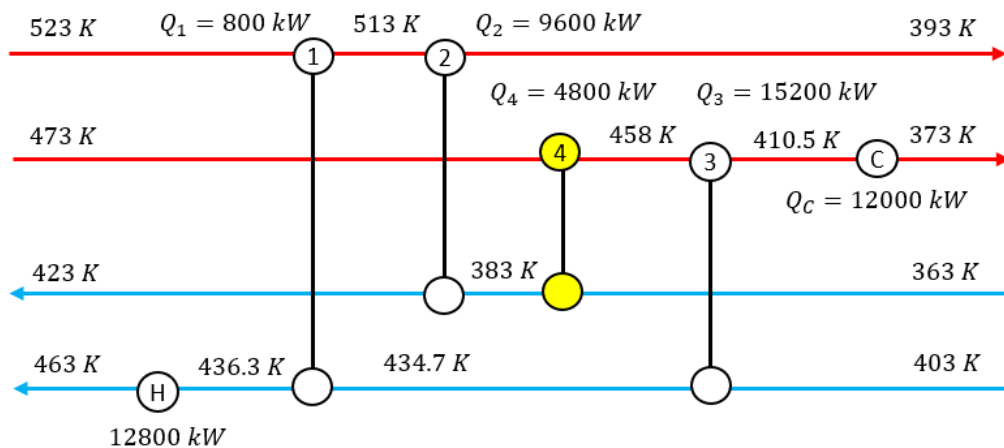


Source: Author's own work, 2024.

The topological modifications alternatives can be classified into:

i) Resequencing: it moves a unit to a new location, preserving the streams in the original match, as depicted in Figure 2.2.

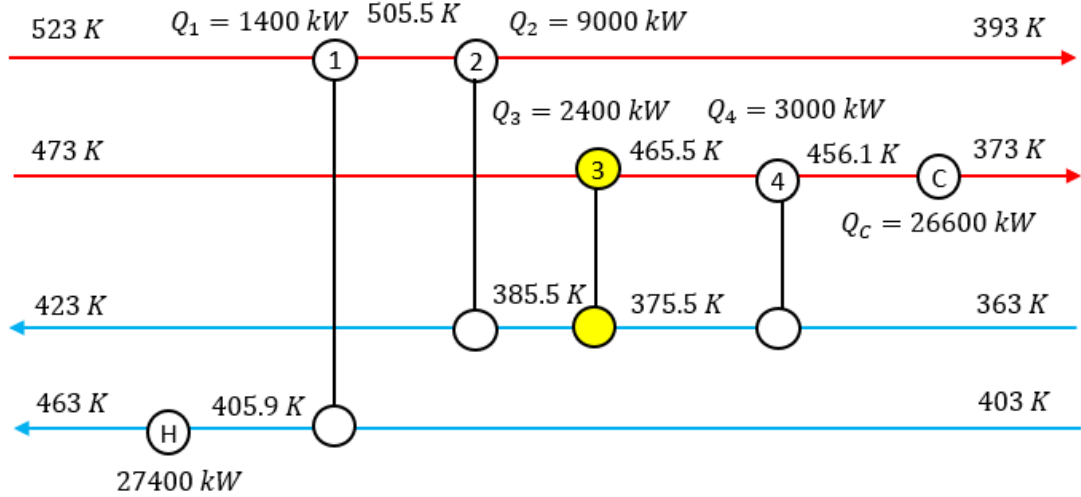
Figure 2.2. Existing HEN with a resequencing.



Source: Author's own work, 2024.

ii) Repiping: the streams involved in the match do not need to be the same as the original one, where one or both streams can be different, as depicted in Figure 2.3.

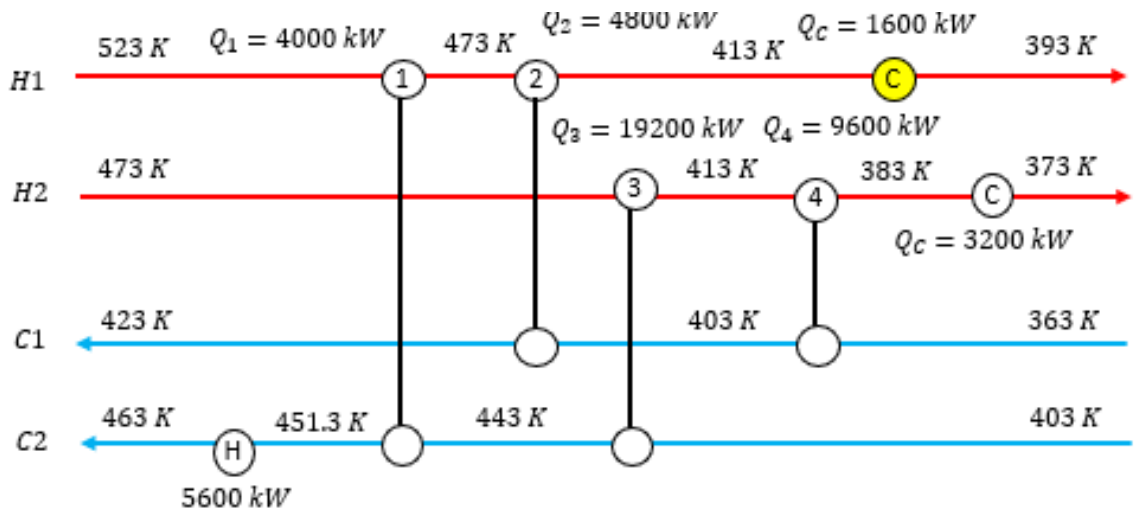
Figure 2.3. Existing HEN with a repiping.



Source: Author's own work, 2024.

iii) Inserting a new match: a new match can be installed in the HEN, as depicted in Figure 2.4.

Figure 2.4. Existing HEN with a new match.



Source: Author's own work, 2024.

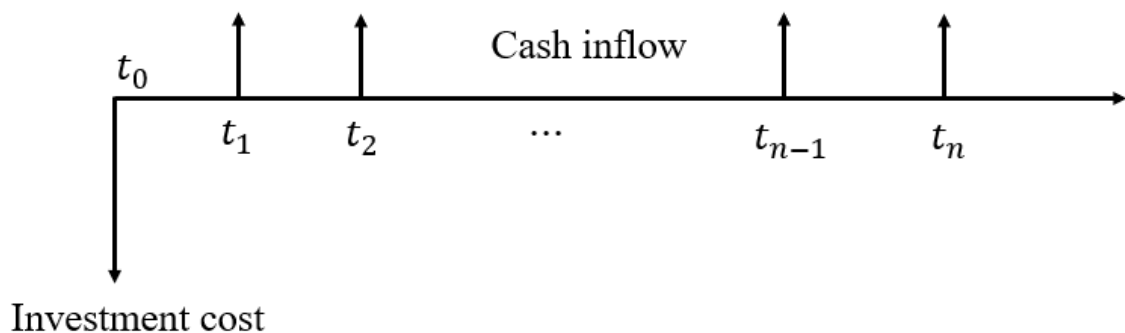
Topological modifications are a multidisciplinary task involving mechanical, civil, and process teams, associated with piping, fittings, safety, maintenance, and control. In addition, the layout team is also essential, as the existing network configuration must consider the availability of physical space and the physical arrangement of the equipment.

2.3. Cash Flow in HEN Retrofit Problems

As briefly discussed, the evaluation of a network retrofit cannot be approached in the same way as a synthesis problem, where the objective is to find the lowest-cost network. In fact, a network retrofit represents a project opportunity in which the company can choose to invest to enhance energy recovery and save money by reducing operational costs.

Conceptually, the literature consistently addresses the same type of problem, which involves retrofitting an existing network with a uniform cash flow, as illustrated in Figure 2.5. The investment cost corresponds to the costs related to the additional thermal equipment and devices that must be purchased to increase the energy recovery of the network. The cash inflow during the time horizon of the project corresponds to the difference between the operating costs of the HEN before and after the retrofit, i.e. it is the economic gain associated with the reduction of the operating costs due to the retrofit.

Figure 2.5. Cash flow of a traditional retrofit problem.



Source: Author's own work, 2024.

However, this representation of the problem does not account for all problems often present in the industrial practice. Therefore, this section presents aspects of the retrofit problem that can modify the cash flow observed in commercial projects.

Some of the issues presented below cannot be solved using the direct application of solution approaches already developed for the conventional problem. Therefore, there is a need for developing new algorithmic tools to solve these problems.

2.3.1. Project size limitations

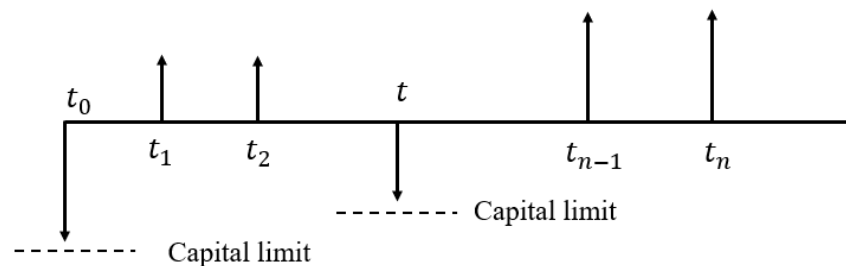
As shown above, the conventional formulation adopted implicitly assumes that the company has unlimited capital, fully available at the beginning of the time horizon of the project, and that the capital comes exclusively from a single source.

However, a scenario usually encountered in industrial practice involves a size limitation, i.e. the retrofit solution must be limited according to a previously established financial cap or other resource limit (e.g. manpower). In this case, a constraint must be added to the problem formulation, which exclude more expensive candidate solutions.

2.3.2. Phased retrofit

A phased project is executed in steps (Bower and Walker, 2007; Alinezhad *et al.*, 2021). After each step, the system is operated until the next step according to the interventions already executed until that moment. This approach can be modelled through multiple cash inflows distributed with time, instead of a single budget limit at the beginning of the project horizon. A phased project can be represented by a set of budget limit associated with each cash inflow. Figure 2.6 represents a cash flow of a phased project organized in two periods.

Figure 2.6. Phased project HEN retrofit.



Source: Author's own work, 2024.

The solution for the HEN retrofit in a phased project can be significantly different from the traditional case. Firstly, an irregular cash flow results in a non-monotonic relationship between the Net Present Value (NPV) and investment, leading to different optimal values among the various metrics used to evaluate the project (NPV, Internal Rate of Return (IRR), and others).

Secondly, since the investment is made in stages, the decisions regarding which modifications will be implemented at each stage may result in a new network that is significantly different from the conventional case.

Aiming at illustrating the impact of a phased project, consider a simplified retrofit of the network presented in Figure 2.7. No topological modifications are considered; therefore, energy recovery is achieved by using the utility path that connects the cooler to the heater through HEX 3. Because of the network topology does not have loops, the selection of a given value of the utility consumption allows the evaluation of the heat loads of all HEXs (i.e. it is a minimum structure network, MSTR, a term presented by Chang *et al.* (2020)).

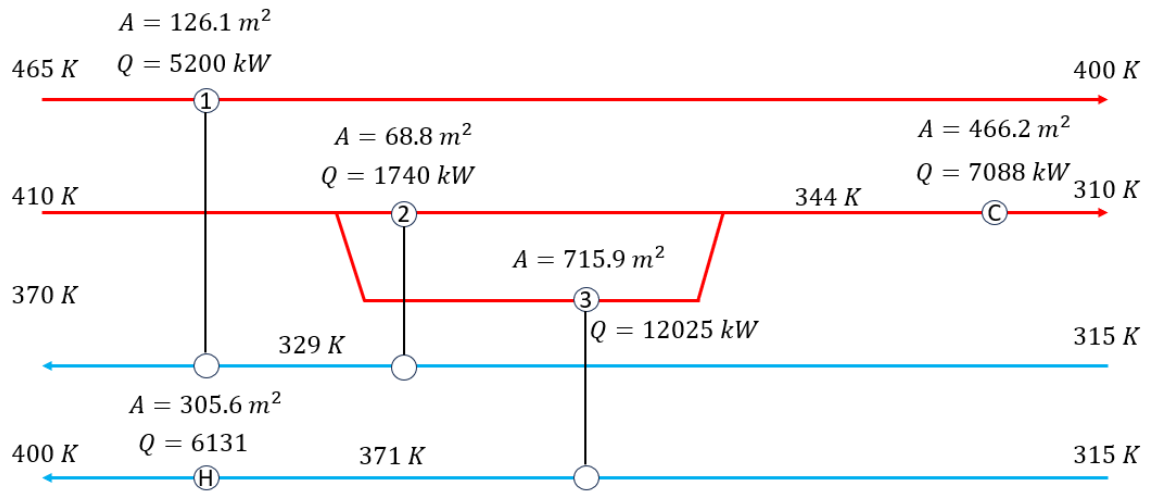
The capital cost evaluation of the additional HEXs is given by:

$$IC = \widehat{FC} + \hat{a}A_{new}^{\hat{b}} \quad (2.2)$$

where \widehat{FC} is a fixed cost, \hat{a} and \hat{b} are cost parameters and A_{new} is the additional area calculated by (the limitations of the use of this simplified relation will be discussed later in this paper):

$$A_{new} = \max\left(0, \frac{Q}{\widehat{U} LMTD} - A_{ex}\right) \quad (2.3)$$

Figure 2.7. Existing HEN A

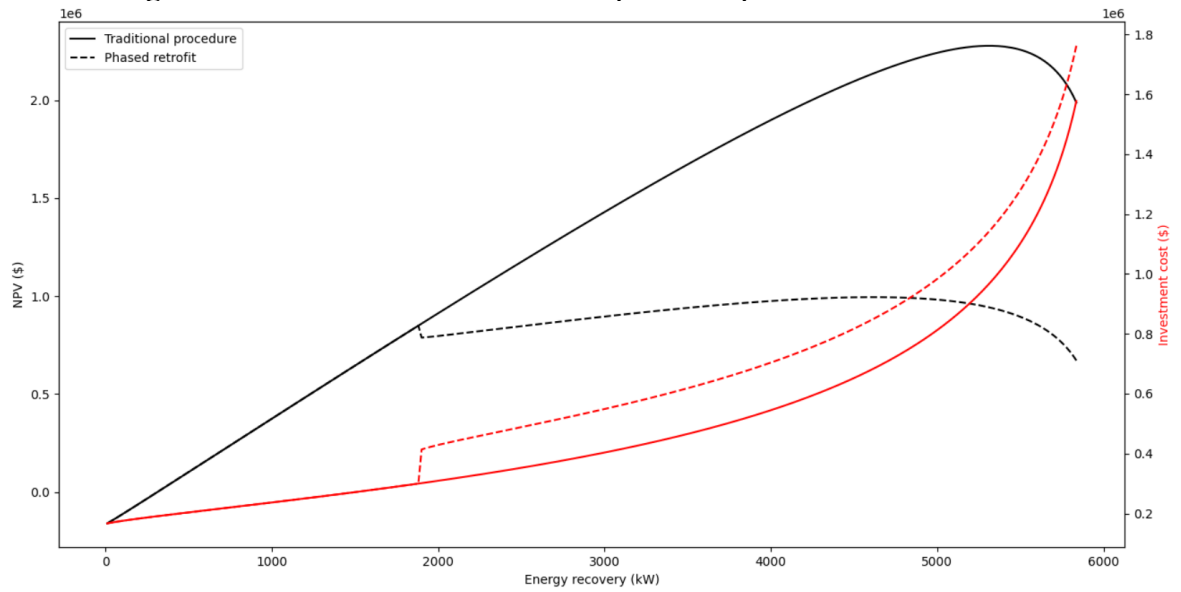


Source: Author's own work, 2024.

The time horizon is 10 years and the discount rate is 9.5%, the available capital at time zero is 300,000 \$, and, after 5 years, a new amount of capital is accessible to make a new investment. Figure 8 below presents the curve of NPV as a function of the energy recovery for the traditional case, i.e. without budget limitations, and the phased retrofit (because the HEN in Figure 2.7 is a MSTR, the construction of the plot in Figure 8 is straightforward).

Figure 2.8 shows that for an energy recovery of 1800 kW, associated with the limited capital cost of 300,000 \$, both curves are equal, because the entire investment can be done at time zero for both cases. However, any increase in the energy recovery requires a higher investment than the available financial limit of the phased project, which means that part of the investment is made after 5 years, causing the modification in the phased retrofit curve and in the investment cost.

Figure 2.8. NPV and Investment cost plot for a phased HEN retrofit



Source: Author's own work, 2024.

The maximum NPV for case without limited resources is 2,278,168 \$ with an energy recovery of 5,340 kW, on the other hand for the second case the maximum NPV is 994,770 \$ with an energy recovery of 4,600 kW. Because the increase in cash flow from new investments in the phased project will be discounted more heavily, since it is postponed due to budget limitations, the optimal solution involves a smaller heat recovery compared to the traditional scenario. Additionally, it should be noted that the capital cost curve is modified due to the presence of an additional shell installed at the beginning of the second period.

The application of the optimal energy recovery considering all the investment at the beginning of the horizon in two steps (i.e. obeying the budget limitations) is associated with an NPV of 891,340 \$, which is 10% smaller than the optimal solution of the phased project. This result indicates that the utilization of the conventional approach to a phased retrofit problem yields a nonoptimal solution.

2.3.3. Portfolio selection problem

It is important to reiterate that, unlike the synthesis problem, the HEN retrofit is classified as a potential investment and should be evaluated using investment analysis concepts. Thus, retrofitting a network represents an investment opportunity aimed at reducing

operational costs in the future. However, it is essential to recognize that, typically, a company's capital is not unlimited, and by investing in network retrofits, the company may forgo other investment opportunities that could potentially yield higher returns. In other words, more broadly, network retrofits fall within the scope of a capital investment portfolio problem and should be addressed in the context of other available investment opportunities.

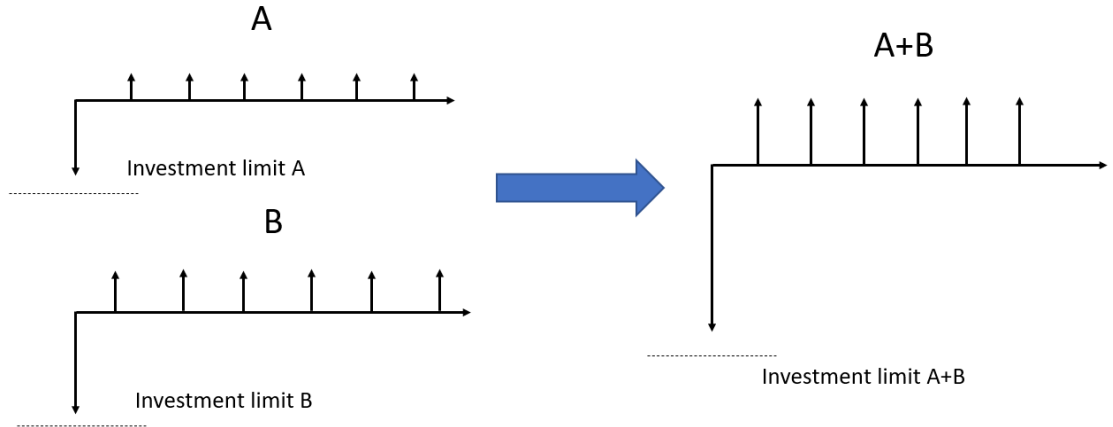
Therefore, the company should seek for the optimal set of projects according to its capital limitations. This set of projects can involve different investment opportunity within the company. For example, a HEN retrofit may compete for budgeting with other projects, such as, the expansion of the production capacity through the debottleneck of an existing plant, the retrofit of the distillation columns of a separation unit, the modification of the reactor internals to decrease the pressure drop, etc.

This analysis can be also explored considering the optimization of multiple HEN retrofit alternatives simultaneously. If the company has multiple plants, the problem can be formulated as the identification of the optimal set of interventions in the different HENs to attain the highest NPV of the investment, constrained by the budget limitation.

To illustrate this problem, consider a company that operates two independent plants, A and B, each one associated with a HEN network that can be retrofitted. This problem can be explored considering excluding alternatives, i.e. by choosing to retrofit network A, the company forgo investing in network B, which could potentially be more profitable, and vice versa. In this case, the solution procedure to this problem would be to retrofit networks A and B independently and select the one that is associated with the higher NPV.

However, larger economic gains may be attained considering the optimal selection of a combination of simultaneous interventions in both networks, i.e. the available budget can be distributed between the two alternatives simultaneously. The cash flow of this problem is illustrated in Figure 2.9.

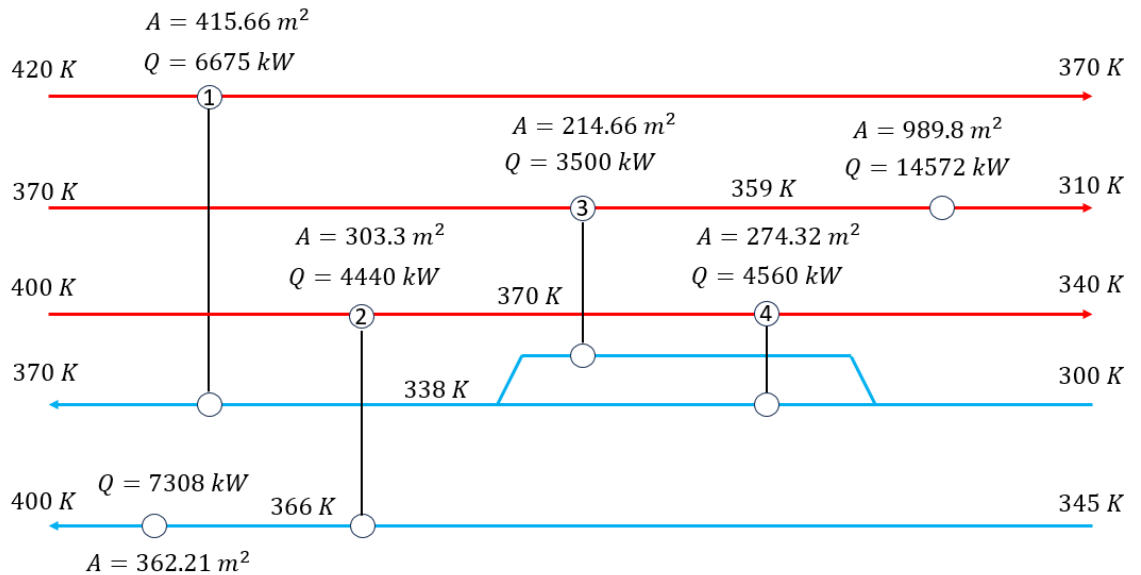
Figure 2.9. Cash flow representation of multiple HEN retrofit.



Source: Author's own work, 2024.

The networks A and B of this example are shown in Figure 2.7 and Figure 2.10, respectively. The same assumptions presented in the previous retrofit example are adopted here. The total budget available is \$ 1,500,000,

Figure 2.10. Existing HEN B

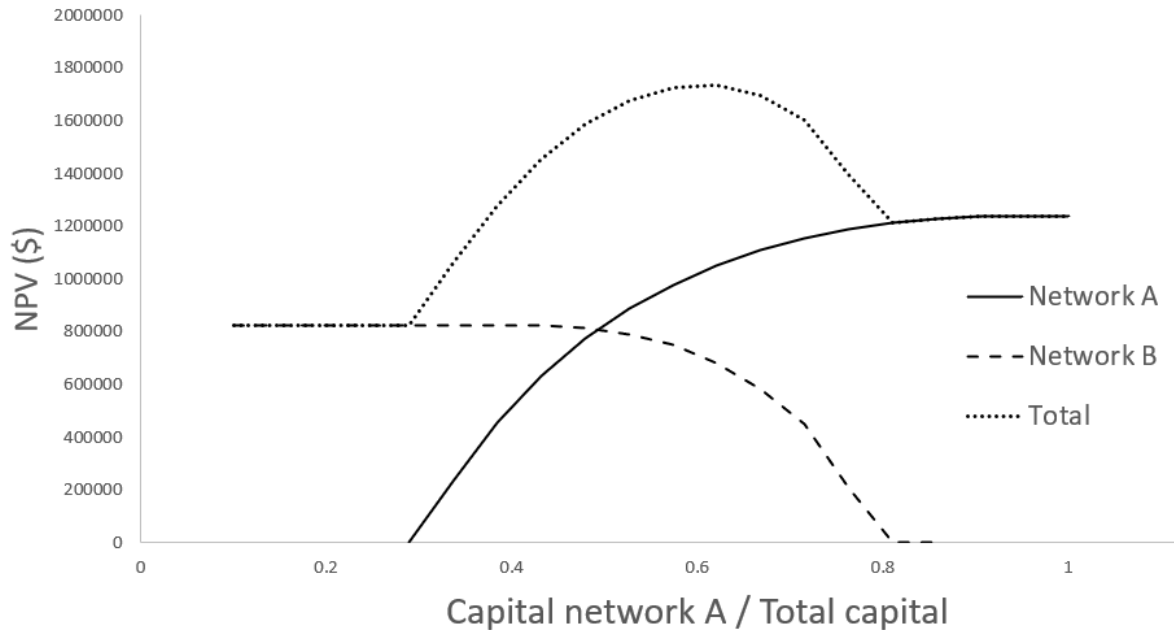


Source: Author's own work, 2024.

Figure 2.11 presents the NPV curves of the retrofit of each network as a function of the fraction of the available budget allocated to network A (the rest is employed in network B). Each point on the curve was obtained by optimizing the retrofit of both networks,

constrained by the corresponding available budget (since the focus here is the nature of the problem, the details of the optimization solutions are not presented).

Figure 2.11. NPV plot for multiple HEN retrofit.



Source: Author's own work, 2024.

Values close to the origin of the x-axis in Figure 2.11 means that a small amount of capital is allocated to network A, any heat transfer area expansion is not economic feasible (i.e. it is associated with a negative NPV), therefore the highest NPV is achieved by retrofitting network B only. In the other end of the axis, the inverse behavior is observed. The optimal solution is located at an intermediate distribution of total capital budget between networks A and B.

Figure 2.11 clearly illustrates the importance of considering possible retrofit projects simultaneously. If the retrofit of each HEN is performed isolated and the best one is selected, it would be selected network A, associated with the optimal NPV close to 1,200,000 \$. However, considering simultaneous retrofit of networks A and B, the optimal solution is a NPV close to 1,800,000 \$, a solution with objective function 50% higher than the isolated problem.

2.3.4. Multiple Financial Sources

The discount rate employed in the evaluation of the objective function of HEN retrofit problems in the literature is a fixed parameter. However, this assumption ignores several issues related to the structure of the capital cost of a company. It is common for companies to utilize loans to finance substantial investments, which necessitates repayment of the debt over time, along with associated interest rates.

The capital cost of the financial resources employed in corporate investments depends on the nature of the source. This evaluation can be conducted using the Weighted Average Cost of Capital (WACC) method (Ross *et al.*, 1998):

$$WACC = \frac{D}{(D + E)} r_d (1 - T) + \frac{E}{(D + E)} k_e \quad (2.4)$$

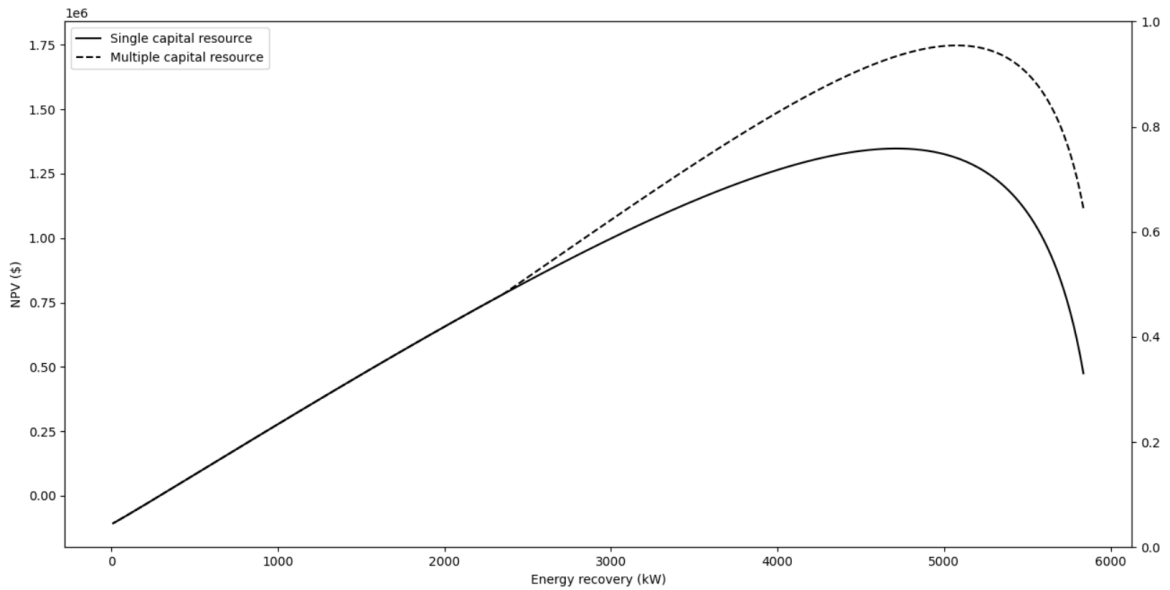
where D and E are the debt and equity amounts employed in the project, r_d and k_e are the corresponding rates of debt and equity and T the corporate tax rate.

Because equity is associated with a higher risk than a debt, the rate associated with an external source is higher than the rate demanded by the stakeholders, i.e. $r_d < k_e$. However, if the debt of a company becomes too high, there is an increase of the financial risk. These financial aspects may be added to the formulation of the retrofit problem, because they can modify the nature of the solution, as illustrated below in a simplified example.

The impact of the presence of multiple source of financial resources can be illustrated using the network depicted in Figure 7. The retrofit of the network was applied using a capital cost rate of 9.5%. However, it is possible to consider a scenario where the government is offering a subsidized loan rate of 3% for additional investments larger than 350,000 \$. The objective is to promote an increase of the energy recovery of the projects, effort that will reduce the carbon footprint. Therefore the interest rate associated to the problem is not a fixed parameter anymore, it becomes part of the problem and the combination of the different financial sources will modify the nature of the solution.

Figure 2.12 presents relation between the NPV and the energy recovery, considering the original problem with a fixed interest rate and the new problem with two financial sources.

Figure 2.12. NPV plot for multiple financial sources.



Source: Author's own work, 2024.

One can observe that the optimal solution is modified. The access of a less expensive financial source yields an increase of the optimal energy recovery, also associated with an increase of the optimal NPV. The subsidized loan corresponds to 68% of the total capital expenditures of the project, i.e. the financial engineering of the project becomes part of the retrofit optimization.

2.3.5. Risk Analysis

As previously discussed, the economic modeling of the HEN retrofit problem is more sophisticated than that of synthesis problems and must align with the full repertoire of investment analysis techniques. A fundamental aspect in this regard is the incorporation of risk analysis into the process.

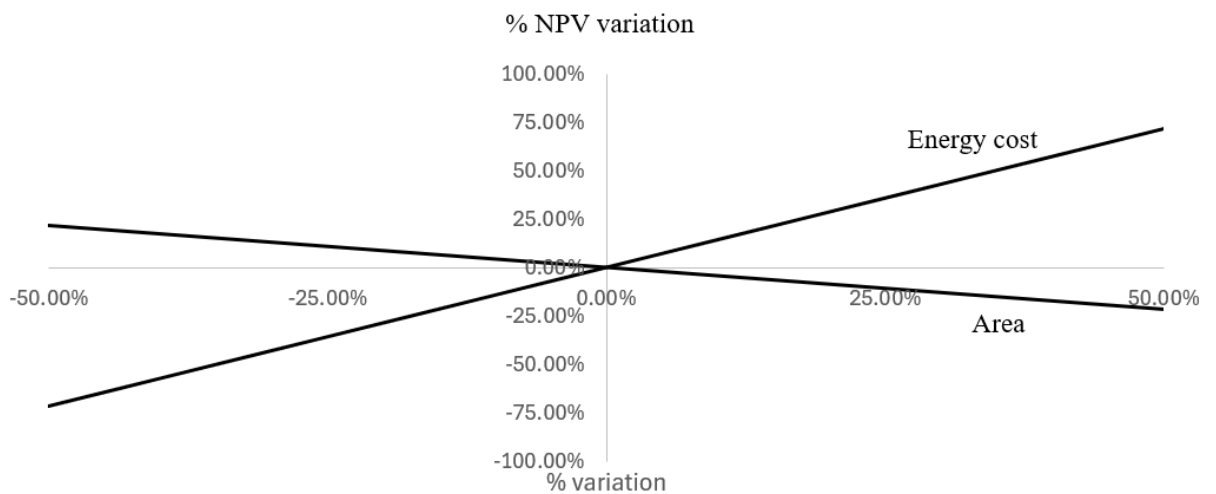
For HEN retrofit projects, various types of risks may arise. These include technical risks, such as inaccuracies in the performance and cost calculations of the equipment, an unexpected fouling behavior, drawbacks associated with the controllability of the retrofitted network, etc. Financial risks are also significant, such as the uncertainty in the energy cost forecasts over time. All cited aspects can reduce the saving money cost compared with the

predicted one in the design stage (i.e. a possible OPEX increase) and/or cause an increase of the investment necessary to acquire the thermal equipment (i.e. a possible CAPEX increase).

Despite the rich literature about optimization with uncertainty developed in the Process Systems Engineering Field, this issue was not sufficiently explored in the context of HEN retrofit.

Aiming at illustrate the importance of a risk analysis, Figure 2.13 presents a Strauss plot (Couper, 2003) related to the conventional retrofit of the HEN described in Figure 2.7.

Figure 2.13. Strauss plot.



Source: Author's own work, 2024.

Figure 2.13 illustrates how the uncertainty in area cost evaluation and energy prices can affect the NPV of the HEN retrofit. Thus, the optimal solution presented in Figure 2.8 is recalculated by varying the area cost and energy prices, generating Figure 2.13.

It illustrates that variations in energy costs can significantly impact the economic performance of a retrofit project. Energy costs are particularly prone to uncertainty due to their high temporal volatility, driven by political crises, inflation, potential wars, and global disruptions such as pandemics. Boldyryev *et al.* (2022) presented a historical distribution of crude oil prices from 1861 to 2020, demonstrating that oil prices can drop by as much as 65% in less than four years. Such a decline would correspond to a sharp reduction in the NPV associated with the retrofit, as evidenced by the analysis of Figure 2.13.

2.4. Design of Heat Exchangers in Retrofit Problems

The HEN retrofit problem involves the need to increase the heat load of some heat exchangers (and also to decrease the heat load in other ones, due to the interconnected structure of the network). Thus, to adapt the existing HEX to the new service, it is necessary to carry out some form of modification in the thermal equipment to enable it to handle the desired new service. These interventions are called here a HEX retrofit.

The vast majority of works in the literature employs retrofit algorithms based on a known and constant value of the overall heat transfer coefficient associated with the existing heat transfer area and with the extra heat transfer area added during the retrofit.

Considering the actual behavior of a HEN, this assumption presents several limitations:

(1) The overall heat transfer coefficient in the existing HEX changes due to, for example, the variation of the flow rate in splits, or some type of topological modification that changes the stream condition (or modify the match at all, like repiping).

(2) The extra heat transfer area added to the network corresponds to a new equipment that must be designed, which may have dimensions different than the original one. These differences may be associated with distinct values of convective heat transfer coefficients and pressure drop.

(3) The extra area added to the network may be organized with different arrangements in relation with the existing units for the hot and cold streams, such as, series-series, series-parallel, parallel-series and parallel-parallel. These different arrangements yield different flow distribution and, consequently, affect the overall heat transfer coefficient.

In fact, the hypothesis adopted in the literature of a unique value of overall heat transfer coefficient (such as in Eq. (2.1)) is only true if the additional area is provided by a HEX identical with the original one, with same geometry and same type, aligned in series with the original unit. However, this is a condition that will seldom occurs.

Despite the limitations mentioned above, the adoption of Eq. (2.1) for the retrofit problem drastically simplifies the problem, but it may hinder the utilization of the retrofit solution in practice and/or it yields nonoptimal solutions.

The limitations of the HEX retrofit in the HEN retrofit problem must be addressed in future papers in order to provide more meaningful retrofit solutions for real problems. This issue has attracted the attention of several authors in the development of solutions for

grassroot HEN synthesis recently (Short *et al.*, 2016; Kazi *et al.*, 2020a; Kazi *et al.*, 2020b; Oliva *et al.*, 2024), but with few exceptions and in a rather limited manner (Wang *et al.*, 2012; Pan *et al.*, 2018), it remains an unexplored field for retrofit problems.

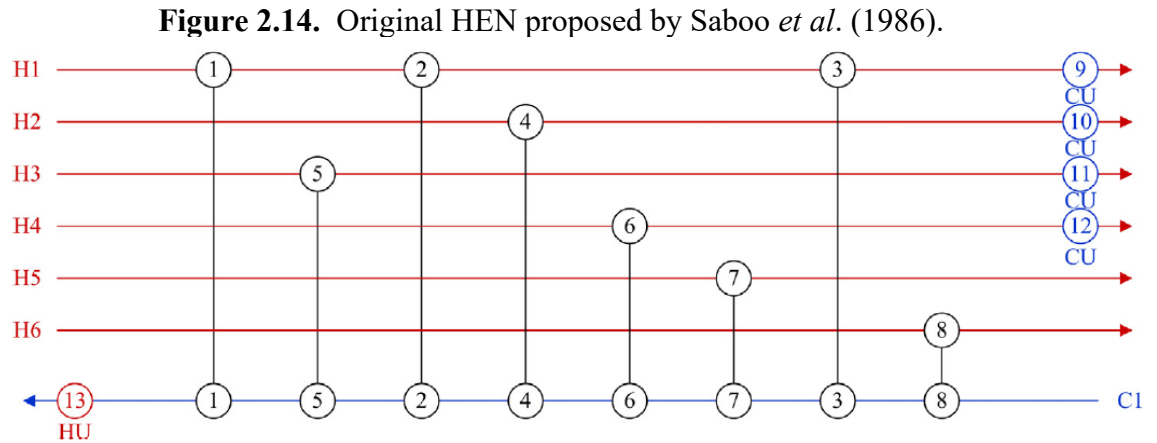
The HEX retrofit of a single unit is a complex problem itself, since there are numerous alternative ways to increase the capacity of an existing heat exchanger. In reality, increasing the capacity of existing HEXs involves a trade-off between the investment and the additional operational costs associated with increased pressure drop. Therefore, it is crucial to evaluate different approaches to enhance the HEX heat load, which may include intensifying the existing HEX, adding a new unit either in series or in parallel. A fundamental consideration is the possibility of aligning a new HEX with a different geometry or even of a different type—for example, coupling a plate heat exchanger in series or parallel with a shell-and-tube heat exchanger.

It should be noted that the new operating conditions of the existing exchanger may differ significantly from the original design, potentially leading to a substantial increase in temperature cross, a reduction in the LMTD, limited tolerance for pressure drop due to preexisting value in the original HEX, or a higher propensity for fouling caused by altered operating conditions (such as flow velocity or temperature). Conversely, the opposite scenario could also arise. Consequently, assuming the addition of new surface area without accounting for these factors—and presuming the new unit shares the same geometry and type as the existing one—can result in interventions that are suboptimal for the required service.

Failing to adopt a more detailed approach to HEX retrofitting risks drastically underestimating the investment cost required to enhance HEX capacity or, worse, proposing a solution that, when rigorously designed, is revealed to be impractical.

In order to exemplify the importance of considering a more detailed HEX retrofit in the HEN retrofit, let consider the following example explored by different authors (Saboo *et al.*, 1986; Briones and Kokossis, 1999; Ma *et al.*, 2000; Rezaei and Shafiei, 2009; Pan *et al.*, 2013, Isafiade, 2018; and Angsutorn *et al.*, 2021). The original network is presented in Figure 2.14.

Consider the existing HEX 5, its heat load is 2,628.1 kW, the inlet and outlet temperatures of the hot stream are 273.0 °C and 258.8°C, the inlet and outlet temperatures of the cold stream are 203.8 °C and 221.6 °C. In addition, the heat capacity flow rates of the hot and cold streams are, respectively, 2400 J/(kg·K) and 2500 J/(kg·K), and their mass flow rate are 76.90 kg/s and 59.16 kg/s (the given data of each stream is the heat capacity flow rate, but using typical values of heat capacity the mass flow rates were estimated).



Source: Author's own work, 2024.

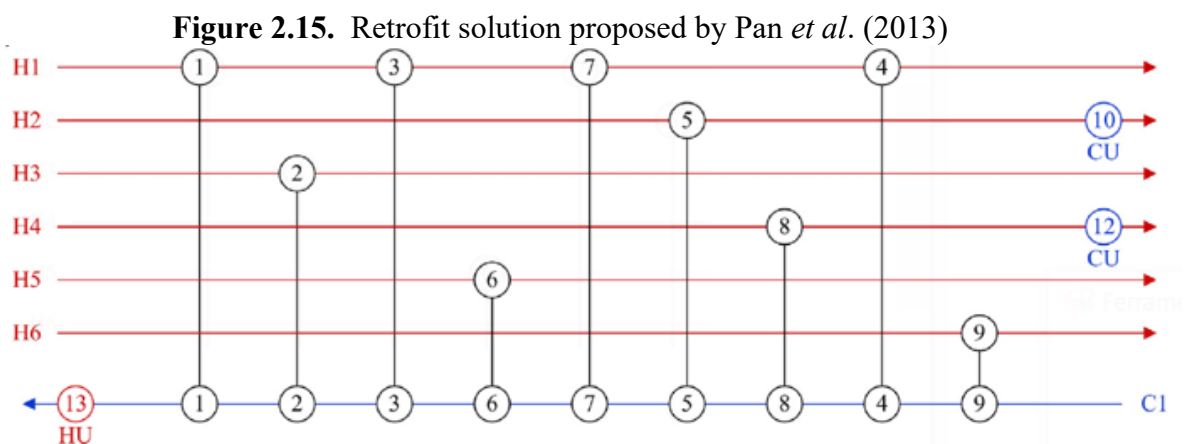
To illustrate the importance of a detailed procedure, the original HEX was designed given the data depicted in Table 2.1, for a shell-and-tube heat exchanger, with the tube-side and shell-side models based on the Dittus-Boelter (Dittus and Boelter, 1930) correlation and the Bell-Delaware method (Serth, 2007), respectively. The resultant design has area and overall heat transfer coefficient very close to the ones used in the paper.

The retrofit solution reported by Pan *et al.* (2013) is presented in Figure 2.15. The retrofit solution proposes to repipe HEX 5 to consider the match between stream H2 and C1. The new design service, associated with the HEX presented in Table 2.1, are associated with a hot stream with inlet, outlet temperatures and mass flow rate of 299 °C, 125.55 °C and 10.19 kg/s. In turn, the cold stream inlet and outlet temperatures are 111.53 °C and 136.6 °C (the mass flow rate is the same).

Table 2.1. HEX 5 details.

Variable	Value
Shell diameter (m)	1.2192
Tube diameter (m)	0.0508
Number of tube passes	6
Pitch ratio	1.25
Layout	Triangular
Tube length (m)	4.8768
Number of baffles	16
Baffle cut (%)	25
Number of tubes	233
Number of shells	1
Fluid allocation	Hot stream in tube
Heat transfer area (m ²)	137.2
Overall heat transfer coefficient (W/m ² K)	268.0
Tube side convective heat transfer coefficient (W/m ² K)	1493.8
Shell side convective heat transfer coefficient (W/m ² K)	520.89
Tube side velocity (m/s)	1.34
Shell side velocity (m/s)	1.01

Source: Author's own work, 2024.



Source: Author's own work, 2024.

Using Eq. (2.1) to calculate the required heat exchanger area, a value of 231.4 m² is obtained, which is associated with an additional area of 44.9 m². Note, however, that the flow

rate of the hot stream decreased drastically, as the solution involves replacing stream H3 with stream H2. In this new arrangement, because the same HEX geometry is used for a smaller mass flow rate, the overall heat transfer coefficient decreases from $264 \text{ W/m}^2\text{C}$ to $140.7 \text{ W/m}^2\text{C}$. Consequently, the required area was drastically underestimated, actually amounting to 435.5 m^2 . This analysis indicates that this proposed retrofit solution will fail, because the heat load of this heat exchanger in the new condition will be considerably lower due to the reduction of the overall heat transfer coefficient.

Another issue of the proposed solution is the stream velocity in the tube side, which reduces from 1.34 m/s to 0.17 m/s , significantly smaller than the recommended value for tube side flow, which is 1 m/s (Smith, 2005). Therefore, this new operational condition may lead to severe fouling problems.

Whenever there is a topological change in the HEN involving repiping, there will be an alteration in the flow velocity within the HEX. In some cases, this change may not result in significant impacts; however, in certain situations, as presented here, it can be highly relevant. Flow rate alteration can also occur when network modifications involve flow redistribution in stream splits, which may or may not have the same level of significance.

This example illustrates the limitation of a typical retrofit solution based on Eq. (1), which ignores the design of HEX and behavior of a HEX when submitted to different thermos fluid dynamic conditions.

2.5. Fouling

Another critical topic, often overlooked in the retrofit literature, is the consideration of fouling in network heat exchangers. The deposit accumulation over the time implies an increase of the utility consumption due to the gradual reduction in the HEXs duty, as well as the associated maintenance and cleaning costs. Moreover, fouling also has a hydraulic impact, increasing the pressure drop of the flow throughout the heat exchangers.

The traditional method to consider fouling effects in heat exchanger is using fouling factor as a thermal resistance in the overall heat transfer coefficient. However, this procedure ignores that the fouling resistance depends on the thermofluid-dynamic behavior of the stream, such as the flow velocity and the temperature. Thus, a more realistic procedure would involve the HEX design using fouling models, which are capable of modelling the fouling

behavior as a function of the heat exchanger geometry and streams conditions (Lemos *et al.*, 2022). The literature has several fouling models that can be used for this purpose (Panchal *et al.*, 1997).

Another aspect to be considered is the dynamic nature of fouling. A fouling factor aims to express the fouling resistance at a terminal condition or, at least, the corresponding fouling resistance at end of the operational run (i.e. considering the period between cleanings).

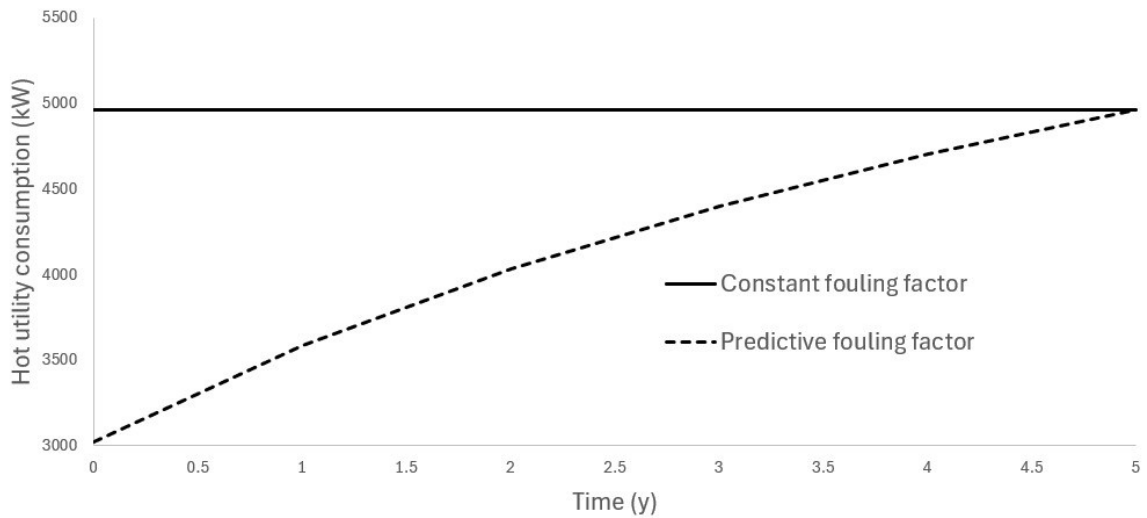
A simplified example below shows how the usual approach to represent the fouling behavior affects the retrofit solution. Let consider a HEX predicted by a retrofit solution to increase the network energy recovery. The cold stream leaves this energy integration heat exchanger and flows towards a heater. The heat load recovered in this heat exchanger decreases the hot utility consumption.

The HEX has an area of 150 m^2 , the clean overall heat transfer coefficient is $400 \text{ W}/(\text{m}^2\text{C})$, the fouling factor is $0.0025 \text{ m}^2\text{C}/\text{W}$ and, consequently, the overall heat transfer coefficient at the dirty condition employed in the design is $200 \text{ W}/(\text{m}^2\text{C})$.

Figure 16 shows the hot utility consumption in the heater downstream HEX in the period between cleanings according to the net present value employed in the evaluation of the objective function in the retrofit problem, i.e. a constant energy recovery during the entire period (see Figure 2.5).

However, let consider that the deposit accumulation in HEX can be modelled as a linear rate with a same fouling resistance at the end of the period between cleanings. Therefore, the HEX starts with a clean heat transfer surface and the deposit layer are gradually increasing. The simulation of the system considering the dynamic behavior yields a considerably lower hot utility consumption, as depicted in Figure 2.16.

Figure 2.16. Utility consumption with constant and predictive fouling factor



Source: Author's own work, 2024.

The solution of the retrofit problem seeks to identify the optimal balance between the investment needed to increase the heat load (CAPEX) and the economic gains associated with the reduction of the utility consumption (OPEX). The differences in the profiles present in Figure 2.16 show that the usual representation of the energy recovery using a constant fouling resistance implies an underestimation of the energy recovery along the operational period. In addition, each HEX in the HEN has a different fouling dynamic. This inaccuracy to evaluate the actual energy recovery compromises the accuracy of the retrofit optimization.

Appropriately accounting for fouling in HEX during HEN retrofits yields a more realistic model, one capable of predicting increased utility consumption over exchanger cleaning cycles as well as anticipating the reduction in heat recovery due to fouling over time. Additionally, another effect of comparable importance is the potential to modify the existing network to accommodate a new topology or heat distribution that mitigates fouling in critical exchangers, especially given the known fouling levels within the existing network.

Consider an existing HEX subjected to substantial fouling. The mitigation of fouling in this HEX can be accommodated in the retrofit problem in several ways, including: (i) intensifying the exchanger to reduce fouling, (ii) determining the feasibility of the installation of a parallel unit to maintain flow velocity, (iii) repositioning the exchanger to a cooler area of the network, swapping it with a less fouled exchanger, (iv) reducing its duty to mitigate network effects from fouling growth, (v) increasing flow rate if the stream exhibits splitting, or (vi) even replacing it with a new exchanger designed with geometry to minimize fouling.

Furthermore, more precise fouling consideration can also inform heat distribution adjustments using energy loops to reduce temperatures in streams susceptible to severe fouling, as well as support accurate design of new matches and units within the network. In sum, it is evident that neglecting proper fouling formation considerations in HEN retrofits can result in considerable discrepancies between the designed and operational networks.

2.6. Layout

Another highly relevant aspect is the layout of the existing plant. Retrofitting an existing HEN must account for the pre-established arrangement of equipment, as well as the physical space available for potential modifications. The current equipment distribution in the plant can clearly impact decisions regarding HEN modifications. For instance, the available space for adding area to an existing HEX may limit the size of the new unit, requiring structural support installations, additional labor for rearranging equipment, or even block the installation of a new exchanger or modification of an existing one at all.

Regarding structural changes to the network, any modification involves additional work of installation of new piping and accessories, as well as the rearrangement of existing HEX units or the installation of new matches. Such tasks require a coordinated effort across several disciplines, such as process engineering, mechanical, civil, layout, safety, and more. Given that the physical layout and space available for an existing HEN are already defined, adding a new match or modifying an existing one may be restricted by space limitations or necessitate new piping, which could be impractical or excessively costly due to increased length and/or pressure drop.

Additionally, an important consideration related to plant layout is safety. For example, suppose that, due to physical and layout constraints, it becomes necessary to route a toxic and/or flammable gas through an initially unclassified area. Such a change would demand a thorough risk assessment to determine the feasibility and necessary protective interventions, potentially driving up implementation costs (e.g. interlock systems) or even rendering the modification unfeasible.

Another key factor tied to layout constraints is the hydraulic components needed for the flow of each stream. Clearly, the cost per unit length for piping and accessories, such as control valves, can vary significantly. For example, transporting a high-flow-rate gas requires

a larger pipe diameter, handling a high-pressure stream demands thicker pipe walls, etc. If handling corrosive components such as sulfur, special materials may be needed, which considerably increases costs. In contrast, transporting a low-pressure, non-hazardous liquid is far less expensive. Therefore, if the layout requires extended piping for certain streams, the proposed modification may be ruled out in practice.

In sum, even if a given modification holds considerable potential for energy recovery, a variety of layout-related factors can impose limitations, require costly interventions, or add complexity to the labor involved, potentially making the modification impractical. This underscores the substantial impact of layout on HEN retrofitting, which has never been considered in any paper in literature.

2.7. Pressure Drop

Considering pressure drop in HEN retrofits is not new and has been included in some studies in the literature, especially those that investigated the use of intensification devices, due to their significant pressure drop penalties (Soltani and Shafiei, 2011; Pan *et al.*, 2013; Pan *et al.*, 2016; Akpomiemie and Smith, 2017). In these studies, pressure drop was addressed by imposing a maximum allowable pressure drop for each stream, which, although it is an advancement, still does not capture the full nuances of the issue. Simply setting a maximum pressure drop for each stream assumes that (i) the target pressure of the stream must be strictly maintained, which is not necessarily true, and (ii) there is no compression or pumping equipment available to compensate for the increased pressure drop.

While assumption (ii) may hold in some cases, many systems already include a compressor or pump, or provision can be made for installing one, particularly in cases of liquid transport, which can often be achieved with low-cost booster pumps that are easy to install and operate.

To be considered more accurately, pressure drop should be formulated in the problem similarly to utility operational costs. The operational cost of pressure drop in the retrofitted network should account for the deviation from the network original condition, as the utility consumption.

For streams where allowable pressure drop is strictly necessary, constraints should be applied in the model. However, for those where strict adherence is not necessary or where additional mechanical power supply is feasible, as discussed, the pressure drop can be relaxed, and costs may include in the model based on the investment needed for increased power and/or enhanced capacity of existing equipment or the purchase of new units.

It should be noted that detailed heat exchanger retrofits can be highly influenced by pressure drop considerations. Suppose, for example, additional shells are needed in series with the existing ones, or flow rates increase in the existing exchanger due to split redistributions, changes in the network stream framework, or even topological modifications like repiping. In such cases, pressure drop can dominate the problem (even for HEX that do now demands increase in the heat transfer), and adding area by installing a new HEX in parallel with the existing one could be an advantageous solution, potentially even reducing the operational pressure drop cost for the HEX.

In sum, despite being addressed in some studies, the pressure drop issue is significantly simplified. Merely setting a maximum pressure drop for each stream may not only unnecessarily constrain promising network modifications, but may also apply to only a limited number of situations, without fully encompassing all relevant aspects. Considering the detailed problem can significantly differ the retrofit solution.

2.8. Challenges of considering these advancements

The challenges inherent in the HEN retrofit problem are widely recognized (Yee and Grossman, 1991; Ma *et al.*, 2000; Wang *et al.*, 2012.; Pan *et al.*, 2013; Akpomiemie and Smith, 2017; Pan *et al.*, 2018), characterized by numerous nonlinearities, non-convexities, and the high-dimensional nature resulted from the multitude of potential interventions in the existing network. These factors lead to significant numerical convergence issues, a high probability of local optima (if a local solver is used) with no means to assess solution quality, dependency on proper initialization of variables, and difficulty in applying these methods to industrial-scale problems—particularly when topological modifications are included in the formulation. It is no surprise, as demonstrated in this thesis, that various simplifications are often necessary to achieve even a feasible solution.

Despite the well-established challenges, it is critical to highlight the discrepancy between academic solutions and industrial needs. After 36 years since one of the first seminal works on HEN retrofit (Tjoe and Linnhoff, 1986), a large number of studies has been published, yet nearly all have aimed to address the same fundamental problem, with minimal progress towards meeting the actual requirements of industry. These studies have consistently revolved around the central challenge of developing a robust, systematic procedure capable of delivering reasonable and practical solutions.

A key issue highlighted in this thesis is the overly simplified modeling of the HEX in the HEN retrofit formulation. As shown, such simplifications can result in significantly underestimated investment and operational costs, as they fail to incorporate detailed calculations and overlook various HEX intervention alternatives. In some instances, they even propose solutions that are not feasible in practice. It is important to emphasize that, although this discussion has been a central aspect of this thesis and supported by a practical example, other authors have also recognized and addressed these issues in some manner (Wang *et al.*, 2012; Pan *et al.*, 2018).

Thus, it is essential to include in the HEN retrofit problem HEX retrofit methodologies able to explore various capacity-increasing options, including different types of exchangers and configurations, with HEX of differing geometries. This approach enables the identification of solutions best suited to the new operating conditions, effectively balancing investment and operational costs. However, achieving this requires abandoning the use of constant heat transfer coefficients and incorporating thermofluid dynamic modeling of the HEX into the formulation. It is worth noting that HEX design variables are typically discrete due to how these units are commercially available.

Incorporating these complexities into the formulation would inevitably introduce additional nonlinearities arising from transport coefficient models. For example, even in the context of grassroot design problems for a single HEX, traditional approaches such as mathematical programming and metaheuristics already exhibit challenges related to convergence, significant computational effort, and premature convergence to local optima, as documented in the literature (Lemos *et al.*, 2020; Nahes *et al.*, 2021; Sales *et al.*, 2021).

Consequently, if the existing simplified approaches already struggle with the inherent difficulties of the problem, the very notion of attempting to incorporate the critical factors emphasized in this thesis—despite their undeniable importance—makes it evident that there is a considerable space for new advances.

2.9. Conclusions

This chapter discussed several fundamental aspects of the HEN retrofit problem from the perspective of industrial practice, aiming to highlight the significant gap between the solutions proposed in the academic literature and their practical implementation challenges. To achieve this, we examine the problem in the light of the need of the chemical process industry, encompassing the analysis of different cash flow alternatives, the need to include the thermal equipment design in the retrofit problem, and other issues that have a direct impact in the HEN retrofit (fouling, layout and pressure drop).

To support the discussion, we have created simple examples to illustrate how the solutions may differ when the aspects discussed in this chapter are taken into account. Additionally, we highlight some of the challenges associated with implementing solutions currently proposed in the literature.

It is important to note that this chapter does not present any comprehensive HEN retrofit procedure. Instead, it underscores the importance of incorporating industrial practice considerations and serves as a call to action for future research to address these critical gaps in the field.

ACRONYMS AND ABBREVIATIONS

HEN – Heat exchanger network

HEX – Heat exchanger

IRR – Internal rate of return

LMTD – Logarithmic mean temperature difference

LP – Linear programming

MILP – Mixed integer linear programming

MINLP – Mixed inter nonlinear programming

MSTR – Minimal structure

NPV – Net present value

GPHE – Gasketed plate heat exchanger

STHE – Shell and tube heat exchanger

NOMENCLATURE

\hat{a}	Area cost parameter (\$/m ²)
A	Heat transfer area (m ²)
A_{ex}	Existing heat transfer area (m ²)
A_{new}	Additional heat transfer area (m ²)
\hat{b}	Area cost parameter
\widehat{CF}	Fixed cost (\$)
D	Value of the debt
E	Value of the equity
F	Correction factor
IC	Investment cost (\$)
Q	Heat load (W)
r_e	Debt cost
r_e	Risk adjusted rate of return on equity
r_f	Risk-free rate
T	Corporate tax rate
U	Overall heat transfer coefficient (W/m ² K)
$WACC$	Weighted average cost of capital
β	Beta coefficient

3 A NOVEL PROCEDURE FOR HEAT EXCHANGER RETROFIT CONSIDERING MULTIPLE INTERVENTION ALTERNATIVES

3.1 Introduction

Heat exchanger (HEX) retrofitting involves modifying an existing unit to adapt it to a new operational service (Smith, 2005). This new service may require either an increase or a decrease in the unit heat load. The need to adapt an existing HEX for a new duty is a common occurrence in industrial practice.

This task is typically applied in the retrofitting of Heat Exchanger Networks (HEN), where the increase of heat recovery demands the redistribution of the heat transfer tasks across the network, changing the temperature profiles of the process streams in each HEX, and eventually altering the streams of a given HEX. Another scenario involves repurposing an unused HEX stored in the plant warehouse for a specific new duty, thus reducing the need to purchase a new unit to complete the retrofit.

Despite its significant practical relevance, the HEX retrofitting problem has long been approached with oversimplifications and underestimations. To our knowledge, no study in the literature fully addresses the nuances, complexities, and intricacies involved in retrofitting a single HEX. Instead, the topic typically appears as a secondary consideration in works focused on HEN retrofitting.

Broadly, HEX retrofitting has been tackled in two main ways. The first and most prevalent approach in the literature involves increasing a HEX heat load by adding additional heat transfer area (Ciric and Floudas, 1989; Ciric and Floudas, 1990; Yee and Grossmann, 1991; Briones and Kokossis, 1999; Ma *et al.*, 2000; Soršak and Kravanja, 2004; Ponce-Ortega *et al.*, 2008; Nguyen *et al.*, 2010; Pan *et al.*, 2013a; Biyanto *et al.*, 2016; Stampfli *et al.*, 2022). Conceptually, this would be achieved by aligning a new HEX in series with the existing unit. The required additional area is simple calculated by:

$$A_{new} = \max\left(\frac{Q}{U LMTD} - A_{ex}; 0\right) \quad (3.1)$$

where A_{new} is the additional area, Q is the heat load, U is the overall heat transfer coefficient, $LMTD$ is the logarithmic mean temperature difference, and A_{ex} is the area of the existing exchanger. However, this equation involves several simplifications:

- (i) The calculation makes no reference to the geometry of the existing HEX.
- (ii) The correction factor, F , is not included, potentially leading to significant underestimation of A_{new} . Furthermore, it overlooks the possibility of requiring multiple shells in series due to temperature cross limitations—a common phenomenon in HEN problems.
- (iii) A single overall heat transfer coefficient is assumed for both the existing and the new HEX, disregarding potential differences in the design between the existing and the new heat exchanger.
- (iv) The equation ignores the critical trade-off between capital investment and operational costs, as pressure drop effects are not considered.
- (v) It fails to account for operational requirements such as, recommended flow velocity ranges, which are vital to preventing fouling, vibration, or erosion in the HEX.

Recently, a second approach has gained traction: the use of intensification devices to enhance the capacity of existing HEXs. The use of intensification devices presents an attractive alternative for increasing the heat load of existing HEX, as they enhance heat transfer without requiring an increase in the heat transfer area. Intensification works typically by boosting convective heat transfer coefficients, thereby increasing the overall heat transfer coefficient. This approach also reduces the propensity for fouling and may be more cost-effective on a per-unit-area basis compared to installing a new HEX.

The application of intensification to increase the heat load of existing HEXs has been investigated in a series of studies, including those by Zhu *et al.* (2000), Wang *et al.* (2012), Pan *et al.* (2012), Pan *et al.* (2013b), Pan *et al.* (2016), and Pan *et al.* (2018). Among these, only Pan *et al.* (2018) incorporated thermofluid-dynamic calculations that accounted for the geometry of the existing HEX, using a model developed through parameter fitting based on the geometry of the existing heat exchangers.

While intensification is an appealing option, it does not address all challenges associated with HEX retrofitting and has notable limitations. Key disadvantages include that intensification often leads to a steep rise in pressure drop, cannot overcome temperature cross constraints, is highly dependent on the dominant thermal resistance being on the intensified side of the exchanger, and can only be applied in certain systems due to the mechanical features of the existing HEX.

In addition, an overlooked but critical challenge is the labor-intensive process of installing intensification devices in an existing HEX. For the cases of tube insert in shell-and-tube heat exchangers, its implementation requires only the head removal to the devices installation and can be easily used. However, the mechanical and civil work for the installation of all other devices is much higher, requiring a retubing procedure (e.g changing segmental baffles to helical ones or changing the number of baffles), or changing the tube bundle at all (e.g using finned tubes). As far as we know, the industry is not so inclined to make this type of complex interventions that may imply in future operational problems to save a few thousands of dollars.

Another critical aspect of HEX retrofit is the necessity to reduce the heat load of an existing unit. This task is especially common in HEN retrofits when increasing the heat duty of one HEX often requires a corresponding reduction in another to balance the network energy flows. To our knowledge, no detailed methodology addressing this issue exists in the literature. The only mention is a brief note in Pan *et al.* (2018), suggesting that such reductions can be achieved through either bypassing the existing HEX or plugging some of its tubes.

Both techniques are indeed effective in reducing the heat transfer capacity, but they come with significant operational implications. For example, both methods alter the flow velocity on the tube side, potentially leading to undesired side effects.

The underestimation of the complexities in HEX retrofitting within the literature is evident. This chapter seeks to address these shortcomings by discussing the problem in depth and presenting a more comprehensive framework that accommodates various intervention strategies. These strategies include:

- Adding a new HEX in series with the existing unit.
- Adding a new HEX in parallel with the existing unit.
- Replacing the existing HEX entirely by a new unit.
- Intensifying the existing HEX.

For the first three options, the newly added or replacing HEX may feature a completely different geometry than the original unit. Consequently, these new configurations would have distinct overall heat transfer coefficients, flow velocities, and pressure drops. The methodology also permits pairing different types of HEXs—such as aligning a gasketed-plate heat exchanger (GPHE) in series with a shell-and-tube heat exchanger (STHE).

This expanded scope is crucial for exploring a broad range of scenarios and responses to the unique demands of the new service conditions imposed on the HEX. By accommodating such diversity, the proposed approach allows to identify the most suitable interventions, by ensuring an appropriate balance between capital expenditure and operational costs, particularly concerning pressure drops.

Given the diverse configurations and interventions, assuming a known and constant overall heat transfer coefficient is not viable. Instead, the overall heat transfer coefficient is rigorously calculated within the proposed approach, using established models in the literature. Furthermore, the equipment design formulation incorporates its representation by a set of independent variables, associated with their geometry, and all key constraints, including geometric limitations, flow velocity thresholds, minimum correction factors, required heat transfer area, and other operational considerations.

A more detailed discussion about heat transfer reduction is also performed in this paper. By considering these elements, this study aims to provide a more comprehensive and practical solution to HEX retrofitting, advancing beyond the current limitations and enabling industrial practitioners to address the multifaceted challenges of HEX adaptation with greater accuracy and reliability.

Finally, it is important to mention that the retrofit solutions are obtained using a proposed optimization algorithm that is robust, without convergence problems, and that always attain the global optimum. The optimization procedure does not involve human intervention, even for tuning algorithmic control parameters.

The rest of the paper is organized as follows. Firstly, HEX retrofit problem is presented, followed by the analysis of the interventions for heat transfer rate increase and, then, heat transfer rate reduction. The application of the proposed methodologies is shown in the result section. Finally, conclusions are presented.

3.2 Problem Statement

Let an existing HEX subject to new operational conditions, different from the original task (e.g. different temperatures, mass flow rates, physical properties or different streams). This chapter focuses on identifying the necessary modifications in the existing HEX to adapt it to the new thermal service. First, it is necessary to determine whether there is a need to

increase or reduce the thermal load of the existing exchanger. This can be done by calculating the ratio between the effective area of the existing HEX (A_{ex}) and the required area (A_{req}):

$$A_r = \frac{A_{ex}}{A_{req}} \quad (3.2)$$

The effective area depends on the type of the existing HEX, which is given by the following equations for a STHE and GPHE, respectively (this paper will focus on these types of heat exchangers, but the proposed is flexible and can be applied for any other equipment type):

$$A_{existing}^{STHE} = NTT \pi Dte L Ns \quad (3.3)$$

$$A_{existing}^{PHE} = (Np - 2) \phi L_w L_p \quad (3.4)$$

where NTT is the total number of tubes, Dte is the outer tube diameter, L is the tube length, Ns is the number of shells, Np the total number of plates, ϕ the enlargement factor, L_w the effective plate width and L_p the effective plate length. The required area is given by:

$$A_{req} = \frac{Q}{U LMTD F} \quad (3.5)$$

where Q and $LMTD$ are the targeted heat load and logarithmic mean temperature difference, and F is the correction factor of the LMTD, all evaluated according to the new thermal task and using the geometry of the existing HEX.

If A_r is higher than $(1 + \widehat{A_{exc\%}}/100)$, where $\widehat{A_{exc\%}}$ is the “excess area”, a design margin added by the designer, it indicates that the heat transfer rate of the existing HEX in the new conditions are larger than the process need and a procedure for reducing heat load may be necessary. In turn, values of A_r smaller than $(1 + \widehat{A_{exc\%}}/100)$ indicates that the existing HEX cannot fulfill the required heat transfer rate, and a procedure for increasing heat load is necessary.

As described before, there are different ways to increase the heat load, based on area addition (inclusion of a new unit in series or parallel with the existing one) or intensifying the existing HEX. The procedures for increasing heat load are discussed in Section 3. The reduction of the heat load in existing HEX, such as using a stream by-pass or plugging tubes, is described in Section 3.4.

3.3 HEX Retrofit - Heat Load Increase

If $A_r < 1$ it indicates that the existing HEX cannot attend the new service, and an intervention is required to increase its heat load. As previously mentioned, there are two different ways to increase the heat load. The first one is supplying the increase in heat load by adding heat transfer area, which can be accomplished by adding a new unit in series or in parallel with the existing one. In addition, the new unit can have a different geometry compared with the existing one or can be of another HEX type at all (e.g. if the existing HEX is a STHE, a new GPHE can be installed in series or parallel).

Because parallel arrangement reduces the flow rate in the existing HEX, its overall heat transfer coefficient also reduces. As a result, the heat transfer rate in the existing HEX decreases and this effect must be included in the analysis of the system. Therefore, the parallel arrangement tends to demand a larger extra heat transfer area. However, the flow rate reduction in the parallel arrangement has the benefit to reduce the pressure drop, which may be a better option if the pumping/compression power is considered in the objective function (i.e. total annualized cost, TAC). Additionally, the pressure drop in the existing and new heat exchangers can be optimized by manipulating the flow rate split of the streams. Therefore, if the pressure drop have an important role in the retrofit, parallel alignment can be an interesting alternative (or the only one in some cases).

The insertion of a new HEX in series does not affect the overall heat transfer coefficient of the existing unit (excluding effects related to the change of the physical properties with the temperature), but it introduces a higher pressure drop. Considering the reduction of the extra area added to the network, the series arrangement is a better option, but it may be infeasible due to the hydraulic limitations. Because the costs of pumping/compression may be considerable, the series arrangement may be more expensive if the objective function is the TAC.

A different alternative to increase the heat transfer is the installation of intensification devices in the existing HEX, two techniques are explored here: twisted-tape and coiled-wire intensification techniques for retrofit purposes.

A crucial aspect that must be emphasized is the possibility of including a new HEX aligned with the existing one, or even replacing it entirely, with a geometry different from the original one. This issue is fundamental because the geometry of a heat exchanger significantly influences its thermofluid dynamic behavior, as well as its capital cost. Furthermore, the new

service may involve design specifications that differ substantially from those for which the existing HEX was originally designed.

Since the characteristics of the new unit to be added depend heavily on both the geometry of the existing HEX and the requirements of the new service, incorporating this design refinement introduces a level of detail and accuracy never previously explored in the literature. This approach enables a more accurate assessment of the overall heat transfer coefficient, pressure drop, and capital cost, thereby allowing the design of a new exchanger adequate to fulfill the retrofit task.

To achieve this level of detail and accuracy, it is essential not only to rigorously evaluate the performance of the existing HEX under the new conditions, but also to employ an optimization procedure for the new HEX that accounts for all of these considerations. Thus, as explained later in this section, the problem of designing a new HEX (grassroot) is embedded in the HEX retrofit procedure.

Indeed, in the next subsection is shown that the proposal procedure consist of, given a modification in the existing HEX, the heat transfer rate in the existing HEX is evaluated, and the difference between the target heat load, \hat{Q}_{req} , and the heat transfer rate in the existing HEX, Q_{ex} , is the heat load that must be provided by the new unit. Thus, the new unit can be designed using a procedure for grassroot design problems.

Thus, we first present in Subsection 3.3.1 a briefly description of the procedure for grassroot design problem, in Subsection 3.3.2 the procedure for HEX retrofit by area addition in series, in Subsection 3.3.3 the addition of area in parallel and in Subsection 3.4 the intensification strategy. Configurations of type series-parallel are not so common and will be not explored in this paper. Additionally, the physical properties are assumed constant, evaluated at a proper temperature reference (Incropera and Dewitt, 2007).

3.3.1. Design problem and optimization of a new unit

The grassroot design problem consists of, given a hot and a cold streams, identifying a new unit that satisfies the thermal task, represented by a set of constraints, minimizing an objective function, typically minimizing area or TAC. Since this paper considers the addition of a new STHE and GPHE, the problem formulation of each type of HEX is presented below.

For a STHE, the basic geometric variables employed to characterize a shell-and-tube heat exchanger in the optimization are: outer tube diameters (d_{te}), shell diameter (D_s), tube

length (L), number of baffles (Nb), number of tube passes (Ntp), tube pitch ratio (rp), and tube layout (lay). The tube thickness and the baffle cut are considered constant and the number of shell passes is assumed equal to 1, i.e. an E-type shell (TEMA, 1999). Due to the commercial availability and/or physical nature of the design variables, their values must be selected among a set of discrete options.

The design constraints of the problem encompass the ratio between the tube length and shell diameter, which must obey the following bounds (Taborek, 2008a):

$$3 D_s \leq L \leq 15 D_s \quad (3.6)$$

Additionally, the baffle spacing must be bounded in relation to the shell diameter (Taborek, 2008b):

$$0.2 D_s \leq lbc \leq 1 D_s \quad (3.7)$$

The area per shell is limited to a maximum value (Smith, 2005):

$$A \leq \hat{A}_{max} \quad (3.8)$$

In this thesis, it is adopted $\hat{A}_{max} = 1000 \text{ m}^2$. In addition, lower and upper bounds on flow velocities in the tube-side and shell-side (vt and vs) are established to avoid fouling and upper bounds are established to avoid vibration and erosion:

$$\widehat{vsmin} \leq vs \leq \widehat{vsmax} \quad (3.9)$$

$$\widehat{vtmin} \leq vt \leq \widehat{vtmax} \quad (3.10)$$

Due to operational issues, the correction factor needs to be higher than a minimum value (Taborek, 2008a):

$$F \geq 0.75 \quad (3.11)$$

The relation between the required heat load (Q) and the required heat transfer area (A_{req}) is based on the *LMTD* method:

$$Q = U A_{req} LMTD F \quad (3.12)$$

Then, the following constraint is added to impose that the STHE area must be higher the required multiplied by a design margin:

$$A \geq \left(1 + \frac{\widehat{A}_{exc}}{100}\right) A_{req} \quad (3.13)$$

where A is evaluated through Eq. (3.3).

For a GPHE, the independent design variables are the total number of plates (Np), plate size (defined by the plate length, Lp , plate width, Lw , and port diameter, Dp), Chevron angle (β), and number of passes of each stream (Nph and Npc , respectively). Similarly to STHE serach space, due to the commercial availability and/or physical nature of the design variables, the values of the design variables must be selected among a set of discrete options. The plate thickness, the surface enlargement factor, and the mean channel spacing are fixed parameters, associated with the plate type and are not included in the optimization.

Bounds on flow velocities of the hot and cold streams through the GPHE channels (vc and vh) are also design constraints:

$$\widehat{vcmin} \leq vc \leq \widehat{vcmax} \quad (3.14)$$

$$\widehat{vhmin} \leq vh \leq \widehat{vhmax} \quad (3.15)$$

Relations between the heat load and the required heat transfer area are also present in the GPHE design problem, represented by the constraints in Eqs. (3.12) and (3.13). The heat transfer area of a GPHE is evaluated through Eq. (3.4).

The objective function of the problem is the total annualized cost (TAC):

$$\min TAC = \hat{r} C_{cap} + (C_{op,h} - C_{op,h}^{ex}) + (C_{op,c} - C_{op,c}^{ex}) \quad (3.16)$$

where $C_{op,h}$ and $C_{op,c}$ are the operational costs of the hot and cold streams, respectively, and C_{op}^{ex} the operational cost of the stream in the original condition. Note that the TAC consider the change of the operational cost caused by the retrofit, not its total value, which is the adequate representation of a retrofit problem. In addition, C_{ap} is the capital cost of new heat transfer area, given by:

$$C_{ap} = \widehat{CF} + \hat{a} A^{\hat{b}} \quad (3.17)$$

where \widehat{CF} is a fixed cost, \hat{a} and \hat{b} are the area cost parameters.

In addition, \hat{r} is the annualization factor (TOWLER and SINOTT, 2008) and C_{op} is the operational cost, given by the following equations:

$$\hat{r} = \frac{\hat{i} (1 + \hat{i})^{\hat{n}}}{(1 + \hat{i})^{\hat{n}} - 1} \quad (3.18)$$

$$C_{op} = \widehat{Nop} \widehat{pc} \left(\frac{\Delta P \widehat{m}}{\hat{\eta} \hat{\rho}} \right) \quad (3.19)$$

where \hat{i} is the interest rate, \hat{n} is the project horizon in years, \widehat{Nop} is the number of operating hours per year, \widehat{pc} is the energy price, $\hat{\eta}$ the pump efficiency, ΔP is the stream pressure drop, \widehat{m} is the mass flow rate, and $\hat{\rho}$ is the fluid density.

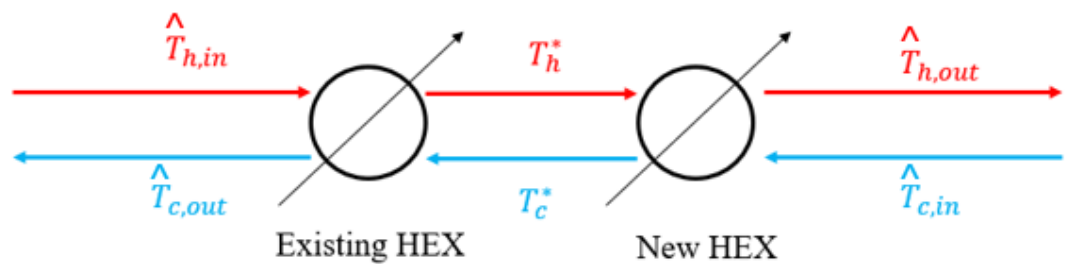
It is important to highlight that the pressure drop is considered in the problem, which is embedded in the objective function considering the trade-off between the capital and operational cost. An alternative representation of the problem, typically found in grassroots design problems is to use in the objective function, instead of the TAC, the capital cost (usually represented by the heat transfer area) and insert constraints associated with upper bounds on the hot and cold streams pressure drop (Nahes *et al.*, 2021).

The design optimization of a new HEX consists of minimizing the TAC subject to the set of constraints presented above. The optimization is performed using the technique called Set Trimming. In this method, the search space is represented by the set of solution candidates. Each candidate is composed of a set of discrete options of the design variables. Starting from an initial set containing all solution candidates, the Set Trimming method is based on the sequential application of the inequality constraints, gradually reducing the number of solution candidates. After the application of all constraints, the resultant set is the feasible region of the problem and the optimal solution can be easily identified by a sorting procedure. Set Trimming has been applied successfully for the global optimization design of several process equipment, such as, STHE (Lemos *et al.*, 2020), kettle vaporizers (Sales *et al.*, 2021), GPHE (Nahes *et al.*, 2021) and intensified HEXs (Chang *et al.*, 2022). A brief representation of how Set Trimming works is described in Supplemental Material (Appendix 1).

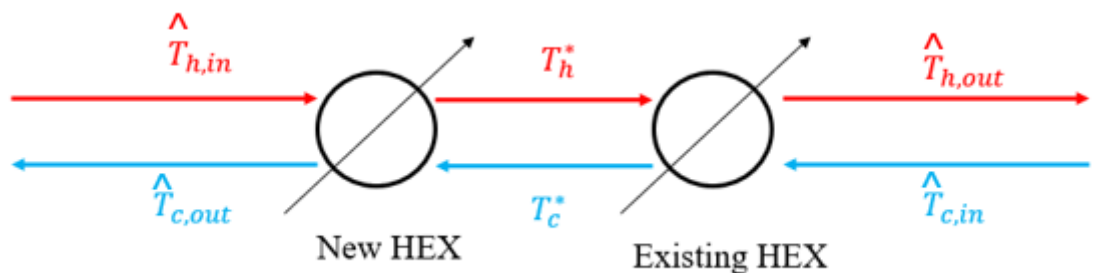
3.3.2. Insertion of a new HEX in series

The focus here is the HEX retrofit by area addition through the installation of a new unit in series with the existing one. Figure 3.1 illustrates two different arrangements for installing a new HEX in series, where the new HEX can be installed in the hot end (Figure 3.1a) or in the cold end (Figure 3.1b).

Figure 3.1. Alternatives of insertion of a HEX in series with the existing one



3.1a - New HEX located in the cold end of the existing HEX



3.1b - New HEX located in the hot end of the existing HEX

Source: Author's own work, 2024.

Note that there are intermediary temperatures, denoted as T_h^* and T_c^* that are unknown. The heat transfer rate equation and the energy balance of the hot and cold stream in the existing HEX can be written as follows:

$$Q_{ex} = \hat{U} \hat{A} LMTD(T_h^*, T_c^*) F(T_h^*, T_c^*) \quad (3.20)$$

$$Q_{ex} = \hat{m}_h \hat{C}_p \hat{p}_h (\hat{T}_{h,in} - T_h^*) \quad (3.21)$$

$$Q_{ex} = \hat{m}_c \hat{C}_p \hat{p}_c (T_c^* - \hat{T}_{c,in}) \quad (3.22)$$

The overall heat transfer coefficient and the heat transfer area are known since the geometric variable of the existing HEX is also known. In addition, F depends on T_h^* and T_c^* . Therefore, the set of Eqs. (20-22) is a system of three nonlinear equations and three variables (Q_{ex}, T_h^*, T_c^*).

This set of equations can be combined in a single one, where the only unknown variable is T_c^* (the variable T_h^* can be substituted through Eqs. (3.21) and (3.22)), as follows:

$$f = \widehat{m}_c \widehat{Cp}_c (T_c^* - \widehat{T}_{c,in}) - \widehat{U} \widehat{A} LMTD(T_c^*) F(T_c^*) \quad (3.23)$$

The solution of Eq. (3.23) gives the temperature T_c^* that, combined with Eqs (3.20) and (3.21) allows the determination of the heat load and all temperatures associated with the existing HEX.

Note that, once T_h^* and T_c^* are obtained, all information about the design service of the new unit is established, since the inlet and outlet temperatures of both streams are known. Thus, the design of the new HEX can be performed using the Set Trimming method.

In addition, it is important to emphasize that because the HEX is added in series, the total pressure drop is the sum of the pressure drop in the existing and new HEXs:

$$\Delta P_c = \Delta P_{c,new} + \Delta P_{c,EX} \quad (3.24)$$

$$\Delta P_h = \Delta P_{h,new} + \Delta P_{h,EX} \quad (3.25)$$

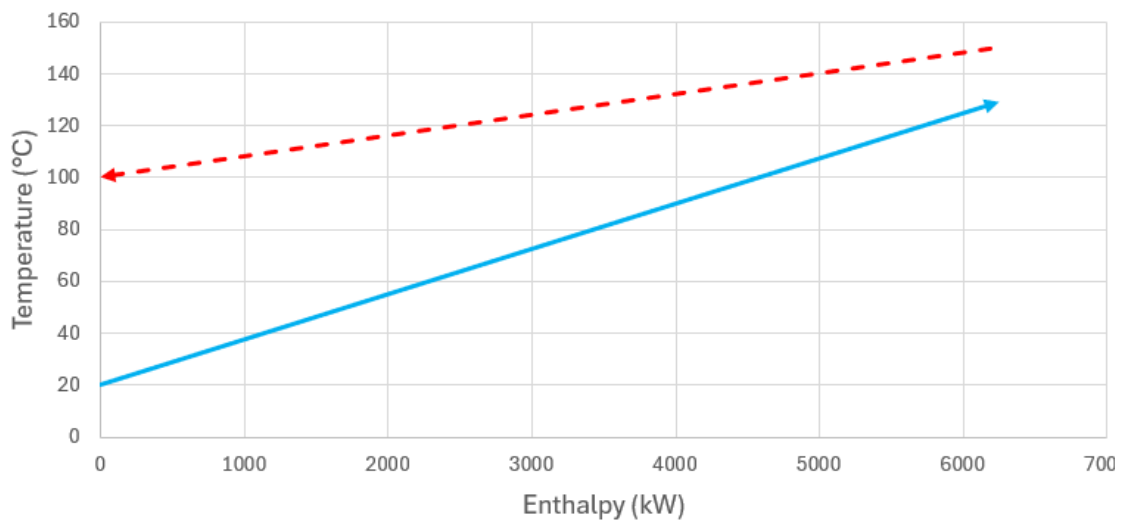
In order to clarify the difference between the two alternatives of insertion of the new HEX, Figure 3.2 presents two typical temperature vs enthalpy diagrams (for streams with uniform heat capacity) associated to a retrofit task. These profiles are associated with different relations between the heat capacity flow rates: $m_h Cp_h > m_c Cp_c$ (Figure 3.2a) and $m_h Cp_h < m_c Cp_c$ (Figure 3.2b).

According to Figure 3.2a, the temperature difference between the hot and cold streams (i.e. the heat transfer driving force) is higher on the cold side of the temperature profiles and decreases as it moves towards the hot side. Thus, if the new unit is installed on the hot side (see Figure 3.1b), the heat transfer driving force in the existing HEX is greater than if the new HEX were installed on the cold side, due to the resultant higher LMTD in the existing HEX. Therefore, the hot side insertion of the new unit implies a higher heat transfer rate of the existing HEX and, consequently, a lower heat load for the new HEX, but associated with a lower LMTD. The insertion of the new HEX in the cold side implies in a task with a higher

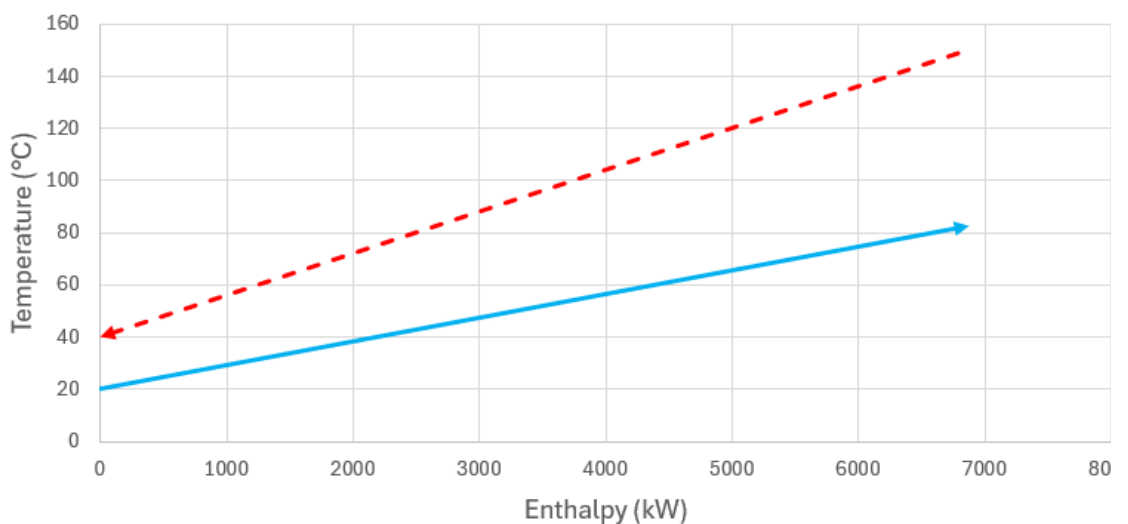
heat load, but associated with a larger LMTD. Temperature profiles similar to that depicted in Figure 1a are associated with analogous conclusions, but ends are inverted (similar to the stream selection rules in Pinch Technology).

Thus, it is not possible to know a priori what the best arrangement is, due to the trade-off between the heat load and driving force of the new HEX. So, it is necessary to evaluate both alternatives, and the solution of the problem is the best one between them.

Figure 3.2. Temperature x Enthalpy diagrams



$$3.2a - m_h C p_h > m_c C p_c$$

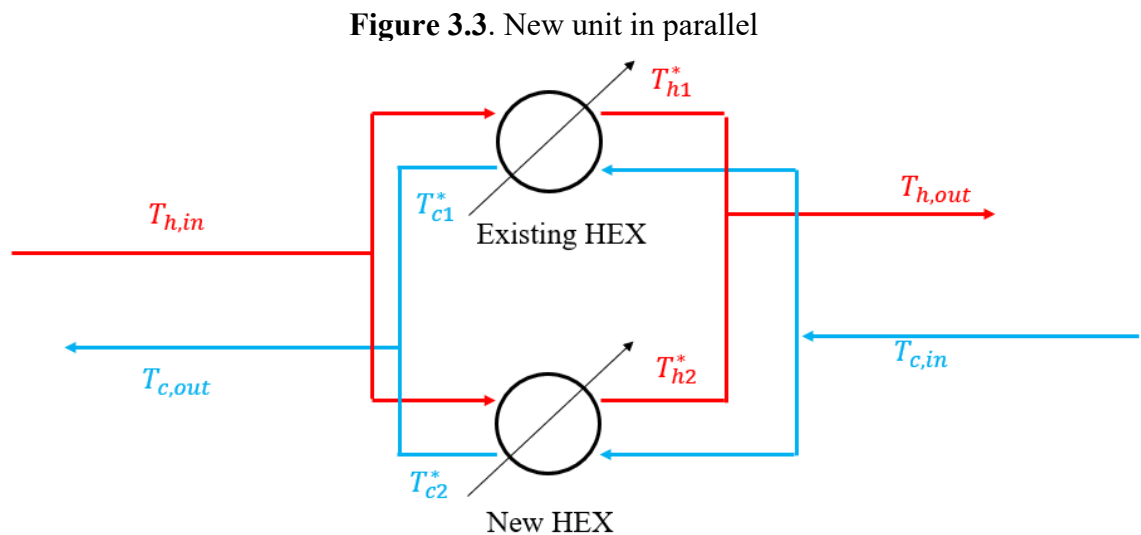


$$3.2b - m_h C p_h < m_c C p_c$$

Source: Author's own work, 2024.

3.3.3. Insertion of a new HEX in parallel

Figure 3.3 illustrates the addition of a new unit in parallel with the existing one. Observe that, in this case, there are four unknown temperatures T_{h1}^* , T_{h2}^* , T_{c1}^* and T_{c2}^* . Those temperatures depend on the split fraction of the hot and cold stream between the new and existing HEX. If a larger fraction of the stream flow rates is diverted to the existing HEX, more heat is transferred in this HEX and the heat duty of the new HEX is smaller. Simultaneously, a larger fraction of the flow rate diverted to the existing HEX, also increases the pressure drop in this HEX and in the system, because the pressure drop in each parallel branch will be the same (any hydraulic unbalance will be compensated by the presence of a valve).



Source: Author's own work, 2024.

Therefore, there are two new degrees of freedom for the problem if the new HEX is added in parallel, which are the split fraction of the cold and hot stream.

Similar to the series alignment, the procedure for the design of a new HEX in parallel starts with obtaining the service of the new unit. Note that, for a given pair of split fractions of the hot stream and cold stream flow rates, the inlet temperatures and the values of the flow rates of the existing HEX are defined. Thus, since the inlet conditions of the existing HEX are known, as well as its geometry (consequently the heat transfer area is known and the overall heat transfer coefficient can be calculated), it is possible to simulate the existing HEX using the $\varepsilon - NUT$ method (Incropera, 2007). The result of this simulation gives the heat load of the existing HEX, which allows the calculation of the heat load of the new HEX that is necessary

to complete the task, which is given by the difference between the desired total heat load and the one in the existing HEX. Therefore, since the heat load of the new HEX can be calculated, it is possible to define its service, and the new HEX in parallel can be designed using the Set Trimming procedure.

Because the split fractions are not previously known, the retrofit using parallel alignment consists of a 2D optimization problem, where the variables are the split fractions of the hot and cold streams. The objective function is evaluated using the procedure described below:

1. For a given pair of split fractions of the hot and cold streams, calculate the heat load of the existing HEX using a simulation procedure.
2. Obtain the thermal task of the new HEX using the evaluated heat load of the existing HEX.
3. Evaluate the outlet temperatures of the HEX (T_{c2}^* and T_{h2}^* in Fig. 3.3) through an energy balance using the heat load of the new HEX.
4. Since the service is defined, the new HEX is optimally designed using the Set Trimming method.

Because this problem presents non-convexities and several discontinuities, the DIRECT optimization method is used to ensure global optimality (Jones and Martins, 2021).

Finally, since the streams are aligned in parallel, the pressure drop is the maximum one between the existing and new HEX:

$$\Delta P_t = \max(\Delta P_{t,new}, \Delta P_{t,EX}) \quad (3.26)$$

$$\Delta P_s = \max(\Delta P_{s,new}, \Delta P_{s,EX}) \quad (3.27)$$

3.3.4. Insertion of intensification devices in the existing HEX

As previously discussed, only the alternatives of tube insert intensification, twisted-tape and coil wired, are explored here. The grassroot design optimization of intensified HEX using Set Trimming have been presented by Chang *et al.* (2022). Thus, its application for the HEX retrofit is a particular case of the original work, since the existing HEX already has its geometric variables. So, the design variables are only the twisted-tape pitch (H) and thickness

(δ) for the twisted-tape intensification, and the coiled-wire helical pitch (P_{cl}) and diameter (E_{cl}) for the coiled-wire intensification.

The problem constraints, along with those presented in Subsection 3.3.1, encompass a set of geometric constraints for each intensification device. The geometric constraints for twisted-tape insert are bounds on the twist ratio y and thickness δ (Jiang *et al.*, 2014):

$$3 \geq y \leq 6 \quad (3.28)$$

$$0.02 \geq \delta \leq 0.04 \quad (3.29)$$

$$y = \frac{H}{dti} \quad (3.30)$$

In addition, for the coiled-wire insert, the geometric constraints are bounds on the helical pitch, P_{CI} , and the helical angle, α_{CI} (Jiang *et al.*, 2014):

$$1.17 \geq P_{CI} \leq 2.68 \quad (3.31)$$

$$32 \geq \alpha_{CI} \leq 61 \quad (3.32)$$

Although, from our perspective, other types of intensification are not commonly considered in industrial practice, but they can be readily included in the procedure if the user wish to take them into account.

3.3.5. Complete procedure

Aiming at identifying the optimal solution among all of the alternatives described above, the exploration of each type of intervention is organized in a single algorithm. The resultant procedure considers different types of HEX retrofit, exploring different arrangements and different types of HEX. The steps of the complete HEX retrofit consist of testing all alternatives sequentially, which are:

- Option 1: Replacing the existing HEX for a new STHE
- Option 2: Replacing the existing HEX for a new GPHE
- Option 3: Inserting twisted-tape in the existing HEX

- Option 4: Inserting coil-wire in the existing HEX
- Option 5: Installing a new STHE in series
- Option 6: Installing a new GPHE in series
- Option 7: Installing a new STHE in parallel
- Option 8: Installing a new GPHE in parallel

All the design tasks for the new unit mentioned above are conducted using Set Trimming for shell-and tube HEX (Lemos *et al.*, 2020) and gasketed plate HEX (Nahes *et al.*, 2021). The incumbent solution of each step is used to eliminate candidates with higher values of the objective function in the subsequent steps, which reduces the computational effort.

Finally, note that Options 1 and 2 involve the replacement of the existing HEX for a new one. In some cases, regarding the new service, it can be the best solution or the only one at all.

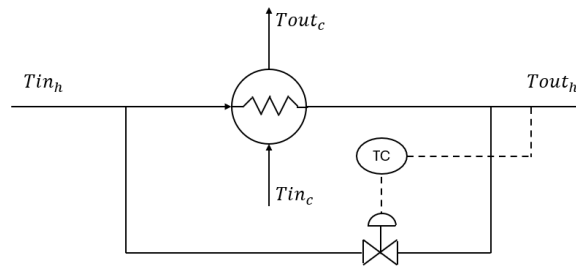
3.4 HEX Retrofit - Heat Load Reduction

If the new thermal task of an existing HEX indicates a significant excess area, the necessity of a system modification to reduce heat transfer depends on an analysis of the nature of the process, considering two different situations.

The first one is when the target temperatures of the streams are strictly important, associated with the type of operation and/or equipment downstream the existing HEX. Some examples are the heat integration between a process stream and a reboiler or a condenser of a distillation column (the heat load interacts with the fractionating control), a heat integration with a feed of reactor (the inlet temperature can affect the conversion or can be limited due to safety reasons), or heat integration in a plant drastically integrated.

In these cases, the capacity of the existing HEX are usually controlled. Figure 3.4 below illustrates a traditional way of controlling the heat transfer in an integration HEX.

Figure 3.4. Typical temperature control in an energy integration HEX



Source: Author's own work, 2024.

The control manipulates the flow rate in the bypass, which affects the heat transfer rate due to the variation in the overall heat transfer coefficient and the *LMTD*. Figure 3.4 presents a bypass in the tube stream, but the shell stream can also be used. It is important to notice that if the existing HEX already has this kind of temperature control, the control loop itself can be used to reduce the heat load. The details on how to use the bypass to reduce the heat load will be discussed further.

The second situation is when there is no need to control the stream temperature during the operation (i.e. the target temperature of the stream is not a hard constraint). In this case, there is no significant impact in the process, i.e. a larger heat load in the existing HEX can be allowed, even if it leads to temperatures different from those initially designed. Some examples are the integration between cold oil before electrostatic treater and hot oil after the treater in a FPSO, some HEXs in crude oil preheating trains in refineries, and heat integration between cold solvents after absorption with hot solvents after regeneration.

In all examples, there is no problem if the outlet temperature of the streams is different from the designed ones, because a utility is used after the HEX, or because the more heat exchanged, the better. If this is the case of an existing HEX subject to a new thermal task that has a significant excess area, it is possible that no intervention is required.

The following subsections explore two alternative ways to reduce the heat load in the existing HEX, if necessary.

3.4.1. Heat load reduction by stream by-pass

Aspects related to the controllability of the control loop are not explored in this paper; instead, the focus here is on the thermo-fluidynamic behavior of the HEX, when a stream bypass is used to reduce the heat load in an existing HEX.

Thus, the goal is to identify the necessary split fraction to make the heat load in the existing HEX be equal to the new service. So, let ψ be the split of the feed stream flow rate that goes to the HEX ($1 - \psi$ is the split associated with the by-pass), ψ can be calculated solving the following equation:

$$Q(\psi) - \hat{Q}_{req} = 0 \quad (3.33)$$

where \hat{Q}_{req} is the heat load of the new service, and Q is the heat load of the existing HEX that is a function of the split ψ . In addition, Q can be evaluated using a simulation procedure like the $\varepsilon - NUT$ method.

We now illustrate the intricacies of some instances of this problem. Consider the retrofit of two hypothetical existing HEXs, where their geometry is depicted in Table 3.1.

Table 3.1. Geometry of existing HEXs subjected to heat load reduction

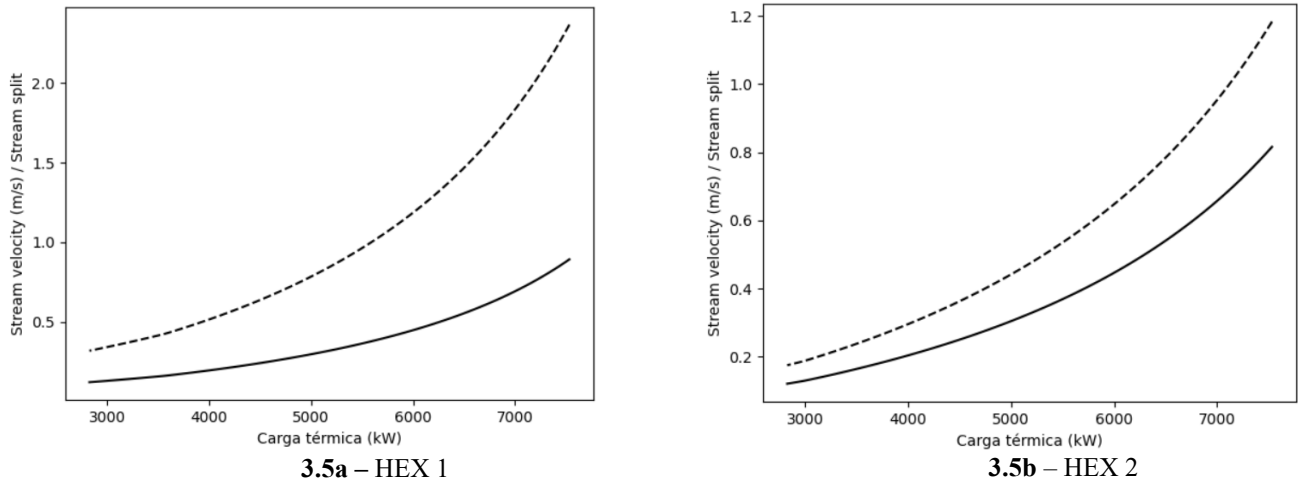
Variable	HEX1	HEX2
Shell diameter (m)	0.5906	0.9906
Outer diameter (m)	0.01905	0.0381
Tube passes	2	4
Pitch ratio	1.25	1.25
Layout	Triangular	Triangular
Tube length (m)	3.0488	3.0488
Number of baffles	8	8
Baffle cut (%)	25	25
Number of tubes	407	278
Number of shells	1	1
Heat transfer area (m ²)	74.26	101.45

Source: Author's own work, 2024.

The original operational condition of both HEX is associated with a hot stream with inlet and outlet temperatures equal to 240 °C and 200 °C, respectively, and a cold stream with inlet and outlet temperatures equal to 52 °C and 85 °C, respectively. The heat duty in the original task is 7,534 kW.

Considering that the by-pass is installed in the tube-side, Figure 3.5 presents the profile of ψ and tube side velocity as a function of the required new heat load.

Figure 3.5. Profiles for using by-pass to reduce heat load. The solid lines are the stream split to the HEX, and the dashed lines are the stream velocity



Source: Author's own work, 2024.

Although both HEX originally operate with the same heat load, they have different thermo-fluidynamic behaviors due to their different geometry. The first one operates with a higher tube-side stream velocity, and the second one with a smaller value. According to the profiles in Figure 3.5, if the heat load of HEX 1 must be smaller than 5,550 kW, the flow velocity in the tube-side becomes smaller than 1 m/s, which is a limit usually imposed to attenuate fouling. On the other hand, for HEX 2, the limit heat load is stricter, equivalent to 6,900 kW, since the HEX 2 operated originally with a small tube-side velocity.

Although a rigorous analysis would require a more detailed study of the fouling phenomenon in the HEX, it illustrates that there is an operational envelope associated with possible values of heat load reduction, without imply a possible operational region prone to fouling. In this example, HEX 1 can reduce only 26% of the original heat load, and HEX 2 only 8.4% without leading to potentially problematic operational conditions.

3.4.2. Heat load reduction by plugging tubes

Plugging tubes is usually applied to allow an HEX to operate even if there some damaged tubes. The plug is inserted into the tubesheets and block the flow through that tube. This approach can be applied in very particular situations to reduce the heat load of a given HEX. This intervention seeks to reduce the heat transfer area through the tube blocking. As a side-effect, the tube-side flow velocity of the remaining tubes increases when other tubes are plugged (and consequently, the overall heat transfer coefficient also increases as also the pressure drop).

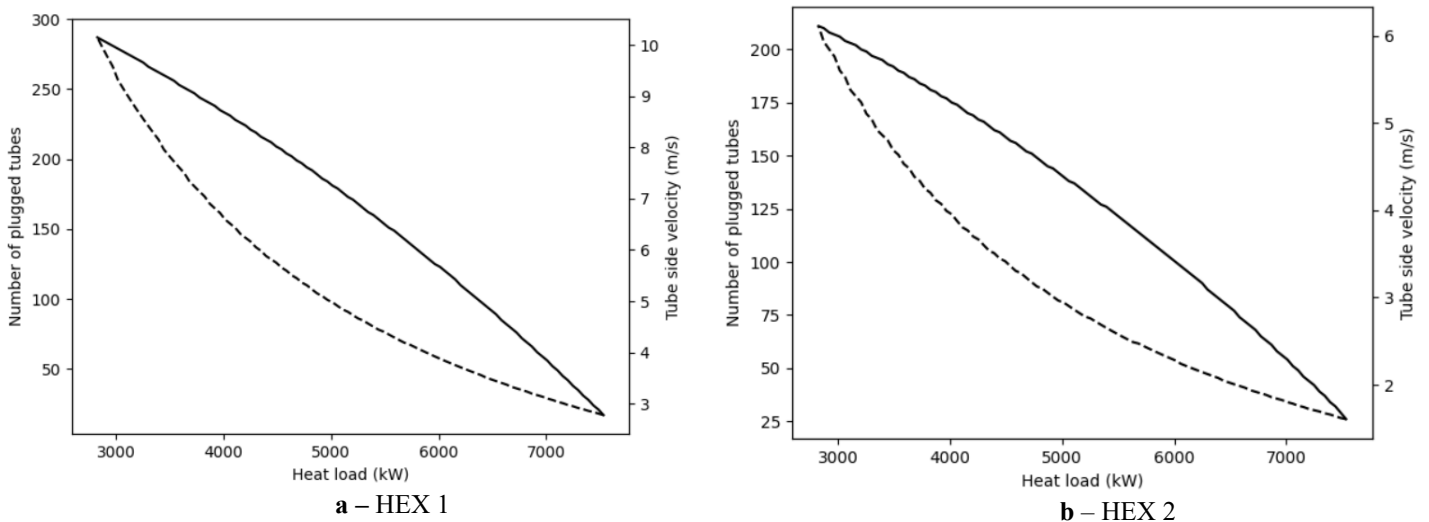
Similarly to the stream by-pass, the number of plugged tubes is obtained solving the following equation:

$$Q(\xi) - \hat{Q}_{req} = 0 \quad (3.34)$$

where ξ is the number of plugged tubes

In order to illustrate the effect of plugging tubes, the same examples in Table 3.1 are considered, and the velocity profile and number of plugged tubes is depicted in Figure 3.6.

Figure 3.6. Profiles for plugging tubes to reduce heat load. The solid lines are the number of plugged tubes, and the dashed lines are the tube stream velocity



Source: Author's own work, 2024.

Figure 3.6 shows a different scenario compared to Figure 3.5. In this case, as the heat load reduces, the stream velocity increases. An upper limit of the tube side velocity,

associated with erosion and vibration problems, usually limits the velocity to 3 m/s in the tube side. Thus, because HEX 1 operates at higher velocities in the original service, small reductions in the heat load already achieve the velocity upper bound. On the other hand, HEX 2, which originally operated at smaller velocities, can achieve higher heat loads reductions without violating the velocity upper bound.

This discussion shows an important pattern. It is not possible to achieve any desired reduction in the heat load of an existing HEX, without imply potentially conditions in the future. If the existing HEX operates originally at a relatively small velocity, plugging tubes can achieve higher heat load reductions, on the other hand using a stream by-pass allows a higher reduction. The limitations of the techniques to reduce the heat load of exiting HEX must be considered if the proposed solution involves a large diminution of the heat transfer rate along the HEN.

Finally, if the new service requires a heat load reduction that can be achieved with both methods, the following guideline can be used: if a control loop with a stream by-pass already exist, use the existing control to increase the stream by-pass. If the valve opening in the new condition is associated with an operational condition of poor controllability, it is possible to install a restriction orifice in the exchanger line, which is associated with a low cost.

However, if the existing HEX does not have any by-pass pipeline, the installation would involve the purchase of piping, fittings and the control valve which can be expensive. Thus, if the head load reduction is necessary, plugging tubes can be a better solution. This guideline involves the smaller change in the existing HEX, and the smallest cost.

3.5 Results

Three retrofit examples are explored involving streams without phase change and applications with process streams (only energy integration HEXs are employed in this section). The STHE model employs the Bell-Delaware method for the shell-side evaluation (Taborek, 2008). It can address the possibility of multiple shells, associated with an E-shell type. The thickness and thermal conductivity of the tubes are equal to 1.22 mm and 50 W/(m·K), respectively. The flow velocity bounds for the STHE are 1 and 3 in the tube-side and 0.5 and 2 m/s in the shell side. The flow velocity bounds for the GPHE are 0.3 and 0.9 m/s.

The GPHE is composed of Chevron-type plates. The thermofluid-dynamic model employed to describe the behavior of the heat exchanger is based on Kakaç and Liu (2002). The plates have thickness and thermal conductivity equal to 0.8 mm and 16.2 W/(m²K), respectively. The enlargement factor associated with the corrugations is 1.15 and the mean channel spacing is 3 mm.

The design variables that represent the search space of each type of HEX are depicted in Tables 3.2, 3.3, and 3.4, and Table 3.5 presents the dimensions of the available plates.

Table 3.2. STHE search space

Design variable	Values
Shell diameter (m)	0.2050, 0.3048, 0.3874, 0.489, 0.5906, 0.6858, 0.7874, 0.8382, 0.889, 0.9398, 0.9906, 1.0668, 1.143, 1.2192, 1.3716, 1.524
Outer diameter (m)	0.00635, 0.009525, 0.0127, 0.01905, 0.0254, 0.03175, 0.0381, 0.05080
Number of tube passes	1, 2, 4, 6
Pitch ratio	1.25, 1.33, 1.5
Tube layout	Triangular, square
Tube length (m)	1.2195, 1.8293, 2.439, 3.0488, 3.6585, 4.8768, 6.0976, 6.706
Number of baffles	1,2,3,...,18,19,20

Source: Author's own work, 2024.

Table 3.3. GPHE search space

Design variable	Values
Number of plates	10,11,12,...,798,799,800
Plate size alternatives (Table 7)	1,2,3,4,5
Chevron angle (deg)	30, 45, 50, 60, 65
Hot and cold number of passes	1, 2

Source: Author's own work, 2024.

Table 3.4. Tube insert search space

Design variable	Values
Twisted-Tapes pitch (m)	From 0.0315 m to 0.3325 m, in increments of 12.7 mm
Twisted-Tapes thickness (m)	From 0.0005 m to 0.004 m, in increments of 0.5 mm
Helical Pitch (m)	0.02, 0.031955, 0.044179, 0.056402, 0.064
Coil-Wire diameter (m)	0.001, 0.0012, 0.0014, 0.0016, 0.0018, 0.0020

Source: Author's own work, 2024.

It is important to note that the design problem involves identifying, among all the options presented in the tables above, a set of independent variables that geometrically define the HEX. The diversity of alternatives available allows the exploration of the trade-offs previously discussed. The investment cost parameters are depicted in Table 3.6.

Table 3.5. Plate dimensions from an industrial supplier (C. J. Mulanix Company, Inc., 2022).

Alternative	Plate length (m)	Plate width (m)	Port diameter (m)
1	0.743	0.845	0.300
2	0.978	0.812	0.288
3	1.281	1.200	0.400
4	1.500	1.220	0.350
5	1.835	0.945	0.300
6	2.092	1.200	0.400
7	1.551	0.909	0.285
8	0.400	0.125	0.03
9	1.845	0.450	0.155
10	1.543	0.812	0.283

Source: Author's own work, 2024.

Table 3.6. Economic parameters

HEX type	Fixed cost	Area cost coefficient	Exponent cost coefficient
STHE (Hajabdollahi <i>et al</i> , 2016)	8500	409	0.85
GPHE (Hajabdollahi <i>et al</i> , 2016)	0	635.15	0.778
Tube insert (Pan <i>et al</i> , 2018)	500	50	1

Source: Author's own work, 2024.

In addition, it is considered a time horizon of 10 years, an energy price of 0.15 \$/kWh, a pump efficiency of 60%, an interest rate of 10% and a number of operating hours per year of 7500 h/y.

The streams physical properties of all examples are depicted in Table 3.7.

Table 3.7: Streams physical properties

	Cold stream	Hot stream
Density (kg/m ³)	870	860
Viscosity (Pa s)	0.0046	0.0004
Heat capacity (J/kg K)	2150	2720
Thermal conductivity (W/(m·K))	0.11	0.132
Fouling factor (m ² K/W)	0.0005	0.0002

Source: Author's own work, 2024.

The data of the retrofit service data and the existing HEX of all three examples are depicted in Table 3.8 and 3.9 (all of them are STHE).

Table 3.8. Retrofit task

	Example 1		Example 2		Example 3	
	Cold stream	Hot stream	Cold stream	Hot stream	Cold stream	Hot stream
Mass flow rate (kg/s)	66.6	40	66.6	40	78	60
Inlet temperature (°C)	62	180	62	190	62	200
Outlet temperature (°C)	111.4	115	107.6	130	110.6	150
Heat load (kW)	7072		6528		8160	

Source: Author's own work, 2024.

Table 3.9. Existing HEXs

Variable	Example 1	Example 2	Example 3
Tube diameter (m)	0.03175	0.0381	0.03175
Tube length (m)	4.8768	6.0976	4.8768
Number of tube passes	6	6	4
Shell diameter (m)	0.9906	1.2192	0.9906
Tube bundle layout	Square	Triangular	Square
Pitch ratio	1.25	1.25	1.25
Number of baffles	18	16	14

Source: Author's own work, 2024.

3.5.1. Example 1

To illustrate the performance of the existing HEX under the new design conditions (presented in Table 3.8), a simulation was conducted, and the thermofluid-dynamic results are presented in Table 3.10.

Table 3.10. Example 1: Existing HEX performance

	Tube side	Shell side
Velocity (m/s)	1.66	0.97
Pressure drop (kPa)	47.313	24.314
Convective coefficient (W/m ² K)	740	1347
Overall heat transfer coefficient (W/m ² K)		309
Heat duty (kW)		5043

Source: Author's own work, 2024.

Because the specified heat load is 7,072 kW, an increase in the heat duty is required. Thus, all retrofit alternatives were conducted. Table 3.11 presents the optimal solution of each one.

Table 3.11. Example 1: Optimal solution of each alternative

Alternative	TAC (\$/y)
Replacement for a new STHE	19,121.5
Replacement for a new GPHE	11,804.9
Twisted-tape insert	Infeasible
Coil-wired insert	Infeasible
Installing a new STHE in series	10,859.7
Installing a new GPHE in series	7,815.9
Installing a new STHE in parallel	19,739.6
Installing a new GPHE in parallel	13,092.0

Source: Author's own work, 2024.

The analysis of Table 3.11 shows that the best alternative is the installation of a new unit in series. The pressure drop in the tube-side and shell-side in the new STHE in series are 67.624 kPa and 29.920 kPa, respectively, and for the new GPHE in series are 14.847 kPa and 25.547 kPa for the cold and hot streams, respectively, which illustrates a significant increase in the total pressure drop. There is no feasible solution using intensification devices, because they cannot accomplish the necessary increase in the heat duty.

3.5.2. Example 2

Table 3.12 illustrates the thermofluid-dynamic variables associated with the performance of the existing HEX under the new service (presented in Table 3.8).

Table 3.12. Example 2: Existing HEX performance

	Tube side	Shell side
Velocity (m/s)	1.18	0.52
Pressure drop (kPa)	25.395	5.636
Convective coefficient (W/m ² K)	511	981
Overall heat transfer coefficient (W/m ² K)		241.68
Heat duty (kW)		5445

Source: Author's own work, 2024.

Because the specified heat load is 6528 kW, an increase in the heat duty is required. Table 3.13 below presents the optimal solution of HEX retrofit alternative.

The analysis of Table 3.13 shows that the best alternative is the installation of intensification devices. The optimal solution using twisted-tape insert increases the tube side heat transfer coefficient to 1159.66 W/m²K, which is an increase of 127 %, giving an overall heat transfer coefficient of 342.83 W/m²K. In addition, the pressure drop in the tube side also increases to 41.778 kPa. In turn, for the coil-wired insert the tube side heat transfer coefficient and the overall heat transfer coefficient increases to 1166.8 W/m²K and 343.5 W/m²K, which is slightly higher than the twisted-tape. The reason why it gives a better solution is associated with the pressure drop, which increases to 32.792 kPa.

Table 3.13 .Example 2: Retrofit solution of each alternative

Alternative	TAC (\$/y)
Replacement for a new STHE	16878.8
Replacement for a new GPHE	9313.9
Twisted-tape insert	4166.8
Coil-wired insert	3307.1
Installing a new STHE in series	4628.6
Installing a new GPHE in series	5077.12
Installing a new STHE in parallel	Infeasible
Installing a new GPHE in parallel	Infeasible

Source: Author's own work, 2024.

Finally, note that there is no solution installing a new unit in parallel, because the original HEX operates very close to the minimum velocity, which avoids the split to the new unit in parallel.

3.5.3. Example 3

Table 3.14 illustrates the thermofluid-dynamic variables associated with the performance of the existing HEX under new service (presented in Table 3.8).

Table 3.14. Example 3: Existing HEX performance

	Tube side	Shell side
Velocity (m/s)	1.94	1.05
Pressure drop (kPa)	62.315	21.071
Convective coefficient (W/m ² K)	889	1599
Overall heat transfer coefficient (W/m ² K)		350
Heat duty (kW)		7119

Source: Author's own work, 2024.

Because the specified heat load is 8,160 kW, an increase in the heat duty is required. Table 3.15 presents the optimal solution of HEX retrofit alternative. The analysis of Table 3.15 shows that the best alternatives are the installation of a new unit in parallel with the existing one. Different to the other examples, the velocity in the existing HEX is high enough to allow a considerable split to the new unit in parallel.

Table 3.15. Example 3: Retrofit solution of each alternative

Alternative	TAC (\$/y)
Replacement for a new STHE	12551
Replacement for a new GPHE	6941
Twisted-tape insert	Infeasible
Coil-wired insert	29416
Installing a new STHE in series	8954
Installing a new GPHE in series	10193
Installing a new STHE in parallel	4842
Installing a new GPHE in parallel	920

Source: Author's own work

The optimal solution with a STHE in parallel involves 37% of the cold stream and 40% of the hot stream diverted to the new unit. The target temperatures in the parallel unit are 116.8 °C for the cold stream outlet temperature and 147.4 °C for the hot stream outlet temperature, associated with a heat load of 3,416 kW.

In turn, for the optimal solution with a GPHE in parallel, 41% of the cold stream and 50% of the hot stream goes to the new unit. The corresponding target temperatures of the outlet cold and hot streams are 118 °C and 153 °C, associated with a heat load of 3,804 kW (note that the heat duty for the GPHE in parallel is higher than for the STHE, because it is associated with a larger split to the new unit).

Another interesting result in Table 3.15 is that a GPHE in series is more expensive than replacing the existing HEX for a new GPHE. It happens because the pressure drop in the existing HEX significantly penalize the objective function, since the pressure drop in the series alignment is the sum of both units.

3.5.4. Comparison with the traditional approach

Although the detailed formulation of an HEX retrofit problem has not been receiving much attention in the literature, the representation of the extension of an existing HEX to fulfill a new thermal task in an HEN retrofit is extensively used in this kind of problem.

Generally, the need to increase heat load in existing exchangers is met by adding heat transfer area using the following equation:

$$A_{new} = \frac{Q}{U LMTD} - A_{existing} \quad (3.35)$$

There are two main underlying assumptions in this equation. The first is that the heat exchangers are operating in a countercurrent configuration. The second, which warrants closer attention, is that both the existing and the new exchanger share the same overall heat transfer coefficient. This assumption holds true only if the existing and new exchangers are not only of the same type but also have a similar geometry.

To illustrate the impact of considering this second hypothesis, the same examples were recalculated assuming that the new shell added has exactly the same geometry as the existing one, with the exception of the tube length that is selected according to the required area. It is worth noting that allowing changes to the tube length keeps the convective heat transfer coefficient on the tube side constant, whereas on the shell side, it undergoes a variation due to changes in the baffle spacing. However, since all other geometric variables remain unchanged, the impact on the overall heat transfer coefficient is minimal. This approach closely aligns with the classical methodology commonly adopted in the literature.

Because parallel alignment involves a variation of the overall heat transfer coefficient and it cannot be known before the evaluation of the HEX, only series alignment is considered. Table 3.16 shows the corresponding results.

Table 3.16. Comparison with traditional approach

	Example 1 TAC (\$/y)	Example 2 TAC (\$/y)	Example 3 TAC (\$/y)
SHE in series – Traditional approach	13,921.0	10,949.3	19,131.0
SHE in series – Proposed approach	10,859.7	4,628.6	8,954.0
Best solution – Proposed approach	7,815.9	3,307.1	920.0

Source: Author's own work, 2024.

Table 3.16 clearly shows the significant difference in the HEX retrofit design if a more detailed procedure is used. If only SHE in series is considered, with similar dimensions of the existing HEX, a solution 28.2% more expensive is found in Example 1, 126% more

expensive in Example 2 and 114% more expensive in Example 3. If all possible alternatives are considered, a higher difference is observed. These results show that to seek new optimal dimensions of the HEX associated with the area addition in HEN retrofit problems can provide considerable cost reductions.

3.6 Conclusions

This section presents a novel procedure for heat exchanger retrofit, which address in detail different alternatives for the increasing and reducing the heat load.

Increasing heat load can be achieved by adding heat transfer area, either through the installation of a new unit in series or parallel with the existing one, or by heat transfer intensification. Each alternative has distinct characteristics and may present the optimal solution depending on the new service of the existing heat exchanger, as illustrated by the examples discussed in the results.

Heat load reduction can be obtained by using a by-pass, or plugging tubes. The first alternative reduces the velocity in the existing HEX, which can cause fouling problems. In turn, plugging tubes increase the velocity in the existing HEX, which can bring erosion and vibration problems.

An important application where the HEX retrofit is embedded is the retrofit of heat exchanger networks. The presented results shows an important aspect never explored before, that can be a relevant contribution to future works about retrofit of HENs.

ACRONYMS AND ABBREVIATIONS

HEN – Heat exchanger network

HEX – Heat exchanger

LMTD – Logarithmic mean temperature difference

LP – Linear programming

MILP – Mixed integer linear programming

MINLP – Mixed inter nonlinear programming

NPV – Net present value

GPHE – Plate heat exchanger

STHE – Shell and tube heat exchanger

TAC – Total annualized cost

NOMENCLATURE

\hat{a}	Area cost parameter (\$/m ²)
A_{ex}	Existing heat transfer area (m ²)
$\widehat{A_{exc\%}}$	Excess area
$A_{existing}^{STHE}$	Area of an existing shell and tube (m ²)
$A_{existing}^{PHE}$	Area of an existing plate heat exchanger (m ²)
A_{new}	Additional heat transfer area (m ²)
Ar	Ratio between effective area and existing area
A_{req}	Required area (m ²)
\hat{b}	Area cost parameter
C_{cap}	Capital cost (\$)
$C_{op,c}$	Cold stream operational cost (\$/y)
C_{opc}^{ex}	Existing cold stream operational cost (\$/y)
C_{oph}^{ex}	Existing hot stream operational cost (\$/y)
$C_{op,h}$	Hot stream operational cost (\$/y)
\widehat{CF}	Fixed cost (\$)
d_{ti}	Tube inner diameter
d_{te}	Tube outer diameter (m)
D_s	Shell diameter (m)
D_p	Port diameter (m)
E_{cl}	Coil wire diameter (m)
F	Correction factor
H	Twisted-tape pitch
\hat{i}	Interest rate (1/y)
L	Tube length (m)
lay	Tube bundle layout
L_w	Plate width (m)
L_p	Plate length (m)

\dot{m}	Mass flow rate (kg/s)
\hat{n}	Project horizon
N_b	Number of baffle
N_p	Number of plates
N_{ph}	Hot stream number of passes
N_{pc}	Cold stream number of passes
$\widehat{N_{op}}$	Number of operating hours per year
N_s	Number of shells
NTT	Total number of tubes
N_{tp}	Number of tube passes
$\widehat{p_c}$	Energy price (\$/kwh)
P_{cl}	Coil-wire helical pitch
Q	Heat load (W)
\widehat{Q}_{req}	Required heat load (W)
Q_{ex}	Heat load in the existing HEX (W)
\hat{r}	Annualization factor (1/y)
rp	Pitch ratio
$T_{c,in}$	Cold stream inlet temperature (°C)
$T_{c,out}$	Cold stream outlet temperature (°C)
$T_{h,in}$	Hot stream inlet temperature (°C)
$T_{h,out}$	Hot stream outlet temperature (°C)
U	Overall heat transfer coefficient (W/m ² K)
vc	Cold stream velocity (m/s)
$\widehat{vc_{min}}$	Minimum cold stream velocity (m/s)
$\widehat{vc_{max}}$	Maximum cold stream velocity (m/s)
vh	Hot stream velocity (m/s)
$\widehat{vh_{min}}$	Minimum hot stream velocity (m/s)
$\widehat{vh_{max}}$	Maximum hot stream velocity (m/s)
vt	Tube side velocity (m/s)
$\widehat{vt_{min}}$	Minimum tube side velocity (m/s)
$\widehat{vt_{max}}$	Maximum tube side velocity (m/s)
vs	Shell side velocity (m/s)

γ	Ratio between twisted-tape pitch and tube inner diameter
β	Chevron angle
ϕ	Enlargement factor
ψ	Mass split fraction to the HEX
ξ	Number of plugged tubes
ΔP	Pressure drop (Pa)
$\hat{\eta}$	Pump efficiency
$\hat{\rho}$	Stream density (kg/m ³)
δ	Twisted-tape thickness (m)

4 HEN RETROFIT WITH DETAILED HEX DESIGN - PART 1: HEAT LOAD MODIFICATIONS

4.1. Introduction

The retrofit of heat exchanger networks (HENs) plays an important role in improving energy efficiency in industrial processes. By enhancing energy recovery, retrofitting reduces utility consumption, while simultaneously contributing to lower environmental impacts. Despite these potential gains, the complexity of modifying an existing network, characterized by a given set of thermal equipment, operational constraints, spatial distribution, etc. makes the retrofit optimization a considerable technology challenge.

HEN retrofit involves proposing interventions in the existing network with the goal of reducing utility consumption. To achieve this, heat transfer is increased in the process-to-process heat exchangers (HEXs) in the network in order to reduce the utility consumption in the heaters and coolers. This intervention alters the service conditions of the existing HEXs, necessitating an increase or decrease in their heat load. These interventions can be divided into two types: retrofits with and without topological modifications in the network (Kemp, 2007).

Topological modifications involve adding new matches to the network or altering existing ones, such as resequencing and repiping (Smith, 2005). These types of interventions are important because they can overcome energy bottlenecks in the HEN, known as pinch matches (Asante and Zhu, 1997), which prevent further energy recovery. However, topological modifications can be challenging to implement in industrial practice, as they involve complex civil and mechanical engineering work (Wang *et al.*, 2012; Pan *et al.*, 2012; Pan *et al.*; 2018), as well as considerations related to the existing plant layout and operations, as described in section 2.

The other type of HEN retrofit does not involve topological modifications. In this case, utility paths and energy loops are used to redistribute heat in the network without altering its topology. The degrees of freedom of the HEN retrofit optimization approach involves the modification of the heat load of the existing HEXs. While this approach does not

overcome pinch matches, they can still attain significant heat recovery without requiring complex and invasive interventions.

Another well-known aspect of HEN retrofits is the numerical difficulties associated with the mathematical models of the problem (Yee; Grossman, 1991; Ma *et al.*, 2000; Pan *et al.*, 2013; Pan *et al.*, 2018). These models exhibit significant nonlinearities, non-convexities, and combinatorial explosion due to the numerous ways of intervening in the network. Therefore, one who attempts to deal with the HEN retrofit needs to handle with numerical and convergence problems, which demand good initialization, high probability to be trapped in a local optimum, which affect the quality of the solution, and may demand elevated computational time.

In light of these challenges, some recent studies have proposed approaches that avoid topological modifications. Although such approaches inherently limit heat recovery, they can result in profitable projects that are easier to implement in practice, which justifies the investigation of such problem (Pan *et al.*, 2012; Wang *et al.*, 2012; Pan *et al.*, 2013; Pan *et al.*, 2018).

According to these two alternative approaches, this work is divided into two parts. Part I presents a procedure for retrofitting HENs without topological modifications, i.e. only the heat load of the existing heat exchangers are modified. Part II extends the methodology to include topological modifications. Consequently, the literature review about HEN retrofit presented below does not include topological changes, the discussion of previous sections that employed such interventions will be addressed in Part II.

Pan *et al.* (2012) discussed the advantages of using heat transfer intensification in HEN retrofit, which allows the enhancement in heat recovery by the increasing of heat transfer coefficients, without changing the heat transfer area and physical size of the HEX. Therefore, the utility consumption can be reduced without the expensive and complex conventional modifications. Thus, they proposed a MILP model with two iterations loops to overcome the nonlinearities of the problem, where the first loop is used for a given energy saving to solve repeatedly a MILP model, where the LMTD is constant in each run, to obtain a feasible solution. The second loop successively seeks the maximum value of energy saving.

Wang *et al.* (2012) discussed that the previous works assumed constant heat transfer coefficients and neglected the streams pressure drop, which is not suitable for practical retrofit applications, because heat transfer coefficients and pressure drops vary with design. In order to avoid the aforementioned disadvantages, a new proposition considering only heat transfer enhancement was proposed, including the detailed evaluation of the HEX including the

correction factor for multiple pass HEX. Thus, the geometric details of existing HEX in the HEN was used to adjust a heat transfer coefficient and pressure drop model using charts presented by Ayub (2005). The suitable HEXs to be enhanced and the new heat transfer distribution is performed under five different heuristics.

Pan *et al.* (2013) discussed that, in addition to increasing the heat transfer coefficients, intensification devices also reduce the propensity of fouling. Thus, fouling models for tube side enhancement were included in the HEN retrofit modelling to evaluate the necessary time for each HEX to be removed for cleaning, given by the moment when the required area turns equal to the effective area. A single example is presented, which is solved considering different minimum HEX operating time. The objective of the problem is to identify which HEX should be intensified to maximize the retrofit profit, obeying the operating time constraint. To deal with the nonlinearities of the model, the same procedure presented by Pan *et al.* (2012) was used.

Pan *et al.* (2016) extended the work of Pan *et al.* (2013) to include HEX cost during cleaning operations and pumping power costs. The cleaning expenditure is evaluated through a cleaning time for each HEX and cleaning cost in \$/time. The pressure drop is evaluated using a regressed model provided by hiTRAN, which expresses the pressure drop as a function of heat transfer coefficients (Pan *et al.*, 2014). Similar linearization techniques addressed in previous works (Pan *et al.*, 2012; Pan *et al.*, 2013) were used to obtain a MILP model.

Pan *et al.* (2018) presented a methodology to incorporate several features proposed in their earlier works (Pan *et al.*, 2012; Pan *et al.*, 2013; Pan *et al.*, 2016) and new advances in a single procedure. In this work, they attempted to address the exchanger detailed performance, including the LMTD and its correction factor (F) calculation, tube and shell side geometry details for intensified heat-transfer coefficients, multiple passes in tube and shell sides, pressure drop constraints, stream bypassing and splitting, and the temperature dependence of stream heat capacities.

Compared to traditional studies involving topological modifications, recent works have demonstrated significant advancements. However, critical limitations still permeate nearly all published articles on the subject. First, it is worth noting that most recent studies focus predominantly on intensification devices. Nonetheless, the potential for heat recovery through the sole intensification of HEX is constrained by several factors: (i) intensification primarily only increases the overall heat transfer coefficient; (ii) the increase in the overall heat transfer coefficient is pronounced only when the dominant thermal resistance is located

on the intensified side; and (iii) intensification devices drastically escalate pressure drop, (iv) HEX with multiple tube passes and in presence of significant temperature cross, (v) altered flow distribution in stream splits can lead to velocities falling outside the recommended range (important to overcome problematic fouling operations, erosion and vibration).

Most of these limitations are not addressed in the existing literature due to the exclusion of HEX geometry considerations, except for Pan *et al.* (2018). However, the example explored in that work does not account for HEXs experiencing temperature cross. In addition, to mitigate the limitations related to the increase of heat transfer rate through an intense rise in the pressure drop, the authors proposed a series of intricate interventions for existing HEXs. For instance, intensifying the shell-side, adjusting baffle spacing, modifying the number of passes on both the shell and tube sides, among other changes, often require extensive procedures such as tube bundle cutting, shell and tubesheet modifications, retubing the bundle, altering heads or endplates and others. These interventions, from a practical standpoint, reintroduce the complexities and challenges of implementation that were previously used to justify avoiding topological modifications.

Even when accepting these considerations, the potential for heat recovery remains inherently limited when the addition of new heat transfer area to existing HEXs is not taken into account. As highlighted in section 3, the retrofit of a single HEX may be a complex task, due to the multitude of possible alternatives. These options may include enhancing the existing exchanger, adding a new unit either in series or in parallel (with the new unit potentially having a different geometry or even being of a different type), or completely replacing the existing exchanger with a new one. It was demonstrated in section 3 that incorporating more detailed options yields significant economic benefits.

To incorporate a more comprehensive HEX retrofit, it is essential, as previously demonstrated, discussed by Wang *et al.* (2012), and corroborated by the results of this study, to employ the modeling of the thermofluid dynamic behavior of the HEX simultaneously with the HEN retrofit. Among the recent paper published about HEN retrofit, only Pan *et al.* (2018) did not assumed a known and fixed overall heat transfer coefficient in the evaluation of the additional heat transfer area, instead of calculating the heat transfer coefficients and pressure drop using correlations according to the HEX dimensions. However, the modeling approach employed by Pan *et al.* (2018) relies on regression methods applicable exclusively to a fixed and predefined HEX geometry.

The need to explore the addition of new HEXs associated with the HEN retrofit with a different geometry or may even with a different HEX type demands the inclusion of

predictive thermofluid dynamic models into the problem formulation. This integration introduces severe nonlinearities and disjunctions, rendering the problem formulation and solution refractory to conventional mathematical programming approaches.

This chapter aims to build on the advances presented in section 2 by fully integrating the retrofit of an individual HEX into a comprehensive framework for the simultaneous HEN retrofit. The resultant HEN retrofit optimization tool with the complete design of new HEX is novel and can provide more realistic solutions, when compared with previous approaches in the literature.

The structure of this chapter is organized as follows. Firstly, the problem statement and the improvements proposed in this work are presented. This is followed by a detailed description of the HEN retrofit procedure based on heat load optimization associated with detailed HEX design. Then, results are shown to demonstrate the power of the proposed approach. Finally, conclusions are presented.

4.2. Problem Statement

The HEN retrofit investigated in this paper is defined by: for a given set of hot and cold streams with their physical properties, inlet and outlet temperatures, cold and hot utility streams, existing HEXs and their basic geometric data, identify the set of new heat loads to increase the energy recovery and the associated dimensions and configuration of the additional thermal equipment to maximize a certain economic objective function, such as, NPV or IRR.

The proposed procedure involves the following features:

1. All geometric variables relevant to the thermofluid dynamic calculations of the existing HEX and for its intervention are considered.
2. Thermofluid dynamic calculations, including flow velocity, pressure drop, and heat transfer coefficients are performed in detail using established models from the literature (e.g., Bell-Delaware method for the shell-side and Dittus-Boelter for the tube-side).
3. The HEX retrofit associated with each heat load modification in the HEN retrofit, aimed at modifying the thermal duty of the existing HEXs, is conducted by evaluating a wide

range of options and different exchanger types (shell-and-tube heat exchangers, STHE, and gasketed-plate heat exchangers, GPHE):

- 3.1. Replacing the existing HEX with a new one
- 3.2. Intensifying the existing HEX
- 3.3. Adding a new unit in series
- 3.4. Adding a new unit in parallel

4. All alternatives presented in the item 3 are evaluated using their complete thermofluid dynamic models, as discussed in item 2. The new unit may have a different geometry from the existing one (or be of other type at all), resulting in a new HEX with different flow velocity, pressure drop, and heat transfer coefficients, which enables aligning a new heat exchanger with the existing one, selecting a type and geometry that better suit to the new service requirements. The design of the new unit considers a broad range of independent variables that define its geometry and is executed through a procedure ensuring global optimality.

5. HEX retrofit calculations take into account velocity constraints, which are crucial for preventing fouling, erosion, and/or vibration issues.

6. The trade-off between the operational cost associated with pressure drop and the investment cost of HEX retrofit is appropriately considered.

7. The calculation of LMTD and correction factor are properly performed considering the possibility of multiples passes and/or multiples shells.

8. If the correction factor in STHE is smaller than 0.75 (a critical condition for ensuring proper equipment operation, Taborek (2008), Cao (2010)) and/or it is not feasible to meet requirements with a single shell, the need for multiple shells is considered. Additionally, the constraint that each shell size is limited by a maximum area (Smith, 2005) is also included to provide realistic solutions, as a consequence, this constraint may imply the presence of multiple shells in the optimal solution.

9. Despite the added nonlinearity and complexity of the problem, the procedure does not present convergence issues, does not require initialization or parameter tuning, and can be solved using any global deterministic optimizer that does not require derivatives (e.g., DIRECT, Jones (2021)) with a reasonable computational time.

10. The procedure effectively handles any objective function, including IRR, ROI, NPV, etc.

Thus, it is evident that this chapter addresses various limitations present in the literature. As previously discussed, among the studies conducted up to this date, the work of

Pan *et al.* (2018) provides the most detailed calculations. However, this study introduces several advancements, as highlighted by items 2, 3, 4, 5, 6, 8, 9 and 10.

The assumptions adopted in this work are listed below:

1. The streams have constant physical properties.
2. The HEN retrofit is conducted through the modifications of the heat loads of the existing heat exchanges associated with the existing HEXs, but without topological modifications.
3. The network is represented by the Synheat superstructure, as proposed by Yee and Grossmann (Yee and Grossmann, 1991). Furthermore, isothermal mixing is assumed.
4. There are only process streams without phase change.

4.3. HEN Retrofit Procedure

Since the HEN retrofit does not consider topological modifications, the procedure consists of exploring a utility path in order to reduce the energy consumption of the existing network. As energy recovery increases, the investment cost also increases, and the goal is to find the optimal solution that maximizes the enterprise profit (NPV, IRR, or another economic metric). In addition, if the network has energy loops, it can also be explored to attain a different energy distribution that minimizes the investment cost for the same utility consumption.

First, a summarized presentation of the problem and solution procedure for HEX retrofit will be provided. The technique applied in this procedure is entirely based on the methodology presented in section 3, which demonstrates a detailed HEX retrofit approach. Thus, while a general overview is provided here, the details are left to be consulted in the original chapter.

After presenting the HEX retrofit, the HEN retrofit without energy loops is presented first, for illustrative purposes. For a given utility consumption, networks with this characteristic have a single energy distribution across the HEN that satisfies the energy balance in all streams. In other words, given a certain utility consumption, the heat loads and the inlet and outlet temperatures (applicable to isothermal mixing, which is assumed in this work) of the streams in all HEXs can be determined directly.

Therefore, for a given level of energy recovery (or utility consumption), the new heat load applied to the existing heat exchangers can be readily calculated, allowing for the detailed retrofit of each HEX using the algorithm presented in section 3. Networks with this feature were explored by Chang *et al.* (2020) and called as Minimal Structures (MSTR).

4.3.1. HEX retrofit

Given an existing HEX that is subject to a new operational condition different from the original task (e.g. different temperatures, mass flow rates, physical properties or different streams), the HEX retrofit consists of identifying the necessary modifications in the existing HEX to adapt it to the new thermal service.

The following retrofit alternatives are considered in the problem: (i) replacing the existing HEX for a new STHE; (ii) replacing the existing HEX for a new GPHE; (iii) inserting twisted-tape in the existing HEX; (iv) inserting coil-wire in the existing HEX; (v) installing a new STHE in series; (vi) installing a new GPHE in series; (vii) installing a new STHE in parallel; or (viii) installing a new GPHE in parallel.

The design formulation of a new STHE, which can be installed in series, in parallel or used to replace the original HEX is now presented. The basic geometric variables employed to characterize a STHE in the optimization are: outer tube diameter (d_{te}), shell diameter (D_s), tube length (L), number of baffles (N_b), number of tube passes (N_{tp}), tube pitch ratio (rp), and tube layout (lay). The tube thickness and the baffle cut are considered constant. The shell is a E-type, i.e. a single shell-side pass (TEMA, 1999).

The design constraints of the problem encompass the ratio between the tube length (L) and shell diameter (D_s), which must obey the following bounds (Taborek, 2008):

$$3 D_s \leq L \leq 15 D_s \quad (4.1)$$

Additionally, the baffle spacing (lbc) must be bounded in relation to the shell diameter (Taborek, 2008):

$$0.2 D_s \leq lbc \leq 1 D_s \quad (4.2)$$

The area per shell is limited to a maximum value (Smith, 2005):

$$A \leq \hat{A}_{max} \quad (4.3)$$

where the value of \hat{A}_{max} adopted in the examples explored here was 1000 m².

In addition, lower bounds on tube-side and shell-side flow velocities (vt and vs) are established to avoid fouling and upper bounds are established to avoid vibration and erosion:

$$\widehat{vsmin} \leq vs \leq \widehat{vsmax} \quad (4.4)$$

$$\widehat{vtmin} \leq vt \leq \widehat{vtmax} \quad (4.5)$$

Due to operational issues, the correction factor needs to be higher than a minimum value (Taborek, 2008; Cao, 2010):

$$F \geq 0.75 \quad (4.6)$$

The relation between the heat load (Q) and the required heat transfer area (A_{req}) is based on the *LMTD* method:

$$Q = U A_{req} LMTD F \quad (4.7)$$

where A_{req} is the required area.

The heat transfer area must be higher than the required area, including a design margin represented by an excess area, \hat{A}_{exc} :

$$A \geq \left(1 + \frac{\widehat{A}_{exc}}{100}\right) A_{req} \quad (4.8)$$

where A is the heat transfer area of the STHE, given by:

$$A = NTT \pi Dte L Ns \quad (4.9)$$

where NTT and NS are the number of tubes per shell and the number of shells.

In turn, for a GPHE, the independent design variables are: total number of plates (Nt), plate size (defined by the plate length, Lp , plate width, Lw , and port diameter, Dp), Chevron

angle (β), and number of passes of each stream (Nph and Npc , respectively). Due to the commercial availability and/or physical nature of the design variables, their values must be selected among a set of discrete options. The plate thickness, the surface enlargement factor and the mean channel spacing are fixed parameters associated with the plate type and are not included in the optimization.

The design constraints of the problem are the bounds on flow velocities on the hot and cold stream velocities (vh and vc):

$$\widehat{vcmin} \leq vc \leq \widehat{vcmax} \quad (4.10)$$

$$\widehat{vhmin} \leq vh \leq \widehat{vhmax} \quad (4.11)$$

The relation between the heat load and the required heat transfer area given by Eqs. (4.7) and (4.8) are also constraints in the GPHE design optimization. The heat transfer area of a GPHE is given by:

$$A = (Np - 2) \phi L_w L_p \quad (4.12)$$

where ϕ is the enlargement factor.

Implementing shell-side intensifications or used finned tube in existing HEXs can be difficult to use in practice. Thus, it is considered only tube insert intensification, using twisted-tape and coil wired. The design variables are only the twisted-tape pitch (H) and thickness (δ) for the twisted-tape intensification, and the coiled-wire helical pitch (P_{cl}) and diameter (E_{cl}) for the coiled-wire intensification.

The problem constraints, along with those presented for the STHE, form an additional set of geometric constraints for each intensification device. The geometric constraints for Twisted-Tape insert are bounds on the twist ratio y and thickness δ (Jiang *et al.*, 2014):

$$3 \geq y \geq 6 \quad (4.13)$$

$$0.02 \geq \delta \geq 0.04 \quad (4.14)$$

$$y = \frac{H}{dti} \quad (4.15)$$

In addition, for the Coiled-Wire insert, the geometric constraints are bounds on the helical pitch, P_{CI} , and the helical angle, α_{CI} (Jiang *et al.*, 2014):

$$1.17 \geq P_{CI} \leq 2.68 \quad (4.16)$$

$$32 \geq \alpha_{CI} \leq 61 \quad (4.17)$$

Although other types of intensification are not commonly used in industrial practice, they can be readily included in the procedure if the user wishes to take them into account.

Thus, for a given new service, all HEX retrofit alternatives cited in this subsection is tested, and the optimal solution is the best one between them. The HEX retrofit objective function for all alternatives is given by:

$$\min TAC = \hat{r} C_{cap} + C_{op,h} + C_{op,c} - \hat{C}_{op,existing} \quad (4.18)$$

where $\hat{C}_{op,existing}$ is the operational cost in the existing HEX in the original condition (i.e. before the retrofit) and C_{cap} is the capital cost, given by:

$$C_{cap} = \widehat{CF} + \hat{a} A_{new}^{\hat{b}} \quad (4.19)$$

where \widehat{CF} is a fixed cost, \hat{a} and \hat{b} are the area cost parameters, and A_{new} is the HEX area.

In addition, \hat{r} is the annualization factor and C_{op} is the operational cost, given by the following equations:

$$\hat{r} = \frac{\hat{i} (1 + \hat{i})^{\hat{n}}}{(1 + \hat{i})^{\hat{n}} - 1} \quad (4.20)$$

$$C_{op} = \widehat{Nop} \frac{\widehat{pc}}{10^3} \left(\frac{\Delta P \widehat{m}}{\hat{\eta} \hat{\rho}} \right) \quad (4.21)$$

where \hat{i} is the interest rate, \hat{n} is the project horizon in years, \widehat{Nop} is the number of operating hours per year, \widehat{pc} is the energy price, $\hat{\eta}$ the pump efficiency, ΔP is the stream pressure drop, \widehat{m} is the stream mass flow rate and $\hat{\rho}$ is the density.

Since the detailed steps of the HEX retrofit will not be presented here, it is worth reiterating some aspects:

i) The design of a new HEX, which will align with the existing unit or replace the existing one, is defined by a search space encompassing all its independent variables that

determine its geometry. This search space consists of a set of discrete values, consistent with the way these components are commercially available. This approach allows the new exchanger to differ in geometry and type from the existing one. All design variables affect the heat transfer coefficients, pressure drop and the investment cost of the new HEX, allowing the new unit to better adapt to the new service, particularly enabling the exploration of the trade-off between investment and operational costs. It was demonstrated in section 3 the significant impact of this in the retrofit of individual HEX, and this chapter also highlights its relevance in network retrofit.

ii) Thermofluid-dynamic calculations are performed in detail, considering exchanger geometry and using reliable models for STHE and GPHE exchanger modeling. This eliminates the need to assume known and constant convection coefficients—an assumption that is often arbitrary and prone to significant error.

iii) The LMTD, its correction factor and flow velocities calculations are incorporated within the optimization constraints.

iv) The trade-off between the capital cost of the HEX and the operational cost associated with the pressure drop associated with the streams flow is accounted for in the objective function, as shown in Eq. (4.18).

4.3.2. MSTR HEN retrofit

As previously discussed, the retrofit procedure for an MSTR network involves utilizing a utility path to increase heat recovery. Given a new level of utility consumption, the heat and temperature distribution of all HEX units and streams can be determined, establishing the new heat loads applied to each one. Consequently, for a given level of consumption, the HEX retrofit algorithm can be executed to derive both the investment cost and the value of the objective function.

Thus, the retrofit of a MSTR effectively becomes a one-dimensional optimization, where the search variable is the energy recovery and the objective function evaluation is performed using the aforementioned procedure. Due to the inherent nonlinearity and discontinuities within the problem, the global optimizer DIRECT (Jones *et al.*, 2021) is employed.

Because DIRECT is a bounded search, it is necessary to define the utility consumption limits, the upper bound is equivalent to that of the existing network, \widehat{E}_{hu}^{curr} , and the minimum consumption is determined by the *PEMin* model (Chang *et al.*, 2020), presented below:

$$PEMin = \underset{\forall(T, Q) \in D_{synheat}}{Min} Ehu \quad (4.22)$$

s.t.

$$Ehu = \sum_{j \in CP} qhu_j \quad (4.23)$$

$$z_{i,j,k} = 1 \quad \forall (i, j, k) \in STR_{match} \quad (4.24)$$

$$z_{i,j,k} = 0 \quad \forall (i, j, k) \notin STR_{match} \quad (4.25)$$

$$zhu_j = 1 \quad \forall (j) \in STR_{heater} \quad (4.26)$$

$$zhu_j = 0 \quad \forall (j) \notin STR_{heater} \quad (4.27)$$

$$zcu_i = 1 \quad \forall (i) \in STR_{cooler} \quad (4.28)$$

$$zcu_i = 0 \quad \forall (i) \notin STR_{cooler} \quad (4.29)$$

where *STR* is a set of binary variables that identifies the existing matches of the structure, given by:

$$STR = STR_{match} \cup STR_{cooler} \cup STR_{heater} \quad (4.30)$$

The *PEMin* is a linear programming (LP) problem, thus the global optimal solution is guaranteed. The solution of the *PEMin* problem gives the minimum energy consumption, Ehu_{min} , of the structure and defines the search space limits of the HEN retrofit problem $[Ehu_{min}, \widehat{E}_{hu}^{curr}]$.

To evaluate the objective function at each optimization point, it is necessary to determine the heat loads and temperature distribution for a given level of heat recovery. This can be achieved using the *PESTR* model (Chang *et al.*, 2020):

$$\forall (T, Q) \in D_{synheat} \quad (4.31)$$

$$\widehat{Ehu} = \sum_{j \in CP} qhu_j \quad (4.32)$$

$$z_{i,j,k} = 1 \quad \forall (i, j, k) \in STR_{match} \quad (4.33)$$

$$z_{i,j,k} = 0 \quad \forall (i, j, k) \notin STR_{match} \quad (4.34)$$

$$zhu_j = 1 \quad \forall (j) \in STR_{heater} \quad (4.35)$$

$$zhu_j = 0 \quad \forall (j) \notin STR_{heater} \quad (4.36)$$

$$zcu_i = 1 \quad \forall (i) \in STR_{cooler} \quad (4.37)$$

$$zcu_i = 0 \quad \forall (i) \notin STR_{cooler} \quad (4.38)$$

$$STR = STR_{match} \cup STR_{cooler} \cup STR_{heater} \quad (4.39)$$

Because the utility consumption is fixed and the network is a MSTR, the *PESTR* model does not have any degree of freedom and it consists of solving the set of synheat constraints, fixing the utility consumption and binary variables, which corresponds to a system of linear equations.

Therefore, the optimization procedure for retrofitting an MSTR network involves the following steps:

1. Given an existing HEN, calculate the minimum utility requirement Ehu_{min} by solving the PEMin model.
2. Run the DIRECT solver with bounds set between Ehu_{min} and the original consumption of the existing network.

3. At each point in the DIRECT, a specific utility consumption E_{hu} is provided, allowing for the calculation of the network heat load and temperature distribution by solving the PESTR model.

4. Once the PESTR model is solved, the thermal loads, inlet and outlet temperatures of all streams across each heat exchanger are determined. Then, each HEX in the HEN is evaluated and retrofitted using the procedure proposed in section 3.

4.3.3. Non MSTR HEN retrofit

The procedure methodology for non MSTR HEN retrofit is analogous. The main difference, however, is that the energy loop presence does not allow the heat and temperature distribution determination only fixing the energy recovery. One degree of freedom is added to the problem for each independent loop in the structure. Thus, to solve the HEN energy balance, it is necessary to fix the utility consumption plus n variables, where n is the number of independent energy loops.

A variable that can be used to represent the degree of freedom associated with each loop is the heat load of one HEX belonging to that loop. Let q_{ijk}^* represent the heat duty of a given exchanger in each loop. The network heat load and temperature distribution can then be determined by solving the PESTRR model presented below.

$$\forall (T, Q) \in D_{synheat} \quad (4.40)$$

$$\widehat{E}_{hu} = \sum_{j \in CP} q_{hu_j} \quad (4.41)$$

$$q_{i,j,k} = \widehat{q}_{ijk}^* \quad \forall (i, j, k) \in M^* \quad (4.42)$$

$$z_{i,j,k} = 1 \quad \forall (i, j, k) \in STR_{match} \quad (4.43)$$

$$z_{i,j,k} = 0 \quad \forall (i, j, k) \notin STR_{match} \quad (4.44)$$

$$zhu_j = 1 \forall (j) \in STR_{heater} \quad (4.45)$$

$$zhu_j = 0 \forall (j) \notin STR_{heater} \quad (4.46)$$

$$zcu_i = 1 \forall (i) \in STR_{cooler} \quad (4.47)$$

$$zcu_i = 0 \forall (i) \notin STR_{cooler} \quad (4.48)$$

$$STR = STR_{match} \cup STR_{cooler} \cup STR_{heater} \quad (4.49)$$

where M^* is the set of matches that represent the selected HEX of each loop. Similar to PESTR, the PESTRR model does not require an optimization procedure.

Thus, optimizing a non-MSTR network involves a search over both energy recovery and the heat duty of these selected matches of each loop. Consequently, like energy recovery, it is essential to establish limits for these thermal loads, $qmin_{ijk}^*$ and $qmax_{ijk}^*$, which can be determined using the *PQMin* and *PQMax* models presented below.

$$PQMin = \underset{\forall (T, Q) \in D_{synheat}}{Min} q_{i,j,k}^* \quad (4.50)$$

s.t.

$$z_{i,j,k} = 1 \forall (i, j, k) \in STR_{match} \quad (4.51)$$

$$z_{i,j,k} = 0 \forall (i, j, k) \notin STR_{match} \quad (4.52)$$

$$zhu_j = 1 \forall (j) \in STR_{heater} \quad (4.53)$$

$$zhu_j = 0 \forall (j) \notin STR_{heater} \quad (4.54)$$

$$zcu_i = 1 \forall (i) \in STR_{cooler} \quad (4.55)$$

$$zcu_i = 0 \forall (i) \notin STR_{cooler} \quad (4.56)$$

$$STR = STR_{match} \cup STR_{cooler} \cup STR_{heater} \quad (4.57)$$

On the other hand, the *PQMax* is analogous, but maximizing $q_{i,j,k}^*$ instead. Both problems consist of LP optimization, where the global optimal solution is guaranteed.

Finally, the determination of the HEXs in the loops can be done using the algorithm called PLOC. If the HEX does not participate in any loop, for a given *Ehu*, there is only one feasible heat duty. On the other hand, if the HEX participates in a loop, for a given *Ehu* there are different values of its heat duty that mathematically solves $D_{synheat}$.

The central idea for identifying whether a given match participates in an energy loop involves attempting to solve the HEN energy balance by fixing its heat load to a slightly different value than a previously determined one. If a feasible solution to the Synheat constraints is found, then the match is part of an energy loop. Otherwise, if only a single viable heat load exists, the HEX does not participate in any loop. Therefore, *PLOC* algorithm is described below:

Step 1) Create an empty list of independent HEX that participates on each loop. This list will contain only one HEX for each loop.

Step 2) Initialize the HEN variables (temperatures and heat loads) with any feasible solution that satisfies $D_{synheat}$ (the existing heat loads and temperature distribution of the existing HEN can be used).

Step 3) Select an untested HEX of the HEN and solve the *PESTRR* model fixing the heat load of this match as the current value plus a small value.

Step 4) If the solution in Step 3 is feasible, then the selected HEX participates of a loop. Thus, add it in the list, and fix its heat load for the next tests.

Step 5) If not all HEXs have been tested yet, return to Step 3. Otherwise, stop the procedure and the list contains one independent HEX for each loop.

Therefore, for a given non-MSTR, the procedure consists of:

- (i) Identify the Ehu_{min} solving the *PEMin* problem,
- (ii) Identify the HEXs for each independent loop solving the *PLOC* algorithm,
- (iii) Determine the minimum and maximum heat loads of the HEXs in the loop by solving *PQMin* and *PQMax*.

Once all of these information are obtained, a multidimension optimization using DIRECT can be performed to identify the optimal values of *Ehu* and $q_{i,j,k}^*$ for all HEXs

associated with the loops. The optimization is bounded between the minimum values $\{Ehu_{min}, qmin_{i,j,k}^*\}$ and maximum values $\{\overline{E}_{hu}^{curr}, qmax_{i,j,k}^*\}$.

Because $qmin_{i,j,k}^*$ and $qmax_{i,j,k}^*$ depend on the Ehu , during the optimization it is possible that a set of $q_{i,j,k}^*$ and Ehu gives an infeasible *PESTRR* solution. In this case, a penalization is applied.

Remark 1: Although it requires solving several mathematical programming problems, each one is a LP model, ensuring global optimum and exhibit a fast convergence. Furthermore, except for *PESTR* (or *PESTRR*, depending on the HEN type), all other models are solved only once. The *PESTR* model, in particular, does not require optimization and can be solved using an efficient linear system solution method. Which means that there are no numerical or convergence problems associated with none of these steps.

Remark 2: The numerical and computational complexity resulting from the proposed enhancements and level of detail is primarily concentrated in the HEX retrofit phase. At this stage, the temperatures and heat loads of all HEXs (i.e., their new thermal service) are already determined, eliminating the need for mathematical programming or any other numerical procedures that could compromise robustness at this point. In essence, for each point in the optimization, every HEX in the network is assessed, and all retrofit alternatives, complete with detailed modeling, are implemented through a robust, efficient algorithm that ensures global optimality (see section 3).

Remark 3: It is essential to emphasize that the cornerstone of this proposed procedure lies in its ability to seamlessly handle any retrofit option, regardless of its complexity, non-linearity, or convergence challenges. If a user wishes to consider additional retrofit alternatives—such as other types of intensification, series-parallel arrangements, or different exchangers like double-pipe HEX or welded plate HEX, an additional option can be simply added in the HEX retrofit phase. Several equipment configurations have already been explored for grassroots problems using Set Trimming (Lemos *et al.*, 2020; Nahes *et al.*, 2021; Sales *et al.*, 2021; Chang *et al.*, 2022). The only trade-off of adding more options is an increase in computational effort, without compromising the method convergence capabilities. As will be shown later, when the HEN retrofit does not involve topological changes, it achieves convergence in remarkably low computational times for real industrial scenarios.

4.4. Results

Two HEN retrofit examples are presented in this chapter. The STHE model employs the Bell-Delaware method for the shell-side evaluation of the heat transfer coefficient and pressure drop (Taborek, 2008) and the Dittus and Boelter correlation for the evaluation of the convective heat transfer coefficient in the tube-side (Incropera, 2007). It can address the possibility of multiple shells, associated with an E-shell type. The thickness and thermal conductivity of the tubes are equal to 1.22 mm and 50 W/(m·K), respectively.

The GPHE is composed of Chevron-type plates. The thermofluid-dynamic model employed to describe the behavior of the heat exchanger is based on Kakaç and Liu (2002). The plates have thickness and thermal conductivity equal to 0.8 mm and 16.2 W/(m²K), respectively. The enlargement factor associated with the corrugations is 1.15 and the mean channel spacing is 3 mm.

The design variables that represent the search space of each type of HEX are depicted in Tables 4.1, 4.2, 4.3, and 4.4.

Table 4.1. STHE search space

Design variable	Values
Shell diameter (m)	0.2050, 0.3048, 0.3874, 0.489, 0.5906, 0.6858, 0.7874, 0.8382, 0.889, 0.9398, 0.9906, 1.0668, 1.143, 1.2192, 1.3716, 1.524
Outer diameter (m)	0.00635, 0.009525, 0.0127, 0.01905, 0.0254, 0.03175, 0.0381, 0.05080
Number of tube passes	1, 2, 4, 6
Pitch ratio	1.25, 1.33, 1.5
Tube layout	Triangular, square
Tube length (m)	1.2195, 1.8293, 2.439, 3.0488, 3.6585, 4.8768, 6.0976
Number of baffles	1,2,3,...,18,19,20

Source: Author's own work, 2024.

Table 4.2. GPHE search space

Design variable	Values
Number of plates	10,11,12,...,798,799,800
Plate size alternatives (Table 7)	1,2,3,4,5,6,7,8,9,10
Chevron angle (deg)	30, 45, 50, 60, 65
Hot and cold number of passes	1, 2

Source: Author's own work, 2024.

Table 4.3. Tube insert search space

Design variable	Values
Twisted-Tapes pitch (m)	From 0.0315 m to 0.3325 m, in increments of 12.7 mm
Twisted-Tapes thickness (m)	From 0.0005 m to 0.004 m, in increments of 0.5 mm
Helical Pitch (m)	0.02, 0.031955, 0.044179, 0.056402, 0.064
Coil-Wire diameter (m)	0.001, 0.0012, 0.0014, 0.0016, 0.0018, 0.0020

Source: Author's own work, 2024.

Table 4.4. Plate dimensions from an industrial supplier (C. J. Mulanix Company, Inc., 2022).

Alternative	Plate length (m)	Plate width (m)	Port diameter (m)
1	0.743	0.845	0.300
2	0.978	0.812	0.288
3	1.281	1.200	0.400
4	1.500	1.220	0.350
5	1.835	0.945	0.300
6	2.092	1.200	0.400
7	1.551	0.909	0.285
8	0.400	0.125	0.03
9	1.845	0.450	0.155
10	1.543	0.812	0.283

Source: Author's own work, 2024.

The cost parameters to evaluate the investment cost of each type of HEX is depicted in Table 4.5.

Table 4.5. Economic parameters

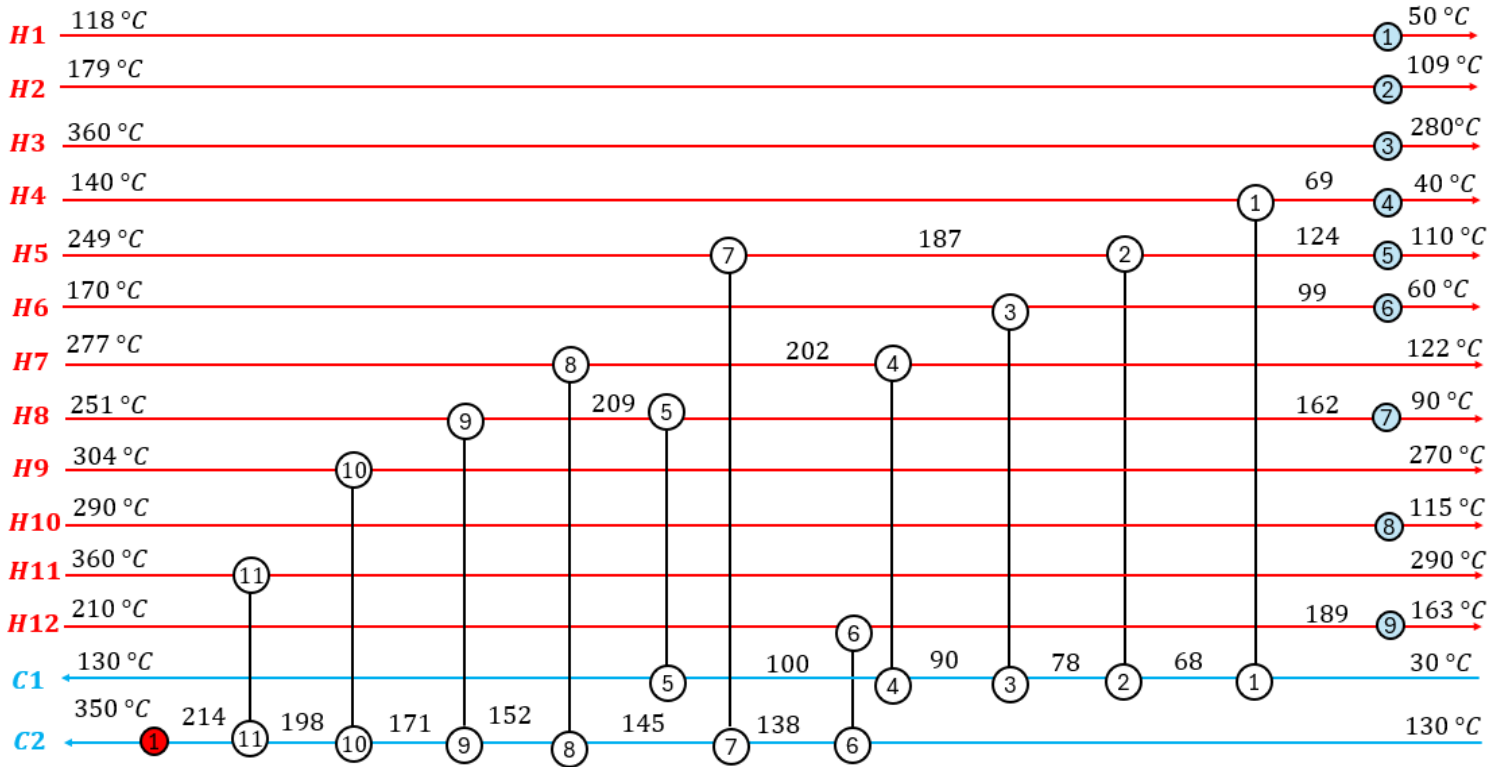
HEX type	Fixed cost	Area cost coefficient	Exponent cost coefficient
STHE (Hajabdollahi <i>et al</i> , 2016)	8500	409	0.85
GPHE (Hajabdollahi <i>et al</i> , 2016)	0	635.15	0.778
Tube insert (Pan <i>et al</i> , 2018)	500	50	1

Source: Author's own work, 2024.

In addition, it is considered a time horizon of 10 years, an electric energy price of 0.15 \$/kWh, a pump efficiency of 60%, an interest rate of 10% and a number of operating hours per year of 7500 h/y. The physical properties and other important information (density, viscosity, thermal conductivity, heat capacity and fouling factor) of the streams are available in Supplementary Material. Both examples consider cooling water as cold utility, the supply and return temperatures for the cooling water in Example 1 are 20 °C and 30 °C, the corresponding values of Example 2 are 38 °C and 53 °C. Since the solutions for the examples did not involve interventions in the utility HEX, their dimensions are provided only in the Supplementary Material to facilitate the readability of the thesis.

4.4.1. Example 1

Example 1 is the retrofit of a HEN based on a crude preheat train, originally proposed by Bagajewicz *et al.* (2013). The unit throughput is 8330 ton/day of a crude oil with an API of 31.8°. It is composed of 12 hot streams and 2 cold streams (the crude oil before and after the desalter). Currently, the furnace heats the crude from 234.8 to 350 °C, with a furnace utility of 39.09 MW. The existing HEN is presented in Figure 4.1.

Figure 4.1: Crude oil preheating train existing HEN.

Source: Bagajewicz *et al.*, 2013.

The stream and existing HEX data are presented in Tables 4.6 and 4.7, and the details of existing HEX are depicted in Table 4.8.

Table 4.6. Example 1: Streams data

Stream	Inlet temperature (°C)	Outlet temperature (°C)	Mass flow rate (kg/s)	Heat capacity (J·kg ⁻¹ ·K ⁻¹)
Hot streams				
H1	117.7	50.0	42.00	2921.4
H2	178.6	108.9	19.13	2477.5
H3	359.6	280.0	7.67	3156.5
H4	140.0	40.0	46.29	2293.9
H5	248.8	110.0	12.73	2513.4
H6	170.1	60.0	14.74	2292.9
H7	277.0	121.9	9.84	2551.3
H8	250.6	90.0	55.10	2375.7
H9	303.6	270.2	81.01	2888.2
H10	290.0	115.0	23.24	1204.1
H11	360.0	290.0	23.42	2830.9
H12	210.0	190.0	46.30	2544.5
Cold streams				
C1	30.0	130.0	96.41	2074.3
C2	130.0	350.0	96;64	2202.0

Source: Bagajewicz *et al.*, 2013.

Table 4.7. Example 1: HEX information in the existing HEN

HEX	1	2	3	4	5	6
Q (kW)	7530	2000	2400	2000	6070	3230
<i>Thi</i> (°C)	140.0	186.6	170.1	201.6	208.8	210.0
<i>Tho</i> (°C)	69.1	124.1	99.1	121.9	162.4	189.1
<i>Tci</i> (°C)	30.0	67.6	77.65	89.6	99.6	130.0
<i>Tco</i> (°C)	67.65	77.6	89.65	99.6	130	138.5
LMTD (°C)	54.0	79.9	44.6	60.5	70.5	65.1
<i>F</i>	0.96	1	0.92	0.96	0.95	0.99
HEX	7	8	9	10	11	
Q (kW)	1990	1880	5470	7800	4640	
<i>Thi</i> (°C)	248.8	277.0	250.6	303.6	360.0	
<i>Tho</i> (°C)	186.6	201.6	208.8	270.2	290.0	
<i>Tci</i> (°C)	138.5	145.4	152.0	171.0	198.1	
<i>Tco</i> (°C)	145.4	152.0	171.0	198.1	214.3	
LMTD (°C)	72.2	86.0	67.5	102.3	116.7	
<i>F</i>	1	1	0.97	0.98	0.98	

Source: Bagajewicz *et al.*, 2013.

Because gasketed-plate heat exchangers are not used in this type of process, it is not considered adding a GPHE during the HEX retrofit. Thus, the alternatives involves replacing the existing one with a new STHE, adding a new STHE in series or parallel, or intensifying the existing HEX.

The retrofitted HEN, aiming at maximizing the NPV, obtained using the proposed procedure is presented in Figure 4.2.

The retrofit solution achieves a heat recovery of 7.6 MW, with an investment cost of 1,495,232 \$ associated with a total addition of 2,860 m² of area. The liquid cash inflow associated with the money saved per year is 769,041 \$, already considering a penalty of 53,819 \$ due to the increase in operational costs due to the larger pressure drop. The optimal NPV is 3,882,290 \$.

In addition, note that HEXs 10 and 11 does not participate in any energy loop or utility path. Consequently, their heat duties remain fixed. Thus, increasing energy recovery was achieved by raising the heat duties of HEXs 6, 7, 8, and 9. It is also observed that increasing the heat duty of these exchangers results in a significant increase in the temperature cross in HEX 9, leading to the need to add two additional shells in series with the existing one (enhancing this HEX cannot overcome the temperature cross issue).

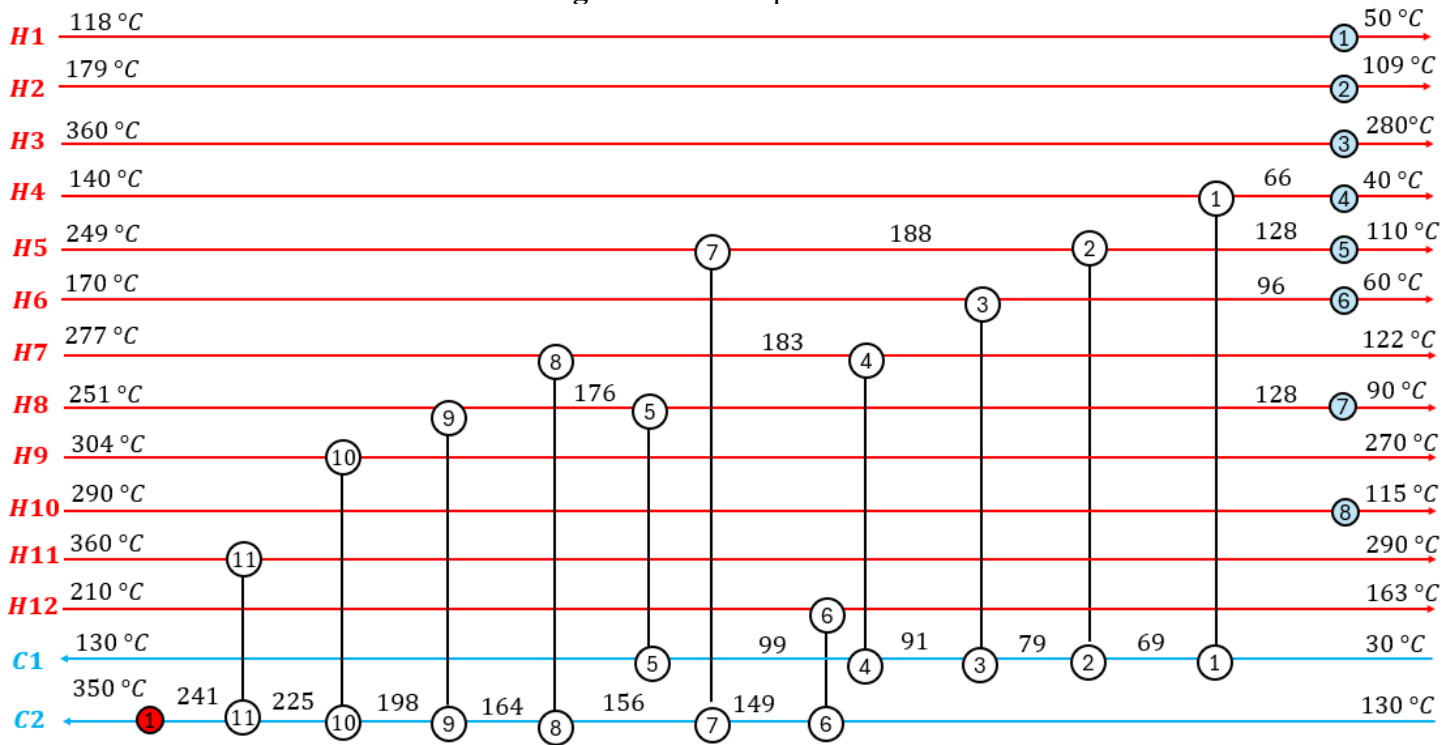
The results of the retrofit related to the HEXs are depicted in Tables 9 and 10.

Table 4.8. Example 1: Design variables of the existing HEXs

HEX	1	2	3	4	5	6
Area (m ²)	757.83	184.89	263.96	521.96	312.38	138.67
Number of shells	2	1	1	1	1	1
U (W/m ² K)	212.5	154.7	248.1	75.3	324.5	305.5
ΔPt_{total} (kPa)	88.0	84.9	100.6	76.9	64.8	26.3
ΔPs_{total} dte (m)	27.5	19.8	23.0	25.3	7.14	16.7
L (m)	0.03175	0.0127	0.0127	0.00635	0.0381	0.0254
Ds (m)	6.0976	6.0976	6.0976	3.0488	6.0976	3.0488
lay	1.143	0.489	0.7874	0.9906	1.143	0.889
Npt	Square	Square	Triangular	Square	Triangular	Square
rp	6	1	6	4	4	6
Nb	1.25	1.25	1.5	1.5	1.25	1.25
Ntt	13	19	7	5	8	5
Tube stream	623	760	1085	2582	428	570
	Cold stream	Cold stream	Hot stream	Hot stream	Cold stream	Hot stream
HEX	7	8	9	10	11	
Area (m ²)	382.08	330.89	363.28	290.91	145.42	
Number of shells	1	1	1	1	1	
U (W/m ² K)	81.14	76.72	262.56	298.54	310.07	
ΔPt_{total}	25.3	29.2	61.1	31.9	18.8	
ΔPs_{total} dte (m)	22.89	13.35	27.6	25.0	16.7	
L (m)	0.009525	0.009525	0.009525	0.0127	0.01905	
Ds (m)	3.0488	3.0488	3.6585	3.6585	3.0488	
lay	0.8382	0.8382	0.9909	0.9398	0.8382	
Npt	Square	Triangular	Square	Square	Square	
rp	1	1	2	2	6	
Nb	1.25	1.25	1.5	1.5	1.33	
Ntt	16	17	6	7	5	
Tube stream	3188	2627	2982	1993	797	
	Cold stream	Cold stream	Hot stream	Hot stream	Hot stream	

Source: Author's own work, 2024.

Figure 4.2. Example 1: Retrofitted HEN



Source: Author's own work, 2024.

Table 4.9: Example 1: HEX information in the retrofitted HEN.

HEX	1	2	3	4	5	6
Q (kW)	7869	1923.4	2501	1524.1	6181	5475.2
T_{hi} (°C)	140.0	188.3	170.1	182.6	175.9	210.0
T_{ho} (°C)	65.9	128.2	96.01	121.9	128.7	163.5
T_{ci} (°C)	30.0	69.3	79.0	91.5	99.1	130.0
T_{co} (°C)	69.3	78.9	91.5	99.1	130	149.0
LMTD (°C)	51.3	81.5	40.3	52.6	37.2	45.9
F^*	0.95	1	0.88	0.97	0.78	0.92
Retrofit alternative	-	-	Coil-wire installation	-	STHE series	STHE series
HEX	7	8	9	10	11	
Q (kW)	1934.4	2368.9	9776	7815	4641	
T_{hi} (°C)	248.8	277.0	250.6	303.6	360.0	
T_{ho} (°C)	188.3	182.6	175.9	270.2	290.0	
T_{ci} (°C)	149.0	155.5	163.9	197.8	225.0	
T_{co} (°C)	155.7	163.9	197.9	225.0	241.1	
LMTD (°C)	62.4	60.0	27.5	75.4	89.2	
F^*	1	1	Indeterminate	0.97	0.97	
Retrofit alternative	-	Coil-wire installation	STHE series	STHE parallel	STHE series	

Note 1: The correction factor presented in this table is its value considering the original HEX geometry (number of tube passes and number of shells).

Note 2: The indeterminate value in HEX 9 arises due to numerical error in calculating the correction factor, caused by the high degree of temperature crossover.

Source: Author's own work, 2024.

Table 4.10. Example 1: Design variables of the HEX retrofit solution

HEX	3	5	6	8	9	10	11
Added area (m ²)	0	338.65	344.70	0	1674.3	158.0	36.8
U (W/m ² K)	299.4	243.13	256.73	154.04	191.23	271.7	240.4
Number of shells added	0	1	1	0	2	1	1
Additional ΔPt	106.0	86.1	45.4	32.2	155	10.0	22.3
Additional ΔPs	0	13.6	34.9	0	92.8	24.0	24.3
dte (m)	-	0.0508	0.01905	-	0.01905	0.01905	0.0508
L (m)	-	6.0976	4.8768	-	6.0976	6.0976	3.6585
Ds (m)	-	1.3716	0.9906	-	1.3716	0.6858	0.7874
lay	-	Square	Square	-	Square	Triangular	Triangular
Npt	-	6	4	-	6	4	4
rp	-	1.25	1.33	-	1.33	1.33	1.5
Nb	-	10	6	-	10	13	5
Ntt	-	348	1181	-	2294	529	63
Helical Pitch (m)	0.064	-	-	0.056	-	-	-
Coil-Wire diameter (m)	0.0012	-	-	0.0014	-	-	-

Source: Author's own work, 2024.

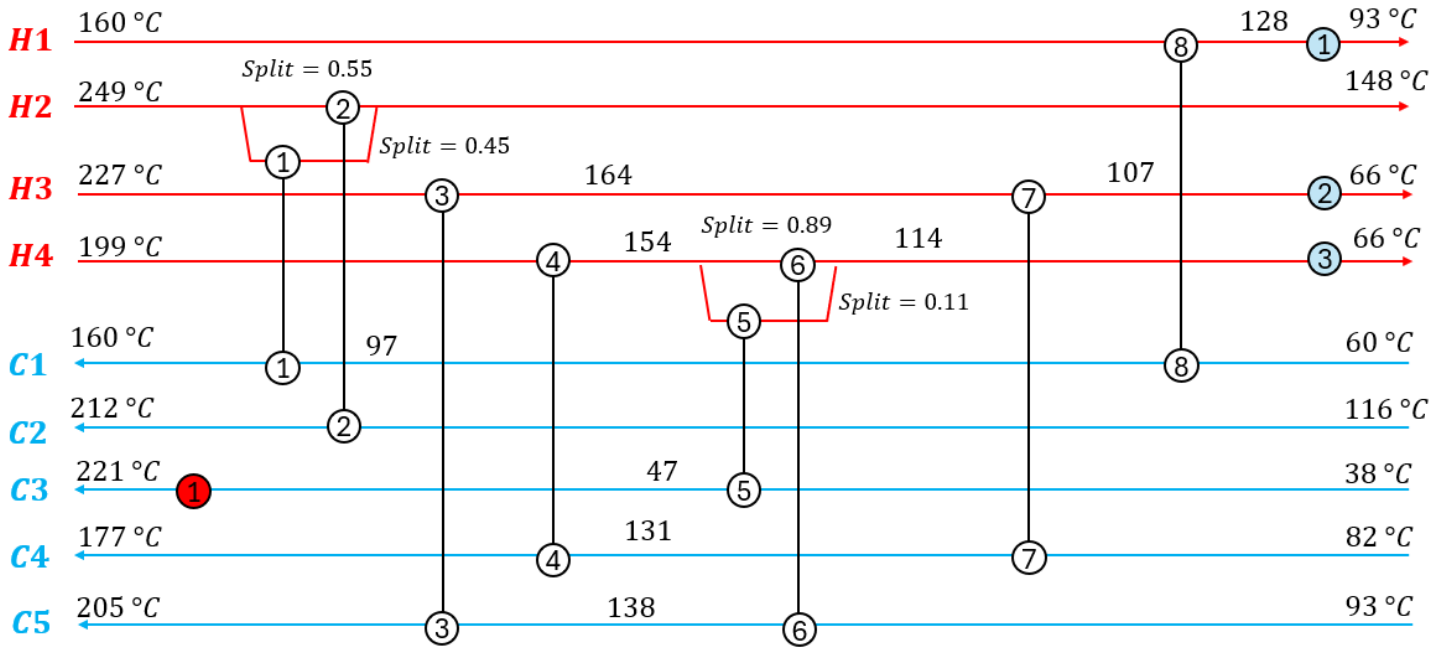
Notice the richness of the solution presented in Table 4.10, where varied retrofit options were proposed, and how a new STHE added can possess a different geometry from the existing one, resulting in distinct overall heat transfer coefficients and pressure drops. This indicates the importance of considering a more detailed HEX retrofit, since new degrees of freedom are included in the problem, allowing the identification of a new shell that is more suit to the new service.

4.4.2. Example 2

Example 2 is an existing HEN that involves 4 hot streams and 5 cold streams. The set of process and utilities streams is inspired in the data presented by Faria *et al.* (2015). Currently, the HEN consumes 15,402 kW of hot utility and 18,556 kW of cold utility. The

existing HEN is presented in Figure 4.3, and the streams data and HEX details are present in Tables 4.11, 4.12 and 4.13.

Figure 4.3. Example 2: Existing HEN



Source: Author's own work, 2024.

Table 4.11. Example 2: Streams data

Stream	Inlet temperature (K)	Outlet temperature (K)	Mass flow rate (kg/s)	Heat capacity ($\text{J}\cdot\text{kg}^{-1}\cdot\text{K}^{-1}$)
H1	160.0	93.0	34.53	2670
H2	249.0	148.0	47.76	2317
H3	227.0	126.0	63.94	2433
H4	199.0	66.0	74.11	2512
C1	60.0	160.0	38.01	2105
C2	116.0	212.0	35.86	1780
C3	38.0	221.0	44.13	2008
C4	82.0	177.0	78.89	2300
C5	93.0	205.0	68.52	2130

Source: Faria *et al.*, 2015.

Table 4.12: Example 2: Information of existing HEX in the original HEN

HEX	1	2	3	4
Q (kW)	5049	6129	9711	8296
<i>Thi</i> (°C)	249.0	249.0	227.0	199.0
<i>Tho</i> (°C)	148.0	148.0	164.4	154.4
<i>Tci</i> (°C)	96.9.0	116.0	138.5	131.3
<i>Tco</i> (°C)	160.0	212.0	205.0	177.0
<i>LMTD</i> (°C)	68.3.0	34.4	23.9	22.6
<i>F</i>	0.94	0.82	1	1
HEX	5	6	7	8
Q (kW)	814	6635	8940	2952
<i>Thi</i> (°C)	154.4	154.4	164.4	160.0
<i>Tho</i> (°C)	114.4	114.4	106.7	128.0
<i>Tci</i> (°C)	38.0	93.0	82.0	60.0
<i>Tco</i> (°C)	47.2	138.5	131.3	96.9
<i>LMTD</i> (°C)	90.9	18.6	28.7	65.52
<i>F</i>	1	0.89	0.83	0.95

Source: Author's own work

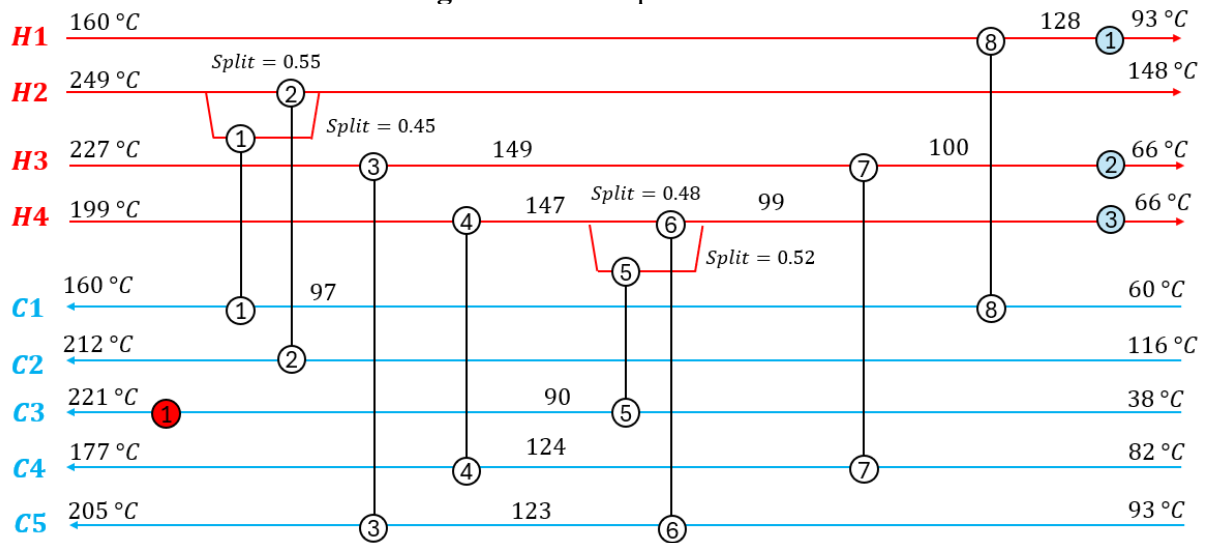
The retrofitted HEN using the proposed methodology aiming at maximizing the NPV is presented in Figure 4.4. The HEX information solution is presented in Table 4.13, and the retrofit details involving the new STHE and the new GPHEs are depicted in Tables 4.14 and 4.15, respectively.

Table 4.13. Example 2: Geometric variables of existing HEXs

HEX	1	2	3	4
Area (m ²)	406.15	1353.7	1486.8	1283.2
Number of shells	2	3	2	2
U (W/m ² K)	215.3	178.8	308.5	320.3
ΔPt_{total} (kPa)	86.4	120.7	103.5	105.7
ΔPs_{total}	54.7	75.3	92.7	95.6
dte (m)	0.01905	0.009525	0.00635	0.00635
L (m)	6.0976	6.0976	6.0976	4.8768
Ds (m)	0.6858	0.7874	0.6858	0.8382
lay	Square	Triangular	Square	Square
Npt	6	6	1	1
rp	1.33	1.33	1.33	1.5
Nb	17	15	9	9
Ntt	506	2473	3557	4595
Tube stream	Hot stream	Hot stream	Cold stream	Hot stream
HEX	5	6	7	8
Area (m ²)	27.7	1243.7	1146.6	167.0
Number of shells	1	3	2	1
U (W/m ² K)	358.6	359.0	361.8	315.6
ΔPt_{total}	8.9	93.9	94.8	53.8
ΔPs_{total}	6.5	71.8	70.3	13.6
dte (m)	0.01905	0.01905	0.009525	0.0127
L (m)	3.0488	6.0976	6.0976	3.0488
Ds (m)	0.3874	0.9398	0.7874	0.6858
lay	Triangular	Triangular	Square	Square
Npt	1	4	2	4
rp	1.33	1.25	1.33	1.25
Nb	18	12	7	5
Ntt	152	1033	3142	1373
Tube stream	Cold stream	Cold stream	Hot stream	Hot stream

Source: Author's own work, 2024.

Figure 4.4. Example 2: Retrofitted HEN



Source: Author's own work, 2024.

Table 4.14. Example 2: HEX information of the retrofitted solution

HEX	1	2	3	4
Q (kW)	5049	6129	12010	9596.2
Th_i (°C)	249.0	249.0	227.0	199.0
Th_o (°C)	148.0	148.0	149.5	147.4
T_{ci} (°C)	96.9	116.0	122.7	124.1
T_{co} (°C)	160.0	212.0	205.0	177.0
LMTD (°C)	68.3	34.4	24.3	22.7
Retrofit alternative	-	-	STHE series	GPHE parallel
HEX	5	6	7	8
Q (kW)	4620.7	4335.4	7640.6	2952
Th_i (°C)	147.5	147.4	149.5	160.0
Th_o (°C)	99.3	99.3	100.3	127.9
T_{ci} (°C)	38.0	93	82	60.0
T_{co} (°C)	90,1	122.7	124.1	96.9
LMTD (°C)	59.3	13.5	21.7	65.5
Retrofit alternative	Replace for a new GPHE	-	GPHE series	-

Source: Author's own work, 2024.

Table 4.15. Example 2: Design variables of the GPHE added to the HEN

HEX	4	5	7
Added area (m ²)	187;6	175.8	137.9
U (W/m ² K)	559.1	554.3	324.3
Additional ΔPh	10.5	10.4	4.8
Additional ΔPc	58.3	18.7	8.9
Lp (m)	2.092	1.543	0.743
Lw (m)	1.200	0.812	0.845
Dp (m)	0.4	0.283	0.3
Nph	2	1	1
Npc	2	1	1
Chevron angle (°C)	30	45	65
Np	65	122	191

Source: Author's own work, 2024.

Table 4.16. Example 2: HEX information of the STHE added to the network

HEX	3
Added area (m ²)	120.9
U (W/m ² K)	330.9
Number of shells added	1
Additional ΔPt	90.1
Additional ΔPs	75.8
dte (m)	0.01905
L (m)	3.0488
Ds (m)	0.7874
lay	Triangular
Npt	2
rp	1.33
Nb	6
Ntt	663

Source: Author's own work, 2024.

The retrofit solution achieves a heat recovery of 3.8 MW, with an investment cost of 109,228 \$ associated with an addition of 313.7 m² of GPHE area and 120.9 m² of STHE. The liquid cash flow of saving money per year is 168,249 \$/y, already considering the additional operating costs of 14,103 \$/y due to the increase of pressure drop. The optimal retrofit NPV is 1,013,821 \$.

This example illustrates a type of HEN rarely explored in the literature for retrofit applications, where several HEX exhibit a significant degree of temperature cross. In the original network, HEX units 1, 2, 4, and 7 display this characteristic.

Note that reducing utility consumption inherently requires increasing the thermal load on HEX 5. However, if the thermal load of HEX 6 remains constant while increasing that of

HEX 5, a substantial increase in the temperature cross in HEX 6 occurs, further reducing its already low LMTD.

To address this, the optimization approach aimed to decrease the thermal load on HEX 6 by redistributing its heat load between HEXs 3 and 4, as shown in Table 13. As a result, four heat exchangers required modification to meet the new thermal demand: HEXs 3, 4, 5 and 7 (despite its reduced thermal load, HEX 7 experienced a drop in its LMTD and a reduction in the correction factor).

This example reveals several noteworthy outcomes. In recent years, the trend in retrofit studies has leaned heavily toward intensification as a preferred solution. However, in this network configuration, none of the solutions involved the installation of tube inserts. For example, HEX 7, although operating at a reduced heat load, would require a 20.5% increase in the overall heat transfer coefficient due to temperature cross and reduced LMTD. Given that the dominant resistance lies on the shell side, this would necessitate a substantial increase in tube-side convection coefficient, severely penalizing pressure drop, a factor that indicates more suitable alternative solutions are preferable. Thus, while intensification is an attractive option, it does not address all challenges in network retrofits.

Another notable result is that the optimal solution for HEX 5 involves completely replacing it with a new GPHE. This choice is driven by the increased heat load, which raises the flow rate of stream H4 through HEX 5, resulting in a shell-side velocity of 2.7 m/s, exceeding the recommended maximum to avoid erosion and vibration. Consequently, intensifying or adding a unit in series would not work. In this case, full replacement was the optimal solution.

4.4.3. Comparison with the traditional approach

The results above clearly underscore the importance of implementing a detailed retrofit with a wider range of modification options for existing exchangers. The assumption that any new heat exchanger installed must maintain the same overall heat transfer coefficient, thus being equal to the existing one, also restricts a key degree of freedom where the new exchanger could adopt a different geometry to better suit the service demands.

We will now demonstrate the difference in results if both examples are solved using the prevalent approach found in the literature, in order to highlight the importance of

considering a detailed HEX retrofit simultaneously with then HEN retrofit. In this conventional method, each existing heat exchanger is primarily characterized by its area and a constant overall heat transfer coefficient. With this assumption, the new required area is calculated by:

$$A_{new} = \max\left(\frac{Q}{U LMTD} - A_{ex}; 0\right) \quad (4.58)$$

In this manner, the network retrofit optimization is conducted following the same approach as previously presented, but with a simplified calculation method for the heat exchanger retrofit. The overall heat transfer coefficient is assumed to be constant and identical for both the existing HEX and the additional area, with its value calculated based on the geometry of the existing exchanger.

Table 4.16 below presents the results obtained using the approach traditionally employed in the literature. These results were generated by optimizing the retrofit of the existing network; however, the HEX evaluation is done using Eq. 4.34. The optimization solution yielded a value for heat recovery and the thermal load of the HEX in the loops. Using this solution, the network was recalculated with the detailed approach based on the procedure presented in section 3. The details of each solution are also depicted in supplementary material.

Table 4.17: Comparison with the traditional approach

	Example 1		Example 2	
	This paper	Traditional approach	This paper	Traditional approach
Energy recovery (MW)	7.6	8.5	3.8	5.4
Investment cost (\$)	1,459,232	2,585,884	109,228	1,578,553
Additional operational cost (\$/y)	53,819	85,127	14,103	75,322
NPV (\$)	3,882,290	2,861,250 \$	1,013,821	- 696,578

Source: Author's own work, 2024.

Table 4.16 demonstrates that, in Example 1, the solution obtained using the traditional approach proposes a network intervention capable of achieving an NPV close of \$2.8 million. However, applying the detailed procedure outlined in this chapter would generate a solution with an NPV \$1 million higher, representing a 35% improvement.

In contrast, for the second example, recalculating the solution derived from the traditional approach using the detailed HEX retrofit procedure presented here resulted in a

negative NPV. The primary cause of this outcome lies in the solution proposed for HEX 7, which exhibits a severe temperature cross phenomenon ($T_{hi} = 159$ °C, $T_{ho} = 88.5$ °C, $T_{ci} = 82$ °C, $T_{co} = 142.2$ °C). Since the HEX retrofit calculation commonly used in the literature lacks detailed modeling, such behavior is not anticipated. Consequently, it necessitates the addition of four more shells in series (resulting in a total of six shells in series) to achieve a correction factor greater than 0.75. This outcome drastically increases both the investment cost and operational cost due to significant pressure drop penalties.

4.5. Conclusions

This paper presents a novel procedure for HEN retrofit addressing several enhancements never explored before. The goal is to incorporate a more detailed description of the HEX retrofit, considering an accurate modelling and a wider range of retrofit options, with different geometries. The benefits of incorporating these features is evident in the results when compared with the traditional approach in the literature. In addition, all details does not affect the procedure capabilities of dealing with the non-linearities, and ensure a robust convergence.

ACRONYMS AND ABBREVIATIONS

HEN – Heat exchanger network
 HEX – Heat exchanger
 IRR – Internal rate of return
 LMTD – Logarithmic mean temperature difference
 LP – Linear programming
 MILP – Mixed integer linear programming
 MINLP – Mixed inter nonlinear programming
 MSTR – Minimal structure
 NPV – Net present value
 GPHE – Gasketed-plate heat exchanger
 ROI – Return on investment
 STHE – Shell and tube heat exchanger
 STR – HEN structure

TAC – Total annualized cost

NOMENCLATURE

\hat{a}	Area cost parameter (\$/m ²)
A	Heat transfer area (m ²)
A_{new}	Additional heat transfer area (m ²)
A_{req}	Required heat transfer area (m ²)
\widehat{A}_{exc}	Excess area (%)
\hat{b}	Area cost parameter
C_{cap}	Capital cost (\$)
$C_{op,c}$	Cold stream operational cost (\$/y)
$C_{op,existing}$	Existing HEX operational cost (\$/y)
$C_{op,h}$	Hot stream operational cost (\$/y)
\widehat{CF}	Fixed cost (\$)
d_{te}	Tube outer diameter (m)
d_{ti}	Tube inner diameter
D_s	Shell diameter (m)
D_p	Port diameter (m)
E_{cl}	Coil wire diameter (m)
E_{hu}	Hot utility consumption (kW)
$E_{hu,min}$	Minimum hot utility consumption (kW)
\widehat{E}_{hu}^{curr}	Hot utility consumption of the existing HEN (kW)
F	Correction factor
H	Twisted-tape pitch
\hat{i}	Interest rate (1/y)
L	Tube length (m)
lay	Tube layout
lbc	Baffle spacing
L_p	Plate length (m)
L_w	Plate width (m)
\dot{m}	Mass flow rate (kg/s)

\hat{n}	Project horizon
Nb	Number of baffles
\widehat{Nop}	Number of operating hours per year
Nph	Hot stream number of passes
Npc	Cold stream number of passes
Nt	Total number of plates
Ntp	Number of tube passes
\widehat{pc}	Energy price (\$/kwh)
P_{cl}	Coil-wire helical pitch
Q	Heat load (W)
qhu_j	Hot utility consumption of cold stream j (kw)
\hat{r}	Annualization factor (1/y)
rp	Pitch ratio
T_{ci}	Inlet cold stream temperature ($^{\circ}\text{C}$)
T_{co}	Outlet cold stream temperature ($^{\circ}\text{C}$)
T_{hi}	Inlet hot stream temperature ($^{\circ}\text{C}$)
T_{ho}	Outlet hot stream temperature ($^{\circ}\text{C}$)
U	Overall heat transfer coefficient ($\text{W}/\text{m}^2\text{K}$)
vc	Cold stream velocity (m/s)
\widehat{vcmin}	Minimum cold stream velocity (m/s)
\widehat{vcmax}	Maximum cold stream velocity (m/s)
vh	Hot stream velocity (m/s)
\widehat{vhmin}	Minimum hot stream velocity (m/s)
\widehat{vhmax}	Maximum hot stream velocity (m/s)
vt	Tube side velocity (m/s)
\widehat{vtmin}	Minimum tube side velocity (m/s)
\widehat{vtmax}	Maximum tube side velocity (m/s)
vs	Shell side velocity (m/s)
\widehat{vsmin}	Minimum shell side velocity (m/s)
\widehat{vsmax}	Maximum shell side velocity (m/s)
y	Ratio between twisted-tape pitch and tube inner diameter
$Z_{i,j,k}$	Binary variable that indicates the match between hot stream i , cold

	stream j in stage k
zcu_i	Binary variable that indicates a cooler for hot stream i
zhu_j	Binary variable that indicates a heater for cold stream j
β	Chevron angle ($^\circ$)
δ	Twisted-tape thickness (m)
ΔP	Pressure drop (Pa)
$\hat{\eta}$	Pump efficiency
$\hat{\rho}$	Stream density (kg/m^3)

5 HEN RETROFIT WITH DETAILED HEX CALCULATIONS- PART 2: TOPOLOGICAL MODIFICATIONS

5.1. Introduction

In the section 4 a retrofit procedure for HENs was presented, focusing exclusively on the heat load modification of the HEXs. Although this approach inherently limits the potential for heat recovery due to the presence of pinch matches (Asante and Zhu, 1997), it enables the identification of heat recovery strategies that can yield significant economic benefits, while requiring less complex and more practical interventions.

However, despite the increased complexity in altering the existing network and installing new components, topological modifications can be useful for enhancing heat recovery potential. In addition, such modifications allow the creation and adjustment of utility paths and energy loops in the network, allowing for a new energy redistribution with reduced investment costs.

The topological modifications commonly addressed in scientific studies include (Kemp, 2007):

- i) Resequencing: it moves a unit to a new location, preserving the streams in the original match.
- ii) Repiping: the streams involved in the match do not need to be the same as the original one, where one or both streams can be different.
- iii) Inserting a new match

The primary challenge highlighted in the literature for implementing topological modifications is the necessity of installing and redistributing piping across the industrial plant. Indeed, regardless of the type of modification among the three main categories listed above, adjustments to the piping (as well as the hydraulic facilities) are required to allow the flow of streams to the newly added or modified matches. However, as discussed in section 2, several additional practical aspects must also be considered. These include the existing plant layout and equipment arrangement, the availability of physical space, safety considerations, controllability, and other factors. Addressing these challenges necessitates a multidisciplinary effort, involving teams specializing in process engineering, mechanical engineering, civil engineering, plant layout, safety, and more.

To the best of our knowledge, among the possible topological modifications, industrial practice is generally more flexible in allowing the addition of new matches to the network. Resequencing may also be considered, albeit with certain caveats. On the other hand, repiping involves far more dramatic interventions and is rarely considered a viable option.

Over the years, researchers have proposed various methodologies to address this problem, primarily based on Pinch Technology, Mathematical Programming and Metaheuristic Methods.

The pioneering work on the application of Pinch Technology to HEN retrofit was presented by Tjoe and Linnhoff (1986). Their approach extends the grassroots design problem using the same principles while introducing the concept of area efficiency, which guides the necessary modifications to improve heat recovery. Following this seminal work, several subsequent studies emerged, like Reisen *et al.* (1995) that presented a prescreening and decomposition method to analyze the HEN retrofit, using a Path Analysis to identify the critical parts of the existing network that should be modified, generating subnetworks.

Lakshmanan and Bañares-Alcántara (1996) discussed the limitations of the application of the visualization tools developed for grassroots problems to retrofit. They proposed a new tool for retrofit visualization, called Retrofit Thermodynamic Diagram, which is a concise graphical representation that facilitates the driving forces visualization in the network. Varbanov and Klemes (2000) presented a methodology based on heuristics to handle cases where the Network Pinch cannot be established, as well as methods to facilitate the decision on topology modifications on the existing network. Nordman and Berntsson (2001) proposed a different approach for HEN retrofit using the Pinch Methodology through new grand composite curves.

Li and Chang (2010) presented a HEN retrofit approach using Pinch Analysis based on the identification and elimination of the cross-pinch heat exchanges. Their work explores the fundamentals of Pinch Technology. Comparing this target information with the existing network, the cross-pinch heat exchanger is identified, and its heat duty is split to overcome the pinch violation. Gadalla (2015) proposed a new graphical method for the analysis of heat recovery systems in retrofit problems. He emphasized the difficulty of the conventional diagrams to incorporate the features of the existing network and proposed a new graphical tool based on the hot stream and cold stream temperatures plot. This new graph divides the systems into different regions, which each region is associated with matches that transfer heat between the pinch or not.

The Pinch Technology can be a good technique for identifying energy saving in retrofit problems and is the most used tool in industrial practice. However, it has important drawbacks: (i) it does not properly account the trade-off between the energy recovery and capital expenditure due to its inaccuracy to evaluate the investment cost; (ii) challenges in developing a systematically procedure, with a strong dependence on designer expertise, and (iii) it has a limited ability to explore a wide range of intervention possibilities within the existing network.

On the other hand, Mathematical Programming based methods are capable of generating a complete automated optimization procedure, usually based on a mixed-integer nonlinear programming (MINLP) formulation or a decomposition strategy based on a nonlinear programming (NLP) – mixed integer linear programming (MILP) formulations. Ciric and Floudas (1989) used a two-stage procedure. The first stage consists of a MILP model, which minimizes the cost of structural modification, identifying all possible matches to attain a target minimum utility consumption associated with a selected HRAT. The second stage consists of a superstructure that addresses all potential units for the selected matches in the first stage, and minimize the investment cost through a NLP model. Ciric and Floudas (1990) proposed an extension of it is previous work, based on the solution of the problem in a single stage, through a MINLP, which overcame the decomposition drawbacks.

Yee and Grossmann (1991) proposed a procedure divided into a prescreening stage and an optimization stage, where the first one determines the economic feasibility of the retrofit and the best saving money achievable, based on cost plots. The second stage involves a simultaneous HEN retrofit optimization based on a MINLP formulation and general superstructure.

Briones and Kokossis (1999) also proposed a procedure divided into a screening stage and an optimization stage. The screening stage encompasses two sub stages, called Auditing and Unit Development stages, both carried out with MILP models. The Auditing stage uses a so called Heat Exchanger Auditing Target model, and the objective is to identify the existing unit that are acceptable and the units that need modification or replacement. In the Unit Development stage, the efficient units are retained and the other ones are considered for reassignment in the Targets for Area and Modifications of an Existing Network model, where the topological modifications are proposed. The result from these models are used to develop retrofit hypertargets, such as the investment-saving plots.

Ma *et al.* (2000) proposed a two-step algorithm, where the first one consist of a MILP where area is calculated considering fixed temperature approaches. The MILP solution is used

to initialize the complete MINLP model used in the second step. Sorsak and Kravanja (2004) proposed a procedure incorporating different HEX types, based on Yee and Grossmann (1990) superstructure. Ponce-Ortega *et al.* (2008) used a MINLP model that was an extension of the Yee and Grossmann (1991) proposal to include process modifications simultaneously with the HEN structure modification, which can lead to better retrofit solutions. The paper also presents a novel procedure to handle with isothermal process streams.

Nguyen *et al.* (2010) proposed a one-step MILP model to HEN retrofit, where the network is separated into several fixed temperature intervals, thus the LMTD in each interval was known and constant.

Pan *et al.* (2013) presented a MILP-based iterative approach, divided in two optimization stages. In the first stage, the most suitable structure modifications are identified, including new exchanger installations, existing exchanger rearrangements and stream repiping, referred to as network structure optimization. In the second stage, the structure proposed in the first one is optimized. Both stages consist of an MILP iterative approach, as proposed in previously works (Pan *et al.*, 2012) and discussed in Part 1 of this paper.

Angsutorn *et al.* (2021) discussed the difficulty of modifying existing heat exchangers and the existing network topology. Thus, they proposed a HEN retrofit approach addressing only new HEXs without increasing heat transfer area of existing HEX.

Although fewer papers explored Metaheuristic Methods to HEN retrofit, there were some previous attempts. Athier *et al.* (1998) proposed a two-stage procedure. The first one, or master problem, addresses the topological modification using a Simulated Annealing procedure (SA). The second one optimizes the required area of the modified network obtained from the master problem, using a NLP model.

Later, Bochenek *et al.* (2006) formulated a single multivariable problem using a structural matrix instead of superstructures, and solved the problem in two levels. The first one addresses the topological modification using a Genetic Algorithm (GA), and the second one is used to obtain the split ratio and areas. Rezaei and Shafiei (2009) discussed the difficulty of GA to handle continuous variables. Therefore, in order to address this limitation, it was proposed to couple the GA with a NLP and ILP models to deal with the continuous variables of the HEN retrofit problem, such as, heat loads, temperatures, split ratios, etc.

Soltani and Shafiei (2011) considered the pressure drop in the retrofit using an iterative algorithm coupling the GA (topological modification), a LP model (network evaluation) and a ILP model (network modification to maximize the profit, where the streams pressure drops are calculated between the LP and ILP runs). Biyanto *et al.* (2016) proposed a

GA method to solve the HEN retrofit based on enhancement tools. Stampfli *et al.* (2022) proposed a GA model for topological modification, followed by a differential evolution (DE) algorithm to optimize the heat loads. They proposed a parallelized procedure for the GA evaluation, where the DE is performed on each chromosome parallel on multiple cores.

As it can be observed, numerous approaches have been proposed to address HEN retrofit considering topological modifications, employing different methodologies. However, in addition to the numerical challenges discussed in Part I, incorporating these modifications introduces combinatorial explosion issues due to the vast possibilities of alteration options. Consequently, applying these techniques to industrial-scale problems remains limited, often struggling to find an optimal solution or even a feasible solution, as highlighted by Pan *et al.* (2012).

Part II of this work extends the work presented in Part I by incorporating topological modifications into the existing network. Following trends in the industrial practice, the interventions considered here exclude repiping, focusing solely on the addition of new matches and the resequencing of existing matches. The proposed approach is based on an enumeration procedure of different structures, where different modifications are generated and each resulting structure (composed of the existing HEN and a given topological modification) is optimized sequentially.

The enumeration strategy is divided into stages, with each stage identifying the best solution requiring the fewest topological modifications, thereby avoiding the combinatorial explosion typically associated with the retrofit problem. The optimization of each structure employs the methodology introduced in Part I, fully accounting for the detailed HEX evaluations in the network. In addition, the optimization of each structure avoids the convergence issues previously discussed, and the final solution is built sequentially from the best interventions in the network. This is in stark contrast to Mathematical Programming-based approaches, whose solution quality is often highly questionable for the reasons outlined earlier.

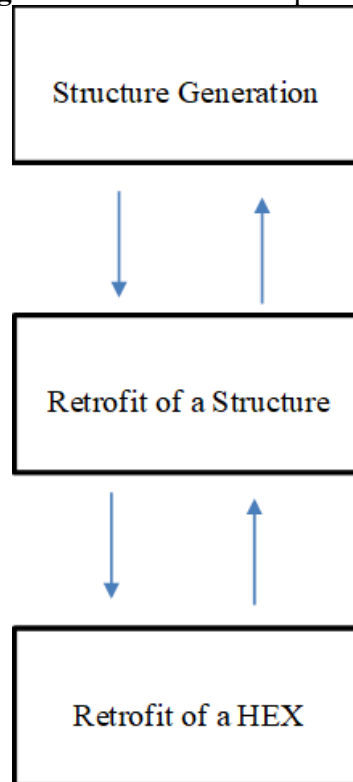
The chapter is organized as follows. The proposed intervention methodology for the network is first presented, followed by the results and conclusions.

5.2. HEN Retrofit Procedure

This chapter extends the procedure presented in Part I of this work (see section 4) by incorporating the possibility of topological modifications. As explained below, this is achieved through an enumeration procedure, wherein various structures, derived from modifications to the existing one, are generated. Each generated structure is optimized using precisely the same methodology outlined in Part I, including all the detailed refinements and enhancements to the retrofit procedure introduced in the first part.

The complete structure of the proposed algorithm in this work is composed of three interconnected subproblems, depicted in Figure 5.1. Each subproblem corresponds to a building blocks that compose the algorithm, as follows.

Figure 5.1: HEN retrofit procedure



Source: Author's own work, 2024.

1) Structure generation: The idea is to create an algorithm to generate different structures, which is associated with the selection of the matches between cold and hot streams. A structure is defined as selecting each match between process streams, as well as

utility matches. Each generated structure is optimized according to the second block of the algorithm.

2) Optimization of a given structure: For each fixed structure generated in the first block, the goal is to identify the optimal energy recovery and heat distribution through the network. The nature of this problem was described in section 4. This step involves the modification of the heat load of existing HEXs, which demands the retrofit of the existing equipment, as presented in the third block.

3) HEX retrofit: For a given new heat load established in the second block, this step involves identifying the optimal intervention for increasing the heat load, as discussed in section 3.

The flexibility of the algorithm allows addressing this problem through the second and third blocks working alone, i.e. a scheme composed only by the second and third blocks would be also an effective HEN retrofit tool, as already presented.

Therefore, it is important to realize that it is being proposed different blocks of structures that is able to perform independent tasks. Each one can be used for a specific proposal, and when coupled and used simultaneously, the HEN retrofit with topological modifications and detailed HEX retrofit is obtained.

Blocks 2 and 3 have already been presented and explored in sections 3 and 4, respectively. Thus, because this section focuses exclusively on the methodology to explore topological modifications in the existing HENs, we present only the details of block 1.

5.2.1. Topological modifications model

The Synheat superstructure, proposed by Yee and Grossman (1990), is employed in this paper, as well as the isothermal mixing. So, the proposed model to generate different structures based on topological modifications in the existing HEN involves the Synheat formulation ($D_{synheat}$) with a set of new constraints. Let \widehat{N} be the total number of matches in the HEN, \widehat{N}_{ex} the number of matches in the existing HEN and \widehat{N}^* the number of matches in the existing HEN that we want to preserve (with the same stage location included), the model is given as follows:

$$PSTRR = \underset{\forall(T, Q) \in D_{synheat}}{Min} \quad \gamma \quad (5.1)$$

s.t.

$$\sum_{i \in HP} \sum_{j \in CP} \sum_{k \in K} z_{i,j,k} + \sum_{j \in CP} zhu_j + \sum_{i \in HP} zcu_i = \widehat{N} \quad (5.2)$$

$$\sum_{i,j,k \in STR} z_{i,j,k} + \sum_{i \in STR} zcu_i + \sum_{j \in STR} zhu_j = \widehat{N}^* \quad (5.3)$$

$$\sum_k z_{i,j,k} \geq \widehat{Nmatc}_{l,j}^{orig} ; \forall i \in HP, j \in CP \quad (5.4)$$

Eq. (5.2) fix the number of matches equal to \widehat{N} and Eq. (5.3) guarantees that \widehat{N}^* matches in the existing HEN are preserved. $\widehat{Nmatc}_{l,j}^{orig}$ is a parameter associated with the number of matches in the existing network between hot stream i and cold stream j . For instance, if stream H1 exchanges heat with stream C1 in Stages 1 and 3, then $\widehat{Nmatc}_{H1,C1}^{orig} = 2$. Consequently, Eq. (5.4) ensures that any modification to an existing match is strictly related to its location, preserving the streams involved in that match. This constraint ensures that alterations to existing matches are limited to resequencing, avoiding repiping.

Thus, the difference between \widehat{N}_{ex} and \widehat{N}^* indicates the extent of resequencing desired in the network, while the difference between \widehat{N} and \widehat{N}_{ex} reflects the number of new matches added to the network.

The generation of structures is performed by running the PSTRR model with an added structure exclusion constraint (Floudas, 1995) to prevent previously visited structures from being regenerated. The procedure involves running the PSTRR model to generate a new structure, followed by optimizing the generated network using the methodology presented in the Part I of this work. Once the generated network is optimized, the PSTRR model is executed again to produce another structure, which is then optimized, and the process is repeated iteratively. Whenever an optimized structure exhibits an objective function better to those of previously evaluated structures, it is updated as the new incumbent. The stopping criterion for the algorithm will be explained shortly.

Unlike Part I of this work, where all the HEX in the network are existing units, the presence of new matches is now possible, which do not have pre-existing equipment. Consequently, these exchangers must be designed rather than retrofitted. The design process follows the Set Trimming methodology developed by Nahes *et al.* (2021) for GPHEs and by

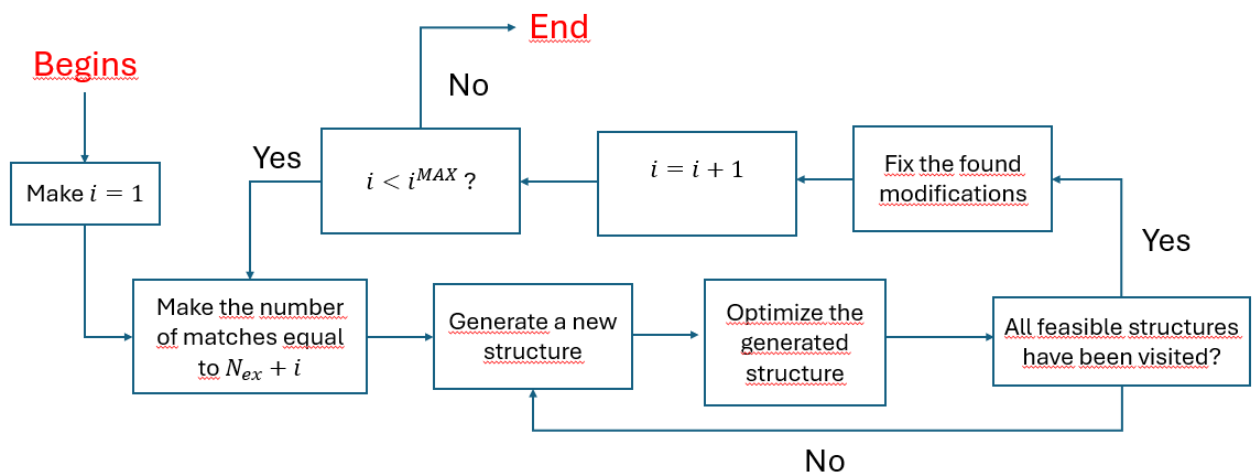
Lemos *et al.* (2020) for STHes. The remaining HEX are calculated using the retrofit procedure outlined in Part I.

The main challenge of the approach proposed in this work lies in the combinatorial explosion of possible structures within the problem. Furthermore, although the optimization of a single structure converges within a reasonable time for practical purposes, optimizing a series of networks renders the computational time of the overall procedure impractical. As a result, it is not feasible to explore all viable structures, necessitating the use of an alternative enumeration procedure.

Thus, the exploration of topological modifications is carried out using an incremental enumeration approach, where the number of modifications allowed in the network is implemented in stages. The first stage involves optimizing the existing network without any modifications, following the exact procedure presented in Part I. The second stage consists of generating all feasible structures by allowing the addition of only one new match and performing a single resequencing within the existing network.

At the end of the second stage, the best solution achievable with the minimum number of topological modifications (one possible new match and one possible resequencing) is obtained. For the third stage, the solution from the second stage is fixed (locking in the resequencing and the new match proposed in the last solution), and the third stage involves generating all viable networks by allowing the addition of one more new match to the structure. The subsequent stages follow the same philosophy. The stopping criterion is based on a maximum number of possible modifications allowed in the network, defined by the value of i^{MAX} . Figure 5.2 depicts the flowchart of the proposed algorithm.

Figure 5.2: Flowchart of the incremental enumeration



Source: Author's own work, 2024.

For a given algorithm stage, where the number of modifications are controlled, the visit of all feasible structures is attained whenever the PSTRR model turns infeasible (which means that there is no more feasible structure with that number of resequencing and new matches).

Remark 1: When proposing topological modifications sequentially rather than simultaneously, the structures generated are heavily dependent on the solution obtained in previous stages. However, it is important to note that the best possible solution with the fewest topological changes is identified at each stage of the procedure. Based on the best intervention proposals from previous stages, subsequent stages build upon these changes to further improve the solution. In other words, the objective function always improves as the process advances.

While this procedure does not guarantee the global optimum, it certainly identifies a robust retrofit solution, all while incorporating the detailed approach presented in Part I. Compared to other methods in the literature, this characteristic is undoubtedly an advantage. For instance, methods based on Mathematical Programming can converge to any local optimum without providing a metric for solution quality and often face numerical challenges (in some cases it is difficult to attain a feasible solution at all, as highlighted in previously papers, like Pan *et al.* (2012)). The results will demonstrate that this procedure achieves high-quality solutions, even surpassing those previously reported in the literature.

Remark 2: Since the procedure relies on an enumeration strategy, various strategies can be implemented to accelerate convergence. Upon identifying an incumbent, the value of its objective function can be used to restrict the DIRECT (Jones, 2021) search space and avoid unnecessary HEX retrofit calculations.

For instance, if the objective function represents the NPV of the project, the incumbent's NPV value (NPV^{inc}) can be used to determine an upper bound for utility consumption:

$$NPV^{inc} = \sum_{t=1}^n \frac{CF_t}{(1 + \hat{i})^t} - IC^{LB} \quad (5.5)$$

where CF_t is the cash inflow, \hat{i} is the interesting rate, n the time horizon and IC^{LB} the investment cost lower bound, which can be calculated using the fixed cost of new matches. Eq. (5) can be solved for CF_t , representing a utility consumption level beyond which the

associated NPV will certainly be lower than the incumbent, as the latter was calculated using a conservative lower bound for the investment cost. Consequently, the upper bound of the utility consumption search space is restricted to this value in the DIRECT run.

Moreover, during each objective function evaluation, the HEX (both retrofitted and newly designed) are sequentially assessed. As each exchanger is evaluated, its investment cost is determined, incrementally updating the objective function. In some cases, this progressive evaluation may reveal that the NPV becomes worse than the incumbent, even before all exchangers are assessed, enabling an early termination of the evaluation for that specific point.

5.3. Results

The results are divided into two parts. The first part aims at demonstrating the performance of the enumeration procedure compared with previous approaches in the literature. This analysis employs two examples with solutions reported in the literature under the assumption of a known and uniform convective heat transfer coefficients. Although one of the key strengths of our work is the detailed modeling of HEXs, the solutions attained in the first part of the results are based on the adoption of this simplification together with the proposed approach (i.e. the third block displayed in Figure 1 is eliminated). Therefore, it is possible to demonstrate the power of the proposed algorithm to explore the space of topological structures, when compared with previous approaches in the literature.

The second part of the results addresses two examples presented in Part I of this study, solving them using the complete approach proposed here, with topological modifications. This set of results aims to quantify the additional gains that can be achievable through the extension of the algorithm to include topological modifications, in comparison with the version with heat load modifications only.

5.3.1. Comparison with previous results from the literature with simplified HEX evaluation

Two examples already employed in the literature are considered. The first example is a small-sized case study, originally proposed by Yee and Grossmann (1987) and has been widely used in numerous previous works in the literature (Ciric and Floudas, 1990; Yee and Grossmann, 1991; Athier *et al.*, 1998; Bochenek and Jeżowski, 2006; Rezaei and Shafiei, 2009; Pan *et al.*, 2013; Angsutorn *et al.*, 2021). The second example is a medium-size and more complicated case study. It is the HEN from a crude preheat train at OEMV Raffinerie Schwechat, Austria, originally proposed by Saboo and co-workers (Saboo *et al.*, 1986). This example has been also widely used in numerous previous articles (Briones and Kokossis, 1999; Ma *et al.*, 2000; Rezaei and Shafiei, 2009; Pan *et al.*, 2013; Isafiade, 2018).

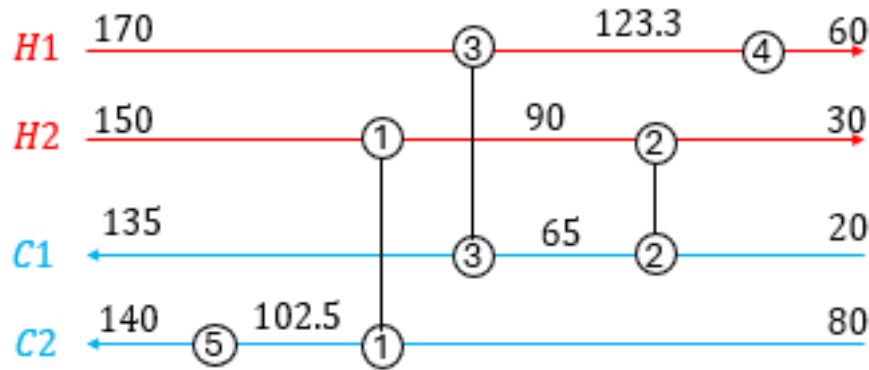
Example 1

The first example involves 2 hot and 2 cold streams, with an existing HEN encompassing five HEX. Figure 5.3 presents the existing HEN, and Tables 5.4 and 5.5 depict the streams and HEX data, respectively.

Table 5.1: Example Based on Yee and Grossmann (1987) - Streams data

Stream	Inlet temperature (K)	Outlet temperature (K)	Heat capacity rate (kW/K)
H1	170	60	30
H2	150	30	15
C1	20	135	20
C2	80	140	40

Source: Yee and Grossmann, 1987.

Figure 5.3. Example Based on Yee and Grossmann (1987) - Existing HEN

Source: Yee and Grossmann, 1987.

Table 5.2. Example Based on Yee and Grossmann (1987) - Information of existing HEX in the original HEN

HEX	1	2	3	4	5
Q (kW)	900.0	900.0	1400.5	1899.0	1500.0
Th_i (°C)	150.0	90.0	170.0	123.3	177.0
Th_o (°C)	90.0	30.0	123.3	60.0	177.0
Tc_i (°C)	80.0	20.0	65.0	20.0	102.5
Tc_o (°C)	102.5	65.0	135.0	40.0	140.0
LMTD (°C)	24.067	16.370	45.664	59.026	53.581
A (m ²)	46.74	68.72	38.32	40.22	34.99

Source: Yee and Grossmann, 1987.

The overall heat transfer coefficient for all HEX is 0.8 kW/(m²·K), the project lifetime is 3 years, the annual interest rate is 33%, the relocation of existing HEX cost is 300 \$ and the investment cost of new HEXs and additional area of existing ones is given, respectively, by:

$$IC_{new\ HEX} = 3000 + 1300A^{0.6} \quad (5.6)$$

$$IC_{ex\ HEX} = 1300A_{new}^{0.6} \quad (5.7)$$

The objective function is the retrofit profit:

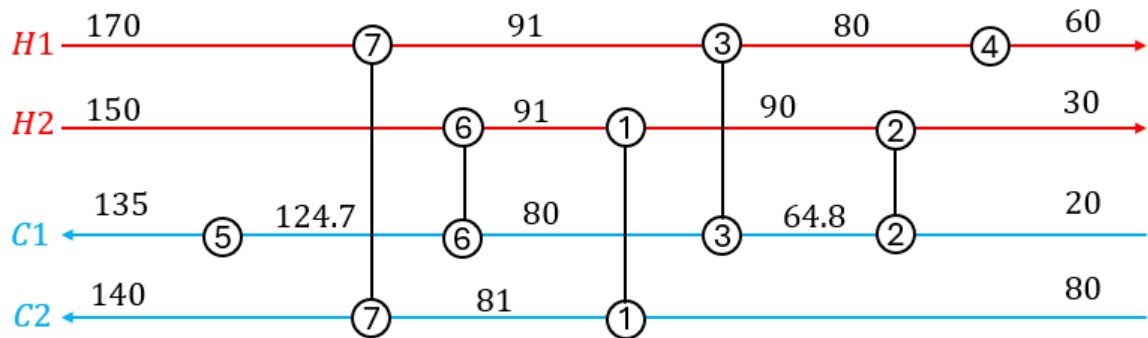
$$\max fobj = FVIFA \cdot SC - IC_{new\ HEX} - IC_{existing\ HEX} - REL_{cost} \quad (5.8)$$

where REL_{cost} is the relocation cost and $FVIFA$ is given by:

$$FVIFA = \frac{\left(1 - \frac{\hat{i}}{100}\right)^{\hat{n}} - 1}{\hat{i}/100} \quad (5.9)$$

The retrofit solution obtained using the proposed approach is associated with a new utility consumption of 201.8 kW of hot utility, and an objective function of 365,300 \$. The proposed topological modifications involve the resequencing of HEX 5, and the addition of two new matches (HEX 6 and 7). The solution is presented in Figure 4, the HEX details in Table 5.3 and the comparison with other works in Table 5.4.

Figure 5.4. Example Based on Yee and Grossmann (1987) - Retrofit solution



Source: Author's own work, 2024.

Table 5.3. Example Based on Yee and Grossmann (1987) - Information of existing HEX in retrofit solution

HEX	1	2	3	4	5	6	7
Q (kW)	25.0	900.0	303.2	601.8	201.8	895	2395
T_{hi} (°C)	91.2	90.0	91.0	80.0	177.0	150.0	170
T_{ho} (°C)	90.0	30.0	80.0	60.0	177.0	91.2	91.0
T_{ci} (°C)	80.0	20.0	65.0	20.0	124.7	80.0	81.2
T_{co} (°C)	81.2	64.8	80.0	40.0	135.0	124.7	140
LMTD (°C)	10.1	16.370	12.36	40.0.	47.01	16.52	18.2
A_{new} (m ²)	0	0	0	0	0	67.7	167.2

Source: Author's own work, 2024.

Table 5.4. Example Based on Yee and Grossmann (1987) - Solution comparison with previous work in literature.

	Objective function
Ciric and Floudas (1990)	368,271
Pan <i>et al</i> (2013)	365,826
Augnstorm <i>et al</i> (2021)	321,251
This work	365,300

Source: Author's own work, 2024.

Table 5.4 shows that the solution obtained in this work outperforms the one proposed by Augnstorm *et al.* (2021) and is slightly lower than those obtained in other studies. The higher value of objective function presented by Ciric and Floudas (1990) and Pan *et al.* (2013)

can be explained because these works involve repiping existing exchangers, a modification not included in our approach, as well as a network configuration that cannot be represented by the Synheat superstructure. Nevertheless, the solution found by this work achieves results very close to theirs, relying on much simpler topological modifications that are more widely accepted in industrial practice.

Example 2

The second example involves 6 hot streams and 1 cold stream, with an existing HEN encompassing thirteen HEXs. Figure 5.5 presents the existing HEN, and Tables 5.5 and 5.6 depict the streams and HEX data, respectively.

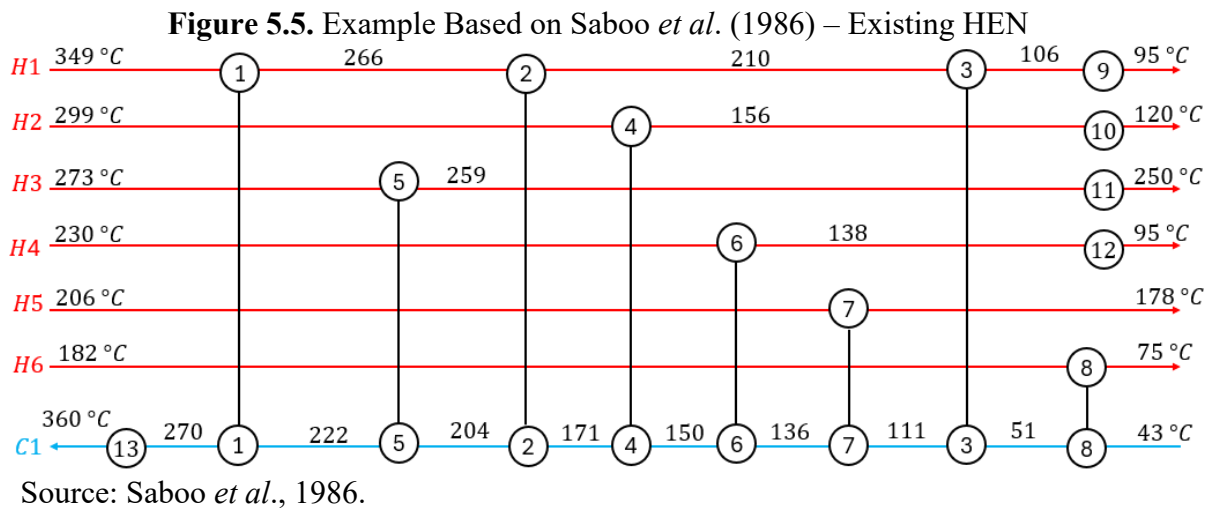


Table 5.5. Example Based on Saboo *et al.* (1986) - Streams data

Stream	Inlet temperature (°C)	Outlet temperature (°C)	Heat capacity rate (kW/K)
H1	349	95	86
H2	299	120	21.4
H3	273	250	184.7
H4	230	95	23.5
H5	206	178	129.4
H6	182	75	11.5
C1	43	360	147.9

Source: Saboo *et al.*, 1986.

Table 5.6. Example Based on Saboo *et al.* (1986) - Information of existing HEX in the original HEN

HEX	1	2	3	4	5	6	7
Q (kW)	7138.5	4849.3	8866.4	3060.6	2618.1	2152.5	3623.2
<i>Thi</i> (°C)	349.0	266.0	206.6	299.0	273.0	230.0	206.0
<i>Tho</i> (°C)	266.0	209.6	106.5	156.0	258.8	138.4	178.0
<i>Tci</i> (°C)	221.6	171.0	51.3	150.3	203.8	135.7	111.3
<i>Tco</i> (°C)	269.8	203.8	111.3	171.0	221.6	150.3	135.8
LMTD (°C)	60.1	49.4	74.7	39.2	53.2	22.6	68.5
<i>A</i> (m ²)	448.0	370.0	447.9	294.4	276.5	359.4	199.7
HEX	8	9	10	11	12	13	
Q (kW)	1230.5	990	770	1620	1020	13335	
<i>Thi</i> (°C)	182.0	106.5	156.0	258.8	138.4	500	
<i>Tho</i> (°C)	75.0	95.0	120.0	250.0	95.0	500	
<i>Tci</i> (°C)	43.0	20.0	20.0	20.0	20.0	269.8	
<i>Tco</i> (°C)	51.3	56.9	48.7	80.3	58.0	360.0	
LMTD (°C)	70.1	61.4	103.6	203.1	77.7	180.8	
<i>A</i> (m ²)	66.2	60.8	28.0	30.1	49.5	278.4	

Source: Saboo *et al.*, 1986.

The overall heat transfer coefficient for all HEXs is 0.265 kW/(m²·K), the project lifetime is 5 years, the annual interest rate is 0%, the relocation of existing HEX cost is 300 \$ and the investment cost of new HEX and additional area of existing ones is given by:

$$IC_{new\ HEX} = 3460 + 300A^{0.6} \quad (5.10)$$

$$IC_{existing\ HEX} = 300A^{0.6} \quad (5.11)$$

The objective function is the same as Example 1. This example has been explored using different values of EMAT (EMAT = 4.2 °C, 12 °C and 14°C) by different authors. The retrofit was conducted here assuming a single EMAT value of 14°C.

The retrofit solution achieves a heat recovery of 4,399.6 kW and an objective function value of \$914,663. With this level of heat recovery, all coolers are rendered unnecessary, resulting in zero cold utility consumption. The topological changes involve the resequencing of HEX 6 and the addition of three new exchangers (HEX 14, 15, and 16).

The solution is presented in Figure 5.6, the HEX details are shown in Table 5.7 and the comparison with other works are presented in Table 5.8.

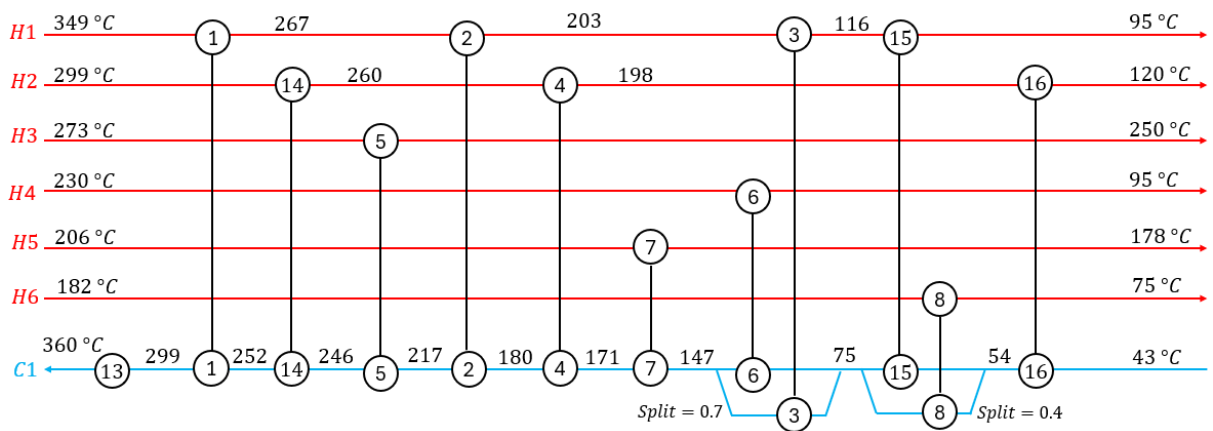
It is noteworthy that the solution obtained through the enumeration procedure represents the best-reported solution to date, even when considering an EMAT of 14°C (lower values would yield better objective functions). Note, however, that the solution proposed in

Example 2 exhibits a characteristic behavior when the synheat model is applied, namely the presence of two splits in series for stream C1. This feature arises from the division of the network into stages and, from a practical standpoint, introduces significant operational complexity and difficulty, often leading to its neglect in industrial applications. A potential solution to this issue would be to replace the synheat model with the sub-stage approach proposed by Kim *et al.* (2017).

This set of results demonstrates that the proposed enumeration procedure is capable of suggesting efficient topological changes to the network. As previously discussed, a significant portion of structures are not explored during the process. However, at each stage, the best intervention is identified, as confirmed by the presented results.

Furthermore, an additional advantage of the proposed procedure, illustrated in the next set of results, is its ability to incorporate an unprecedented level of detail in heat exchanger calculations together with the topological modifications. This is achieved without convergence issues, initialization requirements, or parameter tuning.

Figure 5.6. Example Based on Saboo *et al.* (1986) – Retrofit solution



Source: Author's own work, 2024.

Table 5.7. Example Based on Saboo *et al.* (1986) - Information of retrofit solution

HEX	1	2	3	4	5	6
Q (kW)	7089.1	5449.7	7486.4	1315.9	4247.9	3172.2
T_{hi} (°C)	349.0	266.6	203.2	260	273.0	230.0
T_{ho} (°C)	266.6	203.2	116.1	198.5	250.0	95.0
T_{ci} (°C)	251.6	180.4	74.9	171.5	217.2	74.9
T_{co} (°C)	299.5	217.2	147.0	180.4	246.0	147.0
LMTD (°C)	28.8	34.4	48.3	48.6	29.8	44.3
A_{new} (m ²)	479.5	228.3	136.8	0	349.9	0
HEX	7	8	13	14	15	16
Q (kW)	3623.2	1230.5	8940.9	835.3	1817.8	1675.3
T_{hi} (°C)	206.0	182.0	500.0	299.0	116.1	198.5
T_{ho} (°C)	178.0	75.0	500.5	260.0	95.0	120.2
T_{ci} (°C)	147.0	54.3	299.5	246.0	54.3	43.0
T_{co} (°C)	171.5	74.9	360.0	251.6	74.9	54.3
LMTD (°C)	32.7	52.5		27.4	40.9	107.2
A_{new} (m ²)	137.9	0	0	115.1	167.5	58.9

Source: Author's own work, 2024.

Table 5.8. Example Based on Saboo *et al.* (1986) - Solution comparison

	Objective function (\$)	EMAT
Briones and Kokossis (1999)	636,831	4.2
Ma <i>et al</i> (2000)	769,791	12
Rezaei and Shafiei (2009)	755,608	14
Pan <i>et al</i> (2013)	824,483	14
Augnstorm <i>et al</i> (2021)	890,133	4.2
This work	914,663	14

Source: Author's own work

5.3.2. Comparison with previous results based on heat load modifications only

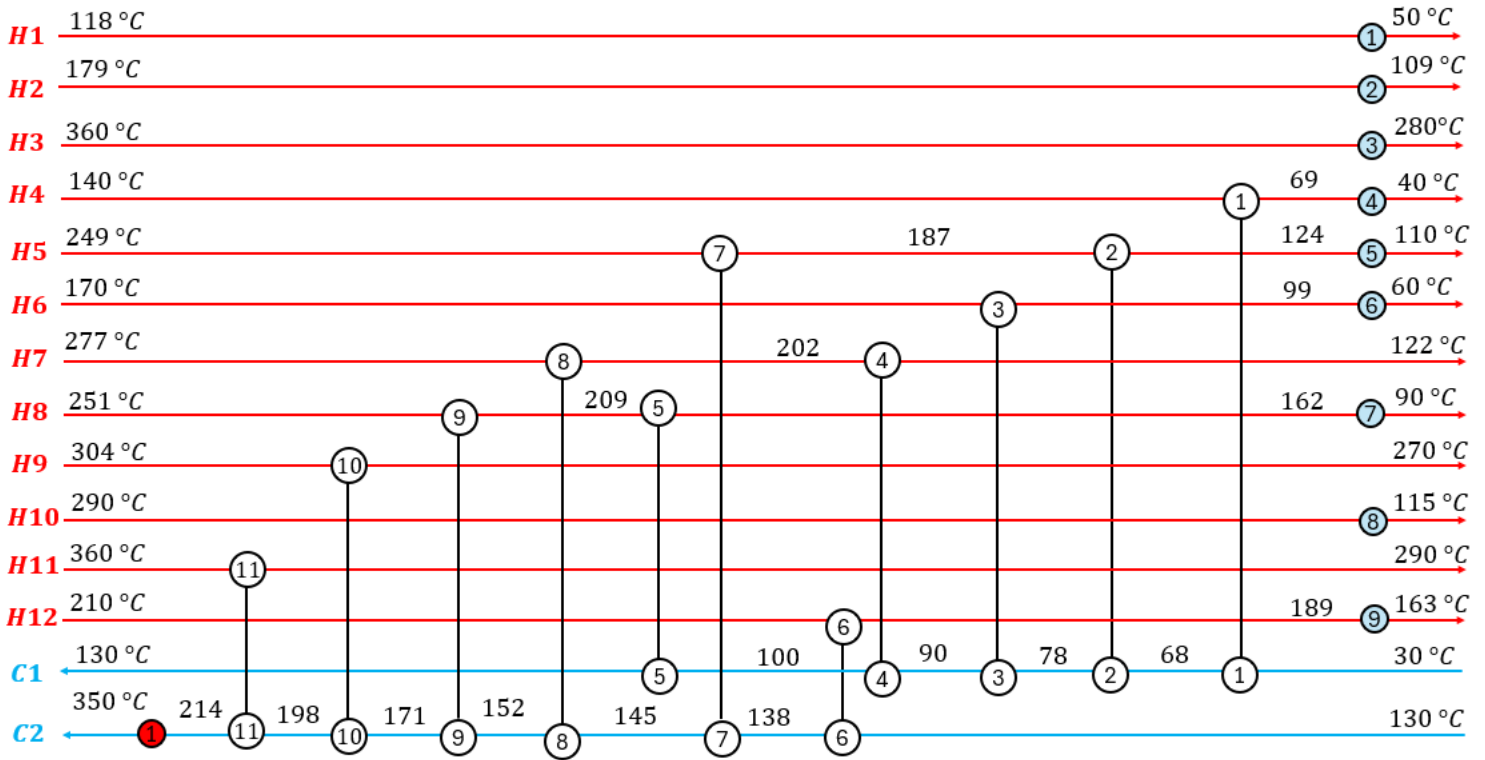
The examples used are the same as those addressed in Part I of this work. To avoid redundantly restating all the necessary data and information that describe the problem, only a few relevant details are repeated here. Readers are encouraged to refer to the first part in this series for a comprehensive understanding (chapter 4).

Example 3

Example 3 involves 12 hot streams and 2 cold streams (crude oil before and after the desalter). Currently, the furnace heats the crude from 234.8 to 350 °C, with a furnace utility of 39.09 MW. The existing HEN is presented in Figure 5.7.

It is important to reiterate that, because gasketed plate HEXs are not used in this type of process, it is not considered adding a GPHE during the HEX retrofit. Thus, the alternatives involve replacing the existing one with a new STHE, adding a new STHE in series or parallel, or intensifying the existing HEX.

Figure 5.7. Example 3: Existing HEN



Source: Bagajewicz *et al.*, 2013.

The stream targets and existing HEX details are presented in Tables 5.9 and 5.10.

Table 5.9. Example 3: Streams data

Stream	Inlet temperature (°C)	Outlet temperature (°C)	Mass flow rate (kg/s)	Heat capacity (J·kg ⁻¹ ·K ⁻¹)
Hot streams				
H1	117.7	50.0	42.00	2921.4
H2	178.6	108.9	19.13	2477.5
H3	359.6	280.0	7.67	3156.5
H4	140.0	40.0	46.29	2293.9
H5	248.8	110.0	12.73	2513.4
H6	170.1	60.0	14.74	2292.9
H7	277.0	121.9	9.84	2551.3
H8	250.6	90.0	55.10	2375.7
H9	303.6	270.2	81.01	2888.2
H10	290.0	115.0	23.24	1204.1
H11	360.0	290.0	23.42	2830.9
H12	210.0	190.0	46.30	2544.5
Cold streams				
C1	30.0	130.0	96.41	2074.3
C2	130.0	350.0	96.64	2202.0

Source: Bagajewicz *et al.*, 2013.

Table 5.10. Example 3: HEX information of the existing HEN

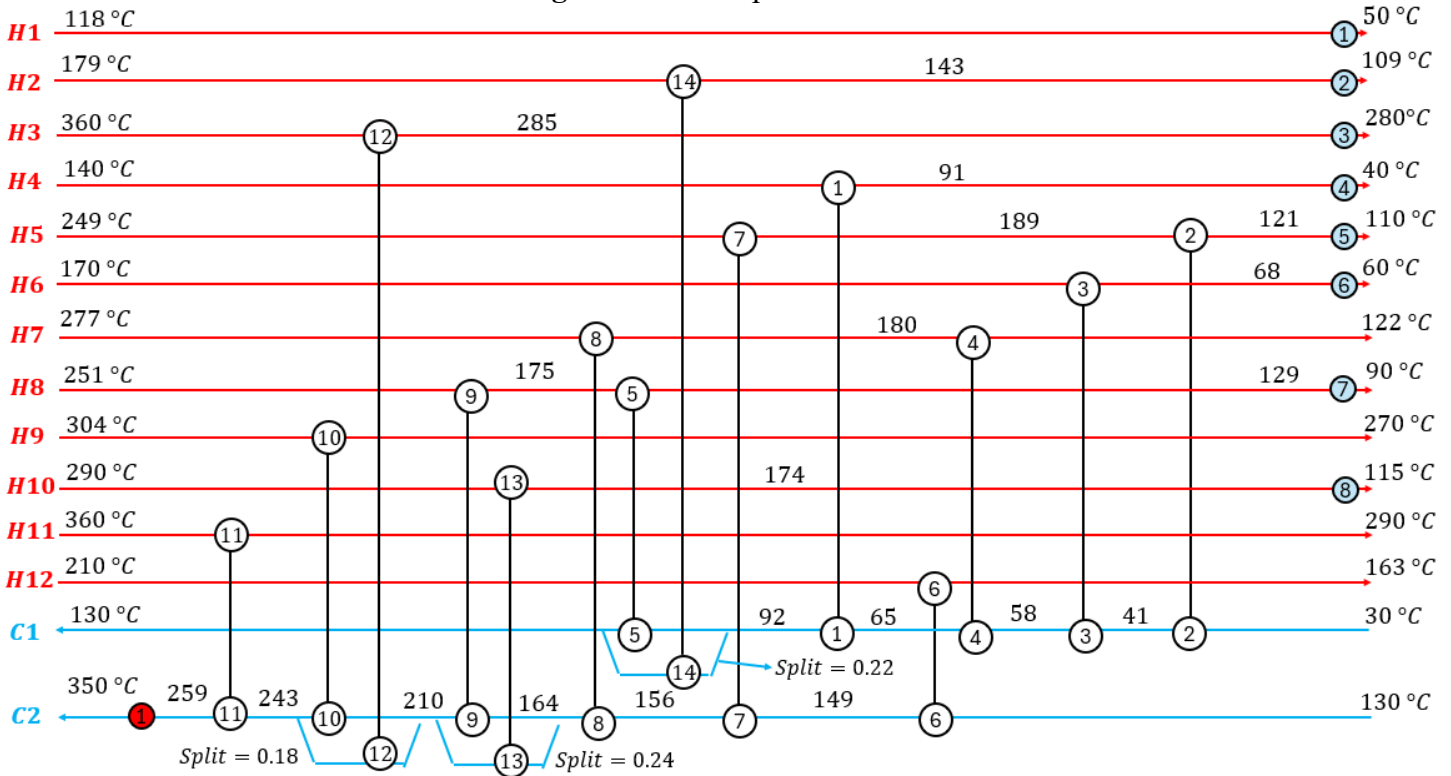
HEX	1	2	3	4	5	6
Q (kW)	7530	2000	2400	2000	6070	3230
<i>Thi</i> (°C)	140.0	186.6	170.1	201.6	208.8	210.0
<i>Tho</i> (°C)	69.1	124.1	99.1	121.9	162.4	189.1
<i>Tci</i> (°C)	30.0	67.6	77.65	89.6	99.6	130.0
<i>Tco</i> (°C)	67.65	77.6	89.65	99.6	130	138.5
LMTD (°C)	54.0	79.9	44.6	60.5	70.5	65.1
<i>F</i>	0.96	1	0.92	0.96	0.95	0.99
HEX	7	8	9	10	11	
Q (kW)	1990	1880	5470	7800	4640	
<i>Thi</i> (°C)	248.8	277.0	250.6	303.6	360.0	
<i>Tho</i> (°C)	186.6	201.6	208.8	270.2	290.0	
<i>Tci</i> (°C)	138.5	145.4	152.0	171.0	198.1	
<i>Tco</i> (°C)	145.4	152.0	171.0	198.1	214.3	
LMTD (°C)	72.2	86.0	67.5	102.3	116.7	
<i>F</i>	1	1	0.97	0.98	0.98	

Source: Bagajewicz *et al.*, 2013.

The retrofit solution attained using the complete algorithm (i.e. with topological modifications) is associated with an energy recovery of 13 MW (5.4 MW higher than the alternative without topological modifications), associated with an NPV of 6,182,838 \$ (59%

higher than the alternative without topological modifications). The proposed topological modifications involves the resequencing of HEX 1, and the addition of three new matches (HEX 12, 13 and 14). The solution is presented in Figure 5.8, the HEX information is depicted in Table 5.11, the details of the solution for retrofitted HEX are presented in Table 5.12, and for new matches in Table 5.13.

Figure 5.8. Example 3: Retrofit solution



Source: Author's own work, 2024.

Table 5.11. Example 3: HEX information in the retrofitted HEN

HEX	1	2	3	4	5	6
Q (kW)	5238.4	2185.6	3464.6	1448.0	5975.2	5496.6
<i>Thi</i> (°C)	140.0	189.5	170.1	179.6	175.1	210.0
<i>Tho</i> (°C)	90.7	121.2	67.6	121.9	129.5	163.3
<i>Tci</i> (°C)	65.5	30.0	40.9	58.2	91.7	130.0
<i>Tco</i> (°C)	91.7	40.9	58.2	65.5	130.0	149.1
LMTD (°C)	35.5	117.6	59.4	86.4	41.3	45.7
HEX	7	8	9	10	11	12
Q (kW)	1896.7	2445.0	9880.8	7815.6	4641	1796.7
<i>Thi</i> (°C)	248.8	277.0	250.6	303.8	360.0	359.6
<i>Tho</i> (°C)	189.5	179.6	175.1	270.2	290.0	285.3
<i>Tci</i> (°C)	149.1	155.7	164.2	209.8	243.1	209.8
<i>Tco</i> (°C)	155.7	164.1	209.7	243.1	259.2	243.1
LMTD (°C)	63.1	57.3	22.7	60.4	70.4	94.5
HEX	13	14				
Q (kW)	3253.4	1688.1				
<i>Thi</i> (°C)	290.0	178.6				
<i>Tho</i> (°C)	174.6	143.0				
<i>Tci</i> (°C)	164.2	91.7				
<i>Tco</i> (°C)	209.8	130.0				
LMTD (°C)	34.2	49.9				

Source: Author's own work, 2024.

Table 5.12. Example 3: Detail solution of retrofitted HEXs

HEX	5	6	8	9	10	11
Retrofit alternative	STHE series	STHE series	Coil-Wire	STHE series	STHE series	STHE series
Added area (m ²)	346.7	365.7	0	2273.9	268.1	99.8
U (W/m ² K)	228.7	246.1	154.04	186.3	205.3	241.5
Number of shells added	1	1	0	3	1	1
Additional ΔPt (kPa)	54.6	43.5	15.1	88.8	36.6	29.5
Additional ΔPs (kPa)	12.8	37.2	0	26.2	18.4	23.6
<i>dte</i> (m)	0.0381	0.01905	-	0.01905	0.0254	0.0381
<i>L</i> (m)	6.0976	4.8768	-	4.8768	4.8768	3.6585
<i>Ds</i> (m)	1.524	1.143	-	1.3716	0.9906	0.889
<i>lay</i>	Triangular	Square	-	Square	Square	Square
<i>Npt</i>	6	4	-	6	2	6
<i>rp</i>	1.5	1.5	-	1.25	1.33	1.5
<i>Nb</i>	18	8	-	8	5	5
<i>Ntt</i>	475	1253	-	2597	689	171
Helical Pitch (m)	-	-	0.064	-	-	-
Coil-Wire diameter (m)	-	-	0.0014	-	-	-

Source: Author's own work, 2024.

Table 5.13. Example 3: Detailed solution of new matches

HEX	12	13	14
Area (m ²)	119.5	662.7	203.1
U (W/m ² K)	179.4	216.3	205.0
Number of shells	1	2	1
Tube stream	Cold stream	Hot stream	Hot stream
ΔPt (kPa)	39.6	59.7	35.7
ΔPs (kPa)	15.4	35.4	17.7
dte (m)	0.01905	0.01905	0.01905
L (m)	3.6585	6.0976	4.8768
Ds (m)	0.6858	0.889	0.7874
lay	Square	Square	Triangular
Npt	6	6	6
rp	1.25	1.33	1.33
Nb	18	18	14
Ntt	473	908	696

Source: Author's own work, 2024.

To highlight the importance of considering a detailed HEX retrofit simultaneously with the HEN retrofit, we also conducted the HEN retrofit using the simplified exchanger design, as was done in Part I and in the first two examples. The simplified design approach dominates the literature, specially considering topological modifications, and has several limitations, as previously discussed (to avoid redundancy, readers are encouraged to refer to the detailed discussion in sections 2 and 3). Here, we will present only the results.

Table 5.14 below presents all the retrofit results obtained, including those using the detailed approach with and without topological modifications (presented in chapter 4), as well as the results with the simplified HEX calculation (presented in appendix 3). It is important to reiterate that the results presented with the simplified approach were obtained as follows: the retrofit of the network was initially carried out using the simplified HEX calculations. Once the solution was obtained, it was then recalculated with the detailed design of the exchangers, leading to the results presented in the table. The details of the solution obtained with the simplified approach is depicted in the supplementary material.

Table 5.14: Comparison between different approaches in example 3

	Detailed HEX evaluation	Detailed HEX evaluation	Simplified HEX evaluation	Simplified HEX evaluation
Topological modification	No	Yes	No	Yes
Energy recovery (MW)	7.6	13	8.5	14.5
Investment cost (\$)	1,459,232	2,719,497	2,585,884	4,293,652
Additional operational cost (\$/y)	53,819	75,531	85,127	145,908
NPV (\$)	3,882,290	6,182,838	2,861,250 \$	4,492,988

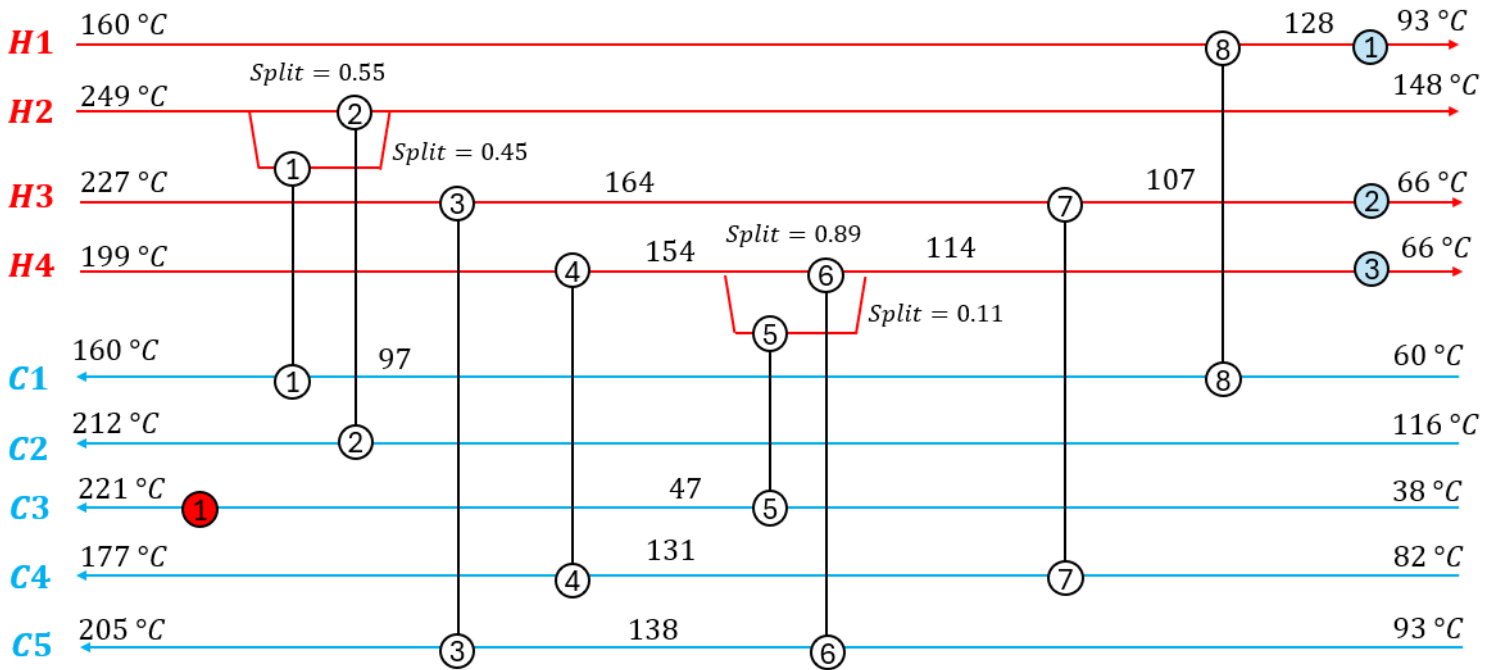
Source: Author's own work, 2024.

Table 5.14 shows that the traditional approach is capable of proposing good results, generating interventions in the network that lead to profitable projects, with an NPV of approximately \$2.8 million and \$4.5 million for retrofit without and with topological modifications, respectively. However, it is noteworthy that there is a significant gain when incorporating all the detailed calculations presented in this series of works, achieving an additional profit of over \$1 million without considering topological changes and up to approximately \$1.7 million when topological changes are considered.

Example 4

Example 4 involves 4 hot streams and 5 cold streams (crude oil before and after the desalter). Currently, the HEN consumes 15,402 kW of hot utility and 18,556 kW of cold utility. The existing HEN is presented in Figure 9, and the streams data and HEX details are present in Tables 5.15 and 5.16.

Figure 5.9. Example 4: Existing HEN



Source: Author's own work, 2024.

Table 5.15. Example 4: Stream data

Stream	Inlet temperature (°C)	Outlet temperature (°C)	Mass flow rate (kg/s)	Heat capacity (J·kg ⁻¹ ·K ⁻¹)
H1	160.0	93.0	34.53	2670
H2	249.0	148.0	47.76	2317
H3	227.0	126.0	63.94	2433
H4	199.0	66.0	74.11	2512
C1	60.0	160.0	38.01	2105
C2	116.0	212.0	35.86	1780
C3	38.0	221.0	44.13	2008
C4	82.0	177.0	78.89	2300
C5	93.0	205.0	68.52	2130

Source: Faria *et al.*, 2015.

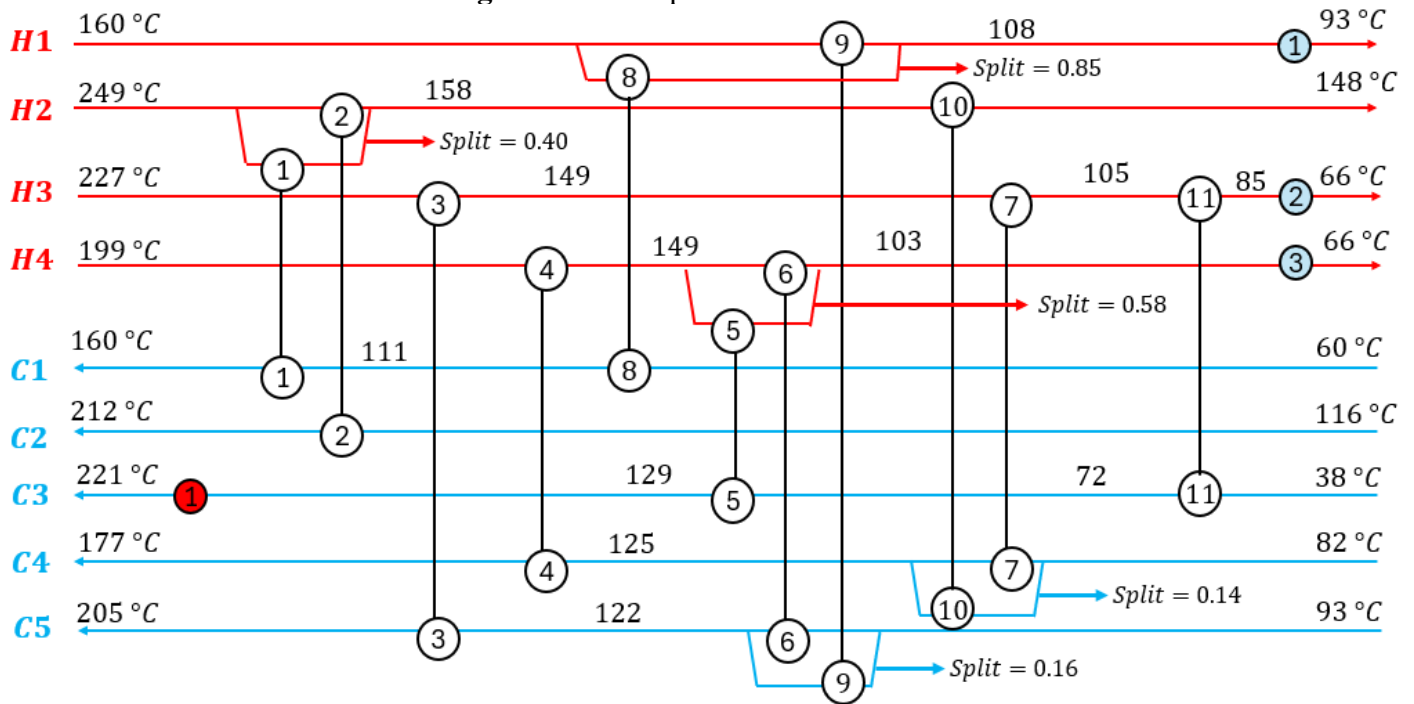
Table 5.16. Example 4: HEX information in the existing HEN

HEX	1	2	3	4	5	6
Q (kW)	5049	6129	9711	8296	814	6635
<i>Thi</i> (°C)	249.0	249.0	227.0	199.0	154.4	154.4
<i>Tho</i> (°C)	148.0	148.0	164.4	154.4	114.4	114.4
<i>Tci</i> (°C)	96.9.0	116.0	138.5	131.3	38.0	93.0
<i>Tco</i> (°C)	160.0	212.0	205.0	177.0	47.2	138.5
<i>LMTD</i> (°C)	68.3.0	34.4	23.9	22.6	90.9	18.6
<i>F</i>	0.94	0.82	1	1	1	0.89
HEX	7	8				
Q (kW)	8940	2952				
<i>Thi</i> (°C)	164.4	160.0				
<i>Tho</i> (°C)	106.7	128.0				
<i>Tci</i> (°C)	82.0	60.0				
<i>Tco</i> (°C)	131.3	96.9				
<i>LMTD</i> (°C)	28.7	65.52				
<i>F</i>	0.83	0.95				

Source: Author's own work, 2024.

The retrofit solution with the complete procedure proposed here is associated with an energy recovery of 7,222 kW (3422 kW higher than the alternative without topological modifications), and a NPV of 1,482,937 \$ (46% higher than the alternative without topological modifications). The proposed topological modifications involve the resequencing of HEX 1, and the addition of three new matches (HEX 9, 10 and 11). The solution is presented in Figure 5.10, the retrofit solution information of each HEX is depicted in Table 5.17, the details of HEX retrofit in Table 5.18 and for new matches in Table 5.19.

Figure 10. Example 4: Retrofit solution



Source: Author's own work, 2024.

Table 5.17. Example 4: HEX information in the retrofitted HEN

HEX	1	2	3	4	5	6
Q (kW)	3937.0	6128.6	12132.7	9374.5	4958.5	3523.1
T_{hi} (°C)	249.0	249.0	227.0	199.0	148.6	148.6
T_{ho} (°C)	158.0	158.0	148.8	148.6	103.1	103.1
T_{ci} (°C)	110.8	116.0	121.9	125.3	72.7	93.0
T_{co} (°C)	160.0	212.0	205.0	177.0	128.7	121.9
LMTD (°C)	65.9	39.5	24.4	22.6	24.8	17.1
HEX	7	8	9	10	11	
Q (kW)	6750.4	4063.9	690.6	1111.9	3077.9	
T_{hi} (°C)	148.8	160.0	160.0	158.0	105.2	
T_{ho} (°C)	105.2	108.4	108.8	148.0	85.4	
T_{ci} (°C)	82.0	60.0	93.0	82.0	38.0	
T_{co} (°C)	125.3	110.8	121.9	152.3	72.7	
LMTD (°C)	23.3	48.8	25.1	47.4	39.5	

Source: Author's own work, 2024.

Table 5.18. Example 4: Detailed solution of HEX retrofit

HEX	3	4	5	8
Retrofit alignment	GPHE series	GPHE parallel	Replace for a new GPHE	GPHE series
Added area (m ²)	137.9	204.9	542.7	89.5
U (W/m ² K)	328.4	518.4	539.7	492.1
Additional ΔPh	5.515	-38.6	38.8	10.0
Additional ΔPc	7.342	-39.9	52.3	13.1
Lp (m)	0.742	2.092	2.092	0.978
Lw (m)	0.845	1.200	1.200	0.812
Dp (m)	0.3	0.4	0.4	0.288
Nph	1	2	2	1
Npc	1	2	2	1
Chevron angle (°C)	60	45	45	45
Np	191	71	188	98

Source: Author's own work, 2024.

Table 5.19. Example 4: Detailed solution of new matches

HEX	9	10	11
Area (m ²)	123.45	115.3	292.7
U (W/m ² K)	261.6	238.4	321.0
Number of shells	2	1	1
Tube stream	Hot stream	Cold stream	Hot stream
ΔPt (kPa)	95.0	63.3	15.5
ΔPs (kPa)	23.5	16.16	13.8
dte (m)	0.01905	0.01905	0.01905
L (m)	4.8768	6.0976	3.6585
Ds (m)	0.3874	0.5906	0.9906
lay	Triangular	Triangular	Square
Npt	6	6	4
rp	1.25	1.33	1.25
Nb	16	10	8
Ntt	141	316	1337

Source: Author's own work, 2024.

Similar to example 1, example 2 is also optimized using the traditional procedure for HEX evaluation. The comparison between each approach is presented in Table 5.20, and the details of the solution obtained with the simplified approach is also depicted in the supplementary material.

Table 5.20: Comparison between each approach in example 4

	Detailed HEX evaluation	Detailed HEX evaluation	Simplified HEX evaluation	Simplified HEX evaluation
Topological modification	No	Yes	No	Yes
Energy recovery (kW)	3800	7222	5395	12063
Investment cost (\$)	109,228	477,758	1,578,553	3,686,762
Additional operational cost (\$/y)	14,103	22,119	75,322	95,721
NPV (\$)	1,013,821	1,482,937	- 696,578	- 857,966

Source: Author's own work, 2024.

Unlike Example 1, Table 5.20 presents a proposed solution from the traditional approach that performs significantly worse, even resulting in a negative NPV. Example 4 is characterized by HEX with high degrees of temperature crossovers and low LMTD values. Since heat exchanger geometry is typically not considered, temperature crossovers are excluded from calculations, severely penalizing the solution when the HEX must be properly designed. Additionally, because pressure drop is often disregarded, the trade-off between capital and operational costs for exchangers, with high heat duties and low LMTD values, is not appropriately addressed, frequently leading to underestimated heat transfer areas (when the trade-off is appropriate account, the heat transfer area tends to increase to reduce the operational cost).

For instance, as detailed in the supplementary material, the new service for HEX 6 involves a heat duty of 8210 kW, with hot stream inlet and outlet temperatures of 159 °C and 103 °C, and cold stream temperatures of 93 °C and 149 °C, respectively, resulting in an LMTD equal to 10 °C. This exchanger experiences a severe temperature crossover, requiring an additional area of 2175 m², distributed across three new shells in series. Note that, because all these aspects is considered simultaneously with the HEN retrofit using a detailed HEX evaluation, in the proposed procedure the optimization seeks an energy and temperature redistribution that avoid the retrofit in this HEX.

These results highlight the critical importance of incorporating detailed exchanger design calculations in retrofit problems. They also underscore that several significant factors are overlooked when a simplified approach is employed.

5.4. Conclusions

This chapter presents an extension of the part I of this work (chapter 4), where topological modifications are also considered in the HEN retrofit. An incremental enumeration procedure is proposed, avoiding the combinatorial explosion that is characteristic of the problem. The first set of examples illustrates that the proposed enumeration procedure can identify good retrofit solutions compared with the literature. Particularly, in one of the examples, the proposed approach found a better solution than those previously reported in the literature. In addition, the second set of examples introduces all enhancement details described in part I, reinforcing the benefits of considering a more detailed modelling. Finally, comparing solutions without topological modifications, it is possible to observe the HEN retrofit solutions with higher NPV can be achieved, due to the more energy recovery.

ACRONYMS AND ABBREVIATIONS

$D_{synheat}$	– Synheat formulation constraints
HEN	– Heat exchanger network
HEX	– Heat exchanger
LMTD	– Logarithmic mean temperature difference
LP	– Linear programming
MILP	– Mixed integer linear programming
MINLP	– Mixed inter nonlinear programming
NLP	– Non linear programming
NPV	– Net present value
GPHE	– Gasketed-plate heat exchanger
STHE	– Shell and tube heat exchanger

NOMENCLATURE

A	Heat transfer area (m ²)
A_{new}	Additional heat transfer area of existing HEX (m ²)
CF_t	Cash flow in time t (\$/y)
$fobj$	Objective function
$FVIFA$	Future value interest factor of annuity (y)
\hat{i}	Interesting rate
IC^{LB}	Lower bound of investment cost (\$)
$IC_{new\ HEX}$	Investment cost of instaling new HEX (\$)
$IC_{ex\ HEX}$	Investment cost of adding new area of existing HEX (\$)
\hat{n}	Time horizon (y)
\hat{N}	Total number of matches in the HEN
\hat{N}_{ex}	Number of matches in the existing HEN
\hat{N}^*	Number of matches in the existing HEN preserved in the new structure
$\widehat{Nmatc}_{i,j}^{orig}$	Number of matches between hot stream i and cold stream j in the existing
NPV^{inc}	Net present value of the incumbent (\$)
REL_{cost}	Relocating HEX cost (\$)
SC	Saving money cost (\$/y)

$z_{i,j,k}$	Binary variable that indicates the match between hot stream i , cold stream j in stage k
zcu_i	Binary variable that indicates a cooler for hot stream i
zhu_j	Binary variable that indicates a heater for cold stream j
γ	Dummy variable

FINAL CONCLUSION

This thesis aimed to revisit the HEN retrofit problem in its broadest scope, reexamining it from foundational concepts to existing proposals in the literature. In chapter 2 is highlighted several significant aspects from the perspective of industrial practice, which are often overlooked by the academic community. The absence of these fundamental aspects in the problem formulation creates a significant misalignment between the solutions proposed in academic articles and the basic needs of industrial practice.

In addition to aspects not yet addressed in the literature, such as different cash flow structures and issues related to network layout, other topics—although superficially mentioned in prior works—were examined in greater depth. For instance, considerations such as pressure drop and fouling were explored, with particular emphasis on the simplified design of the HEXs. Simple examples were presented, illustrating that these simplifications can not only underestimate the investment costs, thereby distorting the actual retrofit return, but also propose solutions that are impractical for real-world implementation.

Finally, we discussed the challenges and difficulties of incorporating these fundamental aspects into HEN retrofit solution procedures. It is well understood that the HEN retrofit problem is inherently complex, and existing methodologies in the literature continue to struggle to provide tools capable of addressing the problem while still relying on numerous simplifications. In this context, it is worth reflecting on whether classical approaches can evolve to meet the level of detail demanded by the problem.

Chapters 3 to 5 present an alternative approach to addressing the HEN retrofit problem, aiming to mitigate some of the limitations and simplifications present in existing studies. Chapter 3 provides a detailed exploration of the retrofit of a single HEX. Various methods for enhancing the heat transfer capacity of existing HEX units are introduced, including adding area by aligning a new unit in series or parallel with the existing one, intensifying the current HEX, or fully replacing it with a new unit.

Additionally, the possibility of aligning different types of HEX units is incorporated, and the assumption of a known and constant overall heat transfer coefficient is discarded. Instead, thermofluid-dynamic calculations are performed in detail using well-established models from the literature. This approach not only enables the exploration of various retrofit alternatives but also represents a significant advancement in the level of model detail.

The results demonstrate that retrofitting a single HEX can be highly complex, with the optimal alternative heavily dependent on the new service conditions to which the HEX is subjected. Another critical aspect highlighted is the importance of allowing the alignment of a heat exchanger with a different geometry from the existing HEX, which better leverages the fundamental trade-off in HEX design between operational and capital costs. In addition to all these features, the procedure is robust, rigorous and free from convergence issues and optimized globally.

Finally, a comprehensive HEN retrofit procedure is introduced, which integrates the detailed calculation of heat exchangers simultaneously with the network retrofit. In Chapter 4, we present a procedure that excludes topological modifications to the network. As demonstrated, while this approach limits the capacity for heat recovery, it offers a solution with less invasive and complex interventions, making implementation simpler while still achieving significant financial returns.

To achieve this, the problem is formulated by leveraging the utility paths and energy loops within the network, with the decision variables being the energy recovery and the thermal load of a heat exchanger within each independent loop. To evaluate the objective function, given the utility consumption and information for each loop, an energy balance is solved to determine the service requirements of all heat exchangers, enabling the retrofit algorithm for HEX, as outlined in Chapter 3, to be employed.

In addition to incorporating several advancements in modeling and retrofit alternatives for heat exchangers, the procedure is designed to embed all numerical challenges inherent in the HEN retrofit problem within the heat exchanger design step. This step, as discussed in Chapter 3, is carried out efficiently and robustly, free of convergence issues, and guarantees global optimality. Consequently, this approach is highly effective in handling the nonlinearities of the problem, even with the extensive detail included in the formulation, requires no initialization or parameter tuning. A comparison with classical approaches demonstrates that, in addition to delivering more profitable solutions, the proposed method avoids suggesting impractical solutions.

Finally, in Chapter 5, we propose a procedure that incorporates topological modifications into the HEN retrofit process. Although these modifications are more complex to implement, they can introduce changes that significantly enhance the network's heat recovery, thereby increasing the retrofit's economic return.

An incremental enumeration technique is presented, where topological modifications are implemented in sequential stages, aiming in each stage to identify the best solution with

the fewest possible modifications. This technique, while excluding a substantial number of potential interventions, mitigates the combinatorial explosion typically associated with the problem. Furthermore, the solution at each stage corresponds to the best topological modification among all feasible options requiring the least number of interventions. This creates a procedure that, as it evolves, incrementally identifies optimal solutions in a structured and systematic manner. The results demonstrate a significant improvement compared to the classical approach, highlighting that topological modifications can yield solutions with greater heat recovery and, consequently, higher profits when such modifications are considered.

Thus, this thesis contributes significantly to the field of HEN retrofit, both through conceptual discussions of the problem and in the development of solution techniques. One of the strengths of the proposed methodology lies in its ability to efficiently handle the numerical complexities of the problem. For cases without topological modifications, there is optimism about incorporating several aspects discussed in this work in future advancements, such as adopting alternative superstructures (e.g., stage and sub-stage models, Kim *et al* (2017)) and integrating more detailed considerations of fouling and cash flow formulations, as presented in Chapter 2.

The main challenge, however, lies in addressing problems that involve topological modifications. A strategy was proposed to include such modifications without incurring a combinatorial explosion, demonstrating significant improvements compared with solutions without topological modifications, and competitive performance relative to previously reported methods. However, to manage computational time effectively, the examples limited the total number of topological changes, allowing for the addition of a maximum of three new matches.

This limitation, coupled with the incremental enumeration strategy, increases the likelihood of excluding potential solutions that might be superior to those reported in the results. Therefore, despite evident progress and contributions, significant challenges remain, particularly in exploring topological modifications in networks. Along with incorporating other aspects presented in this thesis, another avenue for future work involves developing tools to address this difficulty in exploring topologies.

In this regard, parallel computing emerges as a promising direction for future studies. This approach aligns well with the enumeration procedure since it could enable simultaneous optimization of a set of different structures through parallelization.

Another suggestion, which complements the methodology proposed in this thesis, involves the use of upper bounds to bypass the optimization of structures requiring significant computational effort. As the procedure progresses, an incumbent solution—the best solution found up to that point—is identified. Suppose a simplified model is employed as an upper bound to the full model. If the result of this simplified model is worse than the incumbent (e.g., it has a lower NPV), the rigorous solution is guaranteed to be worse as well. Thus, if the upper bound model is computationally inexpensive, it can serve as a preliminary filter to determine whether a structure warrants detailed optimization. These strategies could significantly enhance the methodology's ability to tackle the inherent complexities of the HEN retrofit problem, paving the way for more robust and efficient solutions in future research.

REFERENCES

- AKPOMIEMIE, M.O.; SMITH, R. Pressure drop considerations with heat transfer enhancement in heat exchanger network retrofit. *Applied Thermal Engineering*, v. 116, p. 695-708, 2017.
- ALINEZHAD, R.; ANSARI, R.; MAHDIKHANI, M.; BANIHASHEMI, S.A. Multi-phase Projects Selection and Scheduling Problem: A Multi-objective Optimization Approach. *Iranian Journal of Science and Technology, Transactions of Civil Engineering*, v. 46, p. 2575-2591, 2021.
- ASANTE, N. D. K.; ZHU, X. X. An automated approach for heat exchanger network retrofit featuring minimal topology modifications. *Computers & Chemical Engineering* v. 20, p. 7-12, 1996.
- ASANTE, N. D. K.; ZHU, X. X. An automated and interactive approach for heat exchanger network retrofit. *Chemical Engineering Research and Design*, v. 75, p. 349-360, 1997.
- AUGSUTORN, N.; SIEMANOND, K.; CHUVAREE, R. A robust design method for retrofit of industrial heat exchanger networks using modified stage-wise model. *Chemical Engineering Science*, p. 2021.
- ATHIER, G.; FLOQUET, P.; PIBOULEAU, L.; DOMENECH, S. A mixed method for retrofitting heat-exchanger networks. *Computers & Chemical Engineering*, v. 22, 1998.
- AYUB, Z.H. A new chart method for evaluating single-phase shell side heat transfer coefficient in a single segmental shell and tube heat exchanger. *Applied Thermal Engineering*, v. 25, p. 2412-2420, 2005.
- BAGAJEWICZ, J.M.; VALTINSON, G.; THANH, D.N. Retrofit of Crude Units preheating Trains: Mathematical Programming versus Pinch Technology. *Industrial & Engineering Chemistry Research*, v. 52, p. 14913 – 14926, 2013.
- BIYANTO, T.R.; GONAWAN, E.K.; NUGROHO, G.; CORDOVA, R. H. H.; INDRAWATI, K. Heat exchanger network retrofit throughout overall heat transfer coefficient by using genetic algorithm. *Applied Thermal Engineering*, v. 94, p. 274-281, 2016.
- BOLDYRYEV, S.; GIL, T.; ILCHENK, M. Environmental and economic assessment of the efficiency of heat exchanger network retrofit options based on the experience of society and energy price records. *Energy*, p. 125-155, 2022.
- BRIONES, V.; KOKOSSIS, A. C. Hypertargets: A Conceptual Programming approach for the optimization of industrial heat exchanger networks - II. Retrofit design. *Chemical Engineering Science*. v. 54, p. 541-561, 1999.
- BOCHENEK, R.; JEZOWSKI, J. M.; MARQUARDT, W.; PANTELIDES, C. Genetic algorithms approach for retrofitting heat exchanger network with standard heat exchangers. In *16th European Symposium on Computer Aided Process Engineering and 9th International Symposium on Process Systems Engineering, Elsevier Science: Amsterdam, Netherlands*, 2006.

BOWER, D. C.; WALKER, D.H.T. Planning Knowledge for Phased Rollout Projects. *Project Management Journal*, 38(3), 45-60, 2007.

BIYANTO, T. R.; GONAWAN, E. K.; NUGROHO, G.; CORDOVA, R. H. H.; INDRAWATI, K. Heat exchanger network retrofit throughout overall heat transfer coefficient by using genetic algorithm. *Applied Thermal Engineering*, v. 94, p. 274-281, 2016.

CAO, E. *Heat Transfer in Process Engineering*. New York: McGraw-Hill; 2010.

CHANG, C.; LIAO, Z.; COSTA, A. L. H.; BAGAJEWICZ, M. J. Globally optimal design of intensified shell and tube heat exchangers using complete set trimming. *Computers & Chemical Engineering*. v. 58, 2022.

CHANG, C.; PECCINI, A.; WANG, Y.; COSTA, A. L. H.; BAGAJEWICZ, J. M. Globally optimal synthesis of heat exchanger networks. Part I: Minimal networks. *AIChE Journal*, v. 66, 2020

CIRIC, A. R.; FLOUDAS, C. A. A retrofit approach for heat exchanger networks. *Computers & Chemical Engineering*. v. 13, p. 703-715, 1989.

CIRIC, A. R.; FLOUDAS, C. A. A mixed integer nonlinear programming model for retrofitting heat exchanger networks. *Industrial & Engineering Chemistry Research*. v. 29, p. 239-251, 1990.

DITTUS, F.W.; BOELTER, L.M.K. Heat Transfer in Automobile Radiators of the Tubular Type. *University of California Publications in Engineering*, v. 2, 443-461, 1930.

FLOUDAS, C.A. *Nonlinear and Mixed-Integer Optimization: Fundamentals and Applications*. New York: Oxford Academic, 1995.

GADALLA, M. A. A new graphical method for Pinch Analysis applications: Heat exchanger network retrofit and energy integration. *Energy*, v. 81, p. 159-174, 2015.

INCROPERA, F.P.; DEWITT, D.P. *Fundamentals of heat and mass transfer*. 7. ed. New York: John Wiley & Sons, 2007.

ISAFIADE, A.J. Heat exchanger network retrofit using the reduced superstructure synthesis approach. *Process Integration and Optimization for Sustainability*, v. 2, p. 205–219, 2018.

JIANG, N.; SHELLEY, J.D.; SMITH, R. New models for conventional and heat exchangers enhanced with tube inserts for heat exchanger network retrofit. *Applied Thermal Engineering*, v. 70, 2014.

JONES DR, Martins JRRA. The DIRECT algorithm: 25 years later. *Journal Global Optimization*, v. 79, p. 521-566, 2021.

KAKAÇ, S.; LIU, H. *Heat Exchangers: Selection, Rating, and Thermal Design*. 2. ed. New York: CRC Press, 2002.

KAZI, S.R.; SHORT, M.; ISAFIADE, A.J.; BIEGLER, L.T. Heat exchanger network synthesis with detailed exchanger designs: part 1. A discretized differential algebraic equation model for shell and tube heat exchanger design. *AIChE J*. v. 67, p. 17056, 2020a.

KAZI, S.R.; SHORT, M.; ISAFIADE, A.J.; BIEGLER, L.T. Heat exchanger network synthesis with detailed exchanger designs - 2. Hybrid optimization strategy for synthesis of heat exchanger networks. *AIChE J.* v. 67, p. 17057, 2020b.

KEMP, I. C. *Pinch Analysis and Process Integration*. Oxford: Butterworth-Heinemann, 2007.

KIM, S.Y.; JONGSUWAT, P.; SURIYAPRAPHADILOK, U.; BAGAJEWICZ, M.; Global Optimization of Heat Exchanger Network. Part1: Stages/Substages Superstructure. *Industrial & Engineering Chemistry Research*. v. 56, p. 5944-5957, 2017.

LAKSHMANAN, R.; BAÑARES-ALCANTARA, R. A Novel Visualization Tool for Heat Exchanger Network Retrofit. *Industrial & Engineering Chemistry Research*, v. 35, 4507-4522, 1996.

LEMO, J. C.; COSTA, A. L. H.; BAGAJEWICZ, M. J. Set Trimming Procedure for the Design Optimization of Shell and Tube Heat Exchangers. *Industrial & Engineering Chemistry Research*, v. 59, p. 14048-14054, 2020.

LEMO, J.C.; COSTA, A.L.H.; BAGAJEWICZ, M.J. Design of shell and tube heat exchangers considering the interaction of fouling and hydraulics. *AIChE J.* v. 68, p. 17586, 2022.

LI, B. H.; CHANG, C. T. Retrofitting Heat Exchanger Networks Based on Simple Pinch Analysis. *Industrial & Engineering Chemistry Research*, v. 49, p. 3967-3971, 2010.

LINHOFF, B.; FLOWERS, J.R. Synthesis of heat exchanger networks: I. Systematic generation of energy optimal networks. *AIChE J.*, v. 24, p. 633-642, 1977.

LINHOFF, B.; MASON, D.R.; WARDLE, I. Understanding heat exchanger networks. *Computers & Chemical Engineering*, v. 3, p. 295-302, 1979.

MA, K. L.; HUI, C. W.; YEE, T. F. Constant approach temperature model for HEN retrofit. *Applied Thermal Engineering*. v. 20, p. 1505-1533, 2000.

NAHES, A. L. M.; MARTINS, N. R.; BAGAJEWICZ, M. J.; COSTA, A. L. H. Computational Study of the Use of Set Trimming for the Globally Optimal Design of Gasketed-Plate Heat Exchangers. *Industrial & Engineering Chemistry Research*. v. 60, p. 1746-1755, 2021.

NGUYEN, D. Q.; BARBARO, A.; VIPANURAT, N.; BAGAJEWICZ, M. J. All At-Once and Step-Wise Detailed Retrofit of Heat Exchanger Networks Using an MILP Model. *Industrial & Engineering Chemistry Research*. v. 49, p. 6080-6103, 2010.

NORDMAN, R.; BERNTSSON, T. New Pinch Technology based HEN Analysis methodologies for cost-effective retrofitting. *The Canadian Journal of Chemical Engineering*, v. 79, p. 655-662, 2001.

OLIVA, D. G.; NAHES, A. L. M.; LEMO, J. C.; COSTA, A. L. H.; BAGAJEWICZ, M. J. Globally Optimal Simultaneous Heat Exchanger Network Synthesis and Basic Heat Exchanger Design. *AIChE Journal*, v. 70, e18450, 2024.

PAN, M.; BULATOV, I.; SMITH, R. Heat Transfer Intensification for Retrofitting Heat Exchanger Networks with Considering Exchanger Detailed Performances. *AIChE Journal*, v. 64, 2018

PAN, M.; BULATOV, I.; SMITH, R.; KIM, J. Novel MILP-based iterative method for the retrofit of heat exchanger networks with intensified heat transfer. *Computers and Chemical Engineering*, v. 42, p. 263-276, 2012

PAN, M.; BULATOV, I.; SMITH, R. New MILP-based iterative approach for retrofitting heat exchanger networks with conventional network structure modifications. *Chemical Engineering Science*, v. 104, p. 498-524, 2013a

PAN, M.; BULATOV, I.; SMITH, R.; KIM, J. Optimisation for the retrofit of large scale heat exchanger networks with different intensified heat transfer techniques. *Applied Thermal Engineering*, v. 53, p. 373-386, 2013b

PAN, M.; BULATOV, I.; SMITH, R. Exploiting tube inserts to intensify heat transfer for the retrofit of heat exchanger networks with considering fouling mitigation. *Industrial & Engineering Chemistry Research*, v. 52, p. 2925-2943, 2013c

PAN, M.; BULATOV, I.; SMITH, R. Improving heat recovery in retrofitting heat exchanger networks with heat transfer intensification, pressure drop constraint and fouling mitigation. *Applied Energy*, v. 161, p. 611-626, 2016

PANCHAL, C. B.; KURU, W. C.; LIAO, C. F.; EBERT, W. A.; PALEN, J. W. *Threshold Conditions for Crude Oil Fouling. In Understanding Heat Exchanger Fouling and Its Mitigation*; Bott, T. R., 1. Ed. Lucca, Italy: Begell House, 1997.

PONCE-ORTEGA, J. M.; JIMENEZ-GUTIERREZ, A.; GROSSMANN, I. E. Simultaneous retrofit and heat integration of chemical processes. *Industrial & Engineering Chemistry Research*. v. 47, p. 5512-5528, 2008.

REISEN, J. L. B.; GRIEVINK, J.; POLLEY, G. T.; VERHEIJEN, P. J. T. The placement of two-stream and multi-stream heat-exchangers in an existing network through path analysis. *Computers & Chemical Engineering*, v. 19, p. 143-148, 1995.

REZAEI, E.; SHAFIEI, S. Heat exchanger networks retrofit by coupling genetic algorithm with NLP and ILP methods. *Computers & Chemical Engineering*, v. 33, p. 1451-1459, 2009.

SABOO, A.K., MORARI, M., COLBERG, R.D. RESHEX: An interactive software package for the synthesis and analysis of resilient heat-exchanger networks—I. Program description and application. *Computers & Chemical Engineering*, v. 10, p. 577-589, 1986.

SALES, G.M.; QUEIROZ, E.M.; NAHES, A.L.M.; BAGAJEWICZ, M.J.; COSTA, A.L.H. Globally optimal design of kettle vaporizers. *Thermal Science and Engineering Progress*, 2021.

SERTH, R.W. *Process Heat Transfer: Principles, Applications and Rules of Thumb*. 1. Ed. New York: John Wiley & Sons; 2007.

SHORT, M.; ISAFIADE A.J.; FRASER, D.M.; KRAVANJA, Z. Two-step hybrid approach for the synthesis of heat exchanger networks with detailed exchanger design. *Applied Thermal Engineering*, v. 105, p. 807-821, 2016.

SMITH, R. *Chemical Process Design and Integration*. New York: John Wiley & Sons, 2005.

SOLTANI, H.; SHAFIEI, S. Heat exchanger networks retrofit with considering pressure drop by coupling genetic algorithm with LP (linear programming) and ILP (integer linear programming) methods. *Energy*, v. 36, p. 2381-2391, 2011.

SORSAK, A.; KRAVANJA, Z. MINLP retrofit of heat exchanger networks comprising different exchanger types. *Computers & Chemical Engineering*. v. 28, p. 235-251, 2004.

SREEPATHI, B. K.; RANGAIAH, G. P. Review of Heat Exchanger Network Retrofitting Methodologies and Their Applications. *Industrial and Engineering Chemistry Research*, v. 53, p. 11205-11220, 2014.

STAMPFLI, J. A.; OLSEN, D. G.; WELLIG, B.; HOFMANN, R. A parallelized hybrid genetic algorithm with differential evolution for heat exchanger network retrofit. *MethodsX*, v. 9, p. 101711, 2022.

TABOREK, J. *Input data and recommended practices*. In: *Heat Exchanger Design Handbook*. 1. Ed. New York: G. F. Hewitt, Begell House, 2008a.

TABOREK, J. *Performance evaluation of a geometry specified exchanger*. In: *Heat Exchanger Design Handbook*. 1. Ed. New York: G. F. Hewitt, Begell House, 2008b.

TABOREK J. *Design procedures for segmentally baffled heat exchangers*. 1. Ed. New York: G. F. Hewitt, Begell House, 2008c.

TJOE, T. N.; LINNHOFF, B. Using Pinch Technology for Process Retrofit. *Chemical Engineering Journal*, v. 8, p. 47-60, 1986.

TOWLER, G.; SINNOT, R. *Chemical Engineering Design – Principles. Practice and Economics of Plant and Process Design*, 1. Ed. New York: Butterworth-Heinemann, Burlington, 2008.

VARBANOV, P. S.; KLEMES, J. Rules for paths construction for HENs debottlenecking. *Applied Thermal Engineering*, v. 20, p. 1409-1420, 2000.

WANG, Y.; PAN, M; BULATOV, I.; SMITH, R.; KIM, J. Application of intensified heat transfer for the retrofit of heat exchanger network. *Applied Energy*, v. 89, p. 45-59, 2012.

YEE, T. F.; GROSSMANN, I. E. Simultaneous-Optimization Models for Heat Integration 0.2. Heat-Exchanger Network Synthesis. *Computers & Chemical Engineering*. v. 14, p. 1165-1184, 1990.

YEE, T. F.; GROSSMANN, I. E. A Screening and Optimization Approach for the Retrofit of Heat-Exchanger Networks. *Industrial & Engineering Chemistry Research*. v. 30, p. 146-162, 1991.

ZHU X, ZANFIR M, KLEMES J. Heat transfer enhancement for heat exchanger network retrofit. *Heat Transfer Eng*, v. 21, p. 7-18, 2000.

APPENDIX A - Set Trimming application

This appendix is associated with the supplementary material of the Chapter 3, which involves the article A Novel Procedure for Heat Exchanger Retrofit Considering Multiple Intervention Alternatives.

8.1.1. Set Trimming application.

This appendix presents an example of application of Set Trimming for the grassroots design of STHE. A methanol stream associated with a mass flow rate equal to 130 kg/s needs to be cooled from 160°C to 100°C using a STHE. Thus, a 121.3 kg/s of water stream is used, with inlet and outlet temperatures equals to 60°C and 100°C.

The objective function is the total annualized cost, and it is considered that the hot stream flows in the tube side and the cold stream in the shell side. The search space considered is presented in Table 8.1.

Table 8.1: STHE search space in Set Trimming example

Design variable	Values
Shell diameter (m)	0.2050, 0.3048, 0.3874, 0.489, 0.5906, 0.6858, 0.7874, 0.8382, 0.889, 0.9398, 0.9906, 1.0668, 1.143, 1.2192, 1.3716, 1.524
Outer diameter (m)	0.00635, 0.009525, 0.0127, 0.01905, 0.0254, 0.03175, 0.0381, 0.05080
Number of tube passes	1, 2, 4, 6
Pitch ratio	1.25, 1.33, 1.5
Tube layout	Triangular, square
Tube length (m)	1.2195, 1.8293, 2.439, 3.0488, 3.6585, 4.8768, 6.0976
Number of baffles	1,2,3,...,18,19,20
Baffle cut	15%, 20%, 25%, 30%
Number of shells in series	1,2,3

Source: Author's own work, 2024.

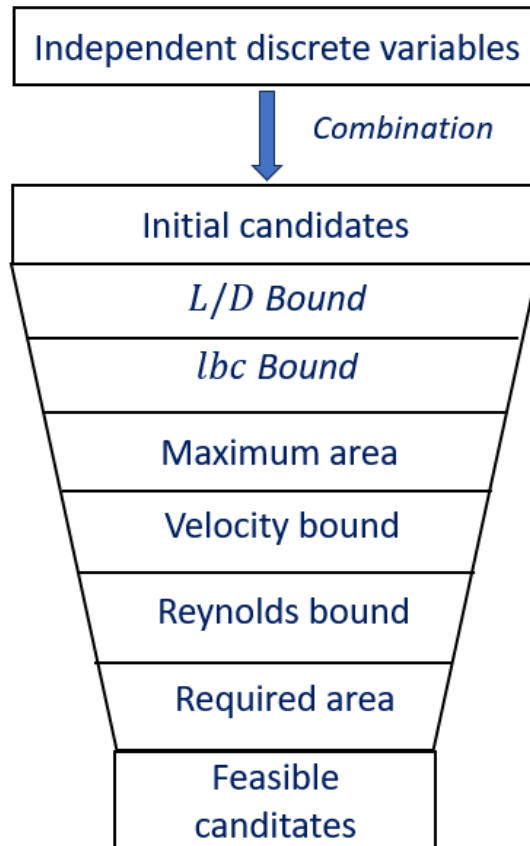
The search space is composed of discrete values of independent design variables. The procedure begins with the generation of initial set of candidates, where each element of the space is one combination of all of the geometric variables. Each element of this representation

is therefore a candidate solution. In the current example, the generation of all combinations of the independent variables gives a set containing 5,160,960 candidates.

Because each candidate is composed of an element of each independent variable, all continuous variables (flow velocities, Reynolds Number, Nuseelt Number, heat transfer coefficients, etc.) can be evaluated for all candidates. Thus, it is possible to evaluate all design constraints for all candidates in a sequential form, eliminating the infeasible ones.

According to the constraints associated with a STHE design, the Set Trimming applied to the STHE is illustrated in Fig 8.1.

Figure 8.1 – Set Trimming application to the STHE



Source: Author's own work, 2024.

Geometric Constraints:

First calculate the ratio between the tube length (L) and shell diameter (Ds) for all 5,160,960 candidates. According to the ratio between the tube length and shell diameter, the ones that have L/D smaller than 3 and higher than 15 are infeasible and can be eliminated from the space. The L/D ratio reduce the space from 5,160,960 to 3,041,280.

We now calculate the baffle spacing (lbc) for all 3,041,280 candidates. The ones that have $lbc < 0.2 D_s$ and $lbc > D_s$ are infeasible and can be eliminated from the space. The lbc bound reduce the space from 3,041,280 to 2,168,064.

We finally calculates the heat transfer area per shell for all 2,168,064. The ones that have the area higher than 1000 m² can be eliminated from the space, reducing the space from 2,168,064 to 2,056,392.

Velocity Bounds:

Now the tube side flow velocity is calculated for all 2,056,392 candidates. After the verification of velocity bounds, the number of candidates reduce to 467,916. Similarly for the shell side, the flow velocity is calculated for the 467,916, reducing the number of candidates to 305,844.

Reynolds Numbers Bounds:

The Reynolds Number in the tube side is calculated for the 305,844 candidates. However, the bounds in Reynolds number in tube side do not eliminate any candidate. Then, the Reynolds Number in shell side is calculated for the same number of candidates, reducing to 263,832.

Pressure Drop Bounds:

Because the objective function is the total annualized cost, the pressure drop is not used.

Minimum correction factor:

The next trimming is the minimum correction factor, but this constraint does not eliminate any candidate.

Heat Transfer Rate Equation:

Finally, the last trimming is the required area, which is calculated for the 263,832 remaining candidates. The application of this trimming reduces to candidates to 118,639.

Objective function evaluation:

Note that all design constraints were used, so all 118,639 surviving candidates are feasible solutions. Thus, now the objective function can be evaluated, and the global optimal solution is identified with a sorting procedure, which corresponds to a TAC equals to 26,101 \$/y.

Is it important to highlight some important aspects of the Set Trimming. First, the fluid allocation is fixed in this example. If the fluid allocation is also a design variable, two Set Trimming is performed, one considering one fluid allocation (e.g. hot stream in the tubes) and the second one considering the other allocation (e.g. cold stream in the tubes). The optimal solution is the smaller objective function between them.

Another aspect is that Set Trimming does not analyze individual candidates employing slow loops, it utilizes computational routines available in different tools to handle large sets of data efficiently (e.g. array operations using NumPy in Python, vectorized operations in Matlab or Scilab, and dynamic sets in GAMS).

APPENDIX B - HEN retrofit without topological modifications results

This appendix is associated with the supplementary material of the Chapter 4, which involves the results of Retrofit with Detailed HEX Design.

Example 1

Tables 8.2 and 8.3 present the complete description of each hot and cold streams

Table 8.2. Hot Stream Data of Example 1

Example	H1	H2	H3	H4	H5	H6
\hat{m} (kg/s)	42	19.1	7.7	46.3	12.7	14.7
Inlet \hat{T} (°C)	117.7	178.6	359.6	140.0	248.8	170.1
Outlet \hat{T} (°C)	50.0	108.9	280.0	40.0	110.0	60.0
ρ (kg/m ³)	655.0	684.0	686.0	746.0	758.0	626.0
$\hat{\mu}$ (mPa·s)	1.13	1.43	5.4	7.8	7.8	1.28
\hat{c}_p (J/kg·K)	2921.4	2477.5	3156.5	2293.92	2513.4	2292.9
\hat{k} (W/m·K)	0.123	0.111	0.126	0.126	0.116	0.137
$\hat{R}f$ (m ² K/KW)	0.275	0.275	0.275	0.275	0.275	0.275
Example	H7	H8	H9	H10	H11	H12
\hat{m} (kg/s)	9.8	55.1	81.0	23.4	23.4	46.3
Inlet \hat{T} (°C)	277	250.6	303.6	290.0	360.0	210.0
Outlet \hat{T} (°C)	121.9	90.0	270.2	115.0	290.0	190.0
ρ (kg/m ³)	613.0	644.0	607.0	736.0	736.0	758.0
$\hat{\mu}$ (mPa·s)	8.3	8.6	1.13	0.58	0.58	1.28
\hat{c}_p (J/kg·K)	2551.3	2375.7	2888.2	1204.1	2830.9	2544.5
\hat{k} (W/m·K)	0.113	0.145	0.102	0.105	0.111	0.125
$\hat{R}f$ (m ² K/KW)	0.275	0.275	0.275	0.275	0.275	0.275

Source: Author's own work, 2024.

Table 8.3. Cold Stream Data of Example 1

Example	C1	C2
\hat{m} (kg/s)	96.4	96.6
Inlet \hat{T} (°C)	30	130
Outlet \hat{T} (°C)	130	350
ρ (kg/m ³)	613	702
$\hat{\mu}$ (mPa·s)	5.7	9.3
\hat{c}_p (J/kg·K)	2074.3	2202.0
\hat{k} (W/m·K)	0.113	0.124
$\hat{R}f$ (m ² K/KW)	0.275	0.275

Source: Author's own work, 2024.

Table 8.8 present the geometry details of the coolers in the HEN.

Table 8.4. Coolers details of Example 1

Cooler	1	2	3	4	5
Area (m ²)	246.2	54.9	28.5	296.4	22.7
Number of shells	1	1	1	1	1
<i>dte (m)</i>	0.0127	0.01905	0.0254	0.009525	0.009525
<i>L (m)</i>	3.0488	2.439	2.439	4.8768	1.2195
<i>Ds (m)</i>	0.8382	0.5906	0.3874	0.5906	0.3048
<i>lay</i>	Triangular	Triangular	Square	Square	Square
<i>Npt</i>	1	2	2	1	1
<i>rp</i>	1.25	1.33	1.3	1.25	1.5
<i>Nb</i>	11	14	18	8	4
<i>Ntt</i>	2024	376	195	2031	348
Tube stream	Cold stream	Cold stream	Cold stream	Cold stream	Cold stream
HEX	6	7	8	9	
Area (m ²)	48.8	98.1	56.9	27.5	
Number of shells	1	1	1	1	
<i>dte (m)</i>	0.0127	0.01905	0.0254	0.01905	
<i>L (m)</i>	3.0488	2.439	3.0488	1.8293	
<i>Ds (m)</i>	0.3874	0.6858	0.5906	0.489	
<i>lay</i>	Triangular	Square	Triangular	Triangular	
<i>Npt</i>	4	1	1	2	
<i>rp</i>	1.25	1.25	1.25	1.33	
<i>Nb</i>	13	3	11	5	
<i>Ntt</i>	401	672	234	251	
<i>Tube stream</i>	Cold stream	Cold stream	Cold stream	Cold stream	

Source: Author's own work, 2024.

Table 8.9 present the service details of each HEX obtained through the HEN optimization using simplified HEX calculations, considering uniform and constant heat

transfer coefficients. In addition, Table 8.10 present the retrofit details of each HEX, when each one was recalculated using the complete procedure.

Table 8.5: HEX information in the retrofitted HEN of example1 using simplified HEX evaluation. The correction factor presented in this table is its value considering the original HEX geometry (number of passes and number of shells). The indeterminate value in HEX 9 arises due to numerical error in calculating the correction factor, caused by the high degree of temperature crossover.

HEX	1	2	3	4	5	6
Q (kW)	9082	2290	2251.9	1256.6	5118	5054
Thi (°C)	140.0	186.4	170.1	171.9	169.4	210.0
Tho (°C)	54.5	114.8	103.5	121.9	130.3	167.1
Tci (°C)	30.0	75.4	86.8	98.1	104.4	130.0
Tco (°C)	75.41	86.9	98.1	104.4	130	147.5
LMTD (°C)	41.3	64.9	37.7	41.9	32.3	48.7
F*	0.89	1	0.89	0.97	0.81	0.94
Retrofit alternative	STHE series	Coil-wire installation	Coil-wire installation	-	STHE series	STHE series
HEX	7	8	9	10	11	
Q (kW)	1996.1	2636.4	10621	7815	4641	
Thi (°C)	248.8	277.0	250.6	303.6	360.0	
Tho (°C)	186.4	171.9	169.4	270.2	290.0	
Tci (°C)	147.5	154.5	163.6	200.5	227.6	
Tco (°C)	154.5	163.6	200.5	227.6	243.8	
LMTD (°C)	625	51.3	20.6	72.7	86.5	
F*	1	1	Indeterminate	0.97	0.97	
Retrofit alternative	Coil-wire installation	STHE series	STHE series	STHE parallel	STHE series	

Source: Author's own work, 2024.

Table 8.6: Geometric variables of the HEX retrofit solution of example 1

HEX	1	2	3	5	6
Added area (m ²)	534	-	-	325.0	271.1
U (W/m ² K)	264.6	-	299.4	241.1	261.5
Number of shells added	1	-	-	1	1
Additional Δ Pt	182	85.2	102.6	87.6	55.4
Additional Δ Ps	35.1	0	0	11.4	27.4
dte (m)	0.03175	-	-	0.0508	0.01905
L (m)	6.0976	-	-	6.0976	4.8768
Ds (m)	1.524	-	-	1.524	0.9906
lay	Triangular	-	-	Triangular	Square
Npt	6	-	-	6	4
rp	1.33	-	-	1.33	1.5
Nb	18	-	-	13	7
Ntt	878	-	-	334	929
Helical Pitch (m)	-	0.060	0.064	-	-
Coil-Wire diameter (m)	-	0.0012	0.0010	-	-
HEX	7	8	9	10	11
Added area (m ²)	-	379.7	2843.1	190.2	50.11
U (W/m ² K)	185.1	80.7	186.4	285.5	226.2
Number of shells added	-	2	3	1	1
Additional Δ Pt	50.9	70.8	184.6	-10.4	22.6
Additional Δ Ps	0	35.4	1.19	5.5	22.4
dte (m)	-	0.01905	0.01905	0.01905	0.0508
L (m)	-	3.6585	6.0976	3.6585	3.0488
Ds (m)	-	0.7874	1.3716	0.9906	0.9906
lay	-	Square	Square	Square	Triangular
Npt	-	2	4	6	6

rp	-	1.25	1.25	1.25	1.5
Nb	-	20	8	10	5
Ntt	-	867	2597	1304	433
Helical Pitch (m)	0.058	-	-	-	-
Coil-Wire diameter (m)	0.014	-	-	-	-

Source: Author's own work, 2024.

Example 2

Tables 8.11 present the complete description of each hot and cold streams

Table 8.7. Streams Data of Example 2

Example	H1	H2	H3	H4	C1	C2	C3	C4	C5
\hat{m} (kg/s)	34.53	47.76	63.94	74.11	38.01	35.86	44.13	78.89	68.52
Inlet \hat{T} (°C)	160	249	227	199	60	116	38	82	93
Outlet \hat{T} (°C)	93	148	126	66	160	212	221	177	205
ρ (kg/m ³)	815	876	872	850	877	908	860	865	850
$\hat{\mu}$ (mPa·s)	0.86	2.8	7.6	0.66	4.2	9.1	2.2	2.5	1.5
\hat{c}_p (J/kg·K)	2670	2317	2433	2512	2105	1780	2008	2300	2130
\hat{k} (W/m·K)	0.10	0.11	0.15	0.13	0.13	0.12	0.14	0.11	0.09
$\hat{R}f$ (m ² K/KW)	0.275	0.275	0.275	0.275	0.275	0.275	0.275	0.275	0.275

Source: Author's own work, 2024.

Table 8.8. Coolers details of Example 2

Cooler	1	2	3
Area (m ²)	66.1	175.0	259.7
Number of shells	1	1	1
<i>dte (m)</i>	0.0127	0.009525	0.0127
<i>L (m)</i>	2.439	2.439	3.6585
<i>Ds (m)</i>	0.5906	0.6858	0.7874
<i>lay</i>	Triangular	Triangular	Square
<i>Npt</i>	1	2	2
<i>rp</i>	1.5	1.25	1.25
<i>Nb</i>	11	6	6
<i>Ntt</i>	679	2398	1779
Tube stream	Cold stream	Cold stream	Cold stream

Source: Author's own work, 2024.

Table 8.13 present the service details of each HEX obtained through the HEN optimization using simplified HEX calculations, considering uniform and constant heat transfer coefficients. In addition, Tables 8.14 and 8.15 present the retrofit details of each HEX when the solution involves a STHE and GPHE, respectively.

Table 8.9: HEX information in the retrofitted HEN of example 2 for the simplified procedure. The correction factor presented in this table is its value considering the original HEX geometry (number of passes and number of shells). The indeterminate value in HEX 9 arises due to numerical error in calculating the correction factor, caused by the high degree of temperature crossover.

HEX	1	2	3	4
Q (kW)	5049	6128	10492	6317
Thi (°C)	249	249	227	199
Tho (°C)	148	148	159.3	165.1
Tci (°C)	96.9	116	133.1	142.2
Tco (°C)	160	212	205	177.0
LMTD (°C)	68.3	34.4	24.0	22.4
F*	0.94	0.82	1	1
Retrofit alternative	-	-	-	-
HEX	5	6	7	8
Q (kW)	6209.2	5853	10918.8	2952
Thi (°C)	165.1	165.1	159.3	160.0
Tho (°C)	100.3	100.3	88.9	128.0
Tci (°C)	38.0	93	82	60.0
Tco (°C)	108.1	133.1	142.2	96.9
LMTD (°C)	59.6	16.7	11.3	65.5
F*	1	0.79	Indeterminate	0.95
Retrofit alternative	Replace for a new GPHE	Replace for a new STHE	STHE series	-

Source: Author's own work, 2024.

Table 8.10: Geometric variables of HEX retrofit involving STHE of example 2.

HEX	6	7
Added area (m ²)	1772.2	2585.1
U (W/m ² K)	286.7	329.8
Number of shells added	3	4
Additional ΔPt	32.1	134.4
Additional ΔPs	11.1	155.5
dte (m)	0.01905	0.01905
L (m)	4.8768	6.0976
Ds (m)	1.2192	1.143
lay	Square	Square
Npt	6	6
rp	1.25	1.25
Nb	16	10
Ntt	2024	1771

Source: Author's own work, 2024.

Table 8.11: Geometric variables of HEX retrofit involving GPHE of example 2.

HEX	5
Added	
area (m ²)	295.2
U (W/m ² K)	456.6
Additional ΔP_h	18.6
Additional ΔP_c	25.3
L _p (m)	1.281
L _w (m)	1.200
D _p (m)	0.400
N _{ph}	2
N _{pc}	2
Chevron angle	
(°C)	50
N _p	167

Source: Author's own work, 2024.

APPENDIX C - HEN retrofit with topological modifications results

This appendix is associated with the supplementary material of the Chapter 5, which involves the results of HEN Retrofit with Detailed HEX Design with topological modifications.

Tables 8.16 and 8.17 present the complete description of each hot and cold streams

Table 8.12. Hot Stream Data of Example 3

Stream	H1	H2	H3	H4	H5	H6
\hat{m} (kg/s)	42	19.1	7.7	46.3	12.7	14.7
Inlet \hat{T} (°C)	117.7	178.6	359.6	140.0	248.8	170.1
Outlet \hat{T} (°C)	50.0	108.9	280.0	40.0	110.0	60.0
ρ (kg/m ³)	655.0	684.0	686.0	746.0	758.0	626.0
$\hat{\mu}$ (mPa·s)	1.13	1.43	5.4	7.8	7.8	1.28
\hat{c}_p (J/kg·K)	2921.4	2477.5	3156.5	2293.92	2513.4	2292.9
\hat{k} (W/m·K)	0.123	0.111	0.126	0.126	0.116	0.137
$\hat{R}f$ (m ² K/KW)	0.275	0.275	0.275	0.275	0.275	0.275
Stream	H7	H8	H9	H10	H11	H12
\hat{m} (kg/s)	9.8	55.1	81.0	23.4	23.4	46.3
Inlet \hat{T} (°C)	277	250.6	303.6	290.0	360.0	210.0
Outlet \hat{T} (°C)	121.9	90.0	270.2	115.0	290.0	190.0
ρ (kg/m ³)	613.0	644.0	607.0	736.0	736.0	758.0
$\hat{\mu}$ (mPa·s)	8.3	8.6	1.13	0.58	0.58	1.28
\hat{c}_p (J/kg·K)	2551.3	2375.7	2888.2	1204.1	2830.9	2544.5
\hat{k} (W/m·K)	0.113	0.145	0.102	0.105	0.111	0.125
$\hat{R}f$ (m ² K/KW)	0.275	0.275	0.275	0.275	0.275	0.275

Source: Author's own work, 2024.

Table 8.13. Cold Stream Data of Example 3

Example	C1	C2
\hat{m} (kg/s)	96.4	96.6
Inlet \hat{T} (°C)	30	130
Outlet \hat{T} (°C)	130	350
ρ (kg/m ³)	613	702
$\hat{\mu}$ (mPa·s)	5.7	9.3
\hat{c}_p (J/kg·K)	2074.3	2202.0
\hat{k} (W/m·K)	0.113	0.124
\hat{R}_f (m ² K/KW)	0.275	0.275

Source: Author's own work, 2024.

Table 8.14 present the geometry details of the coolers in the HEN.

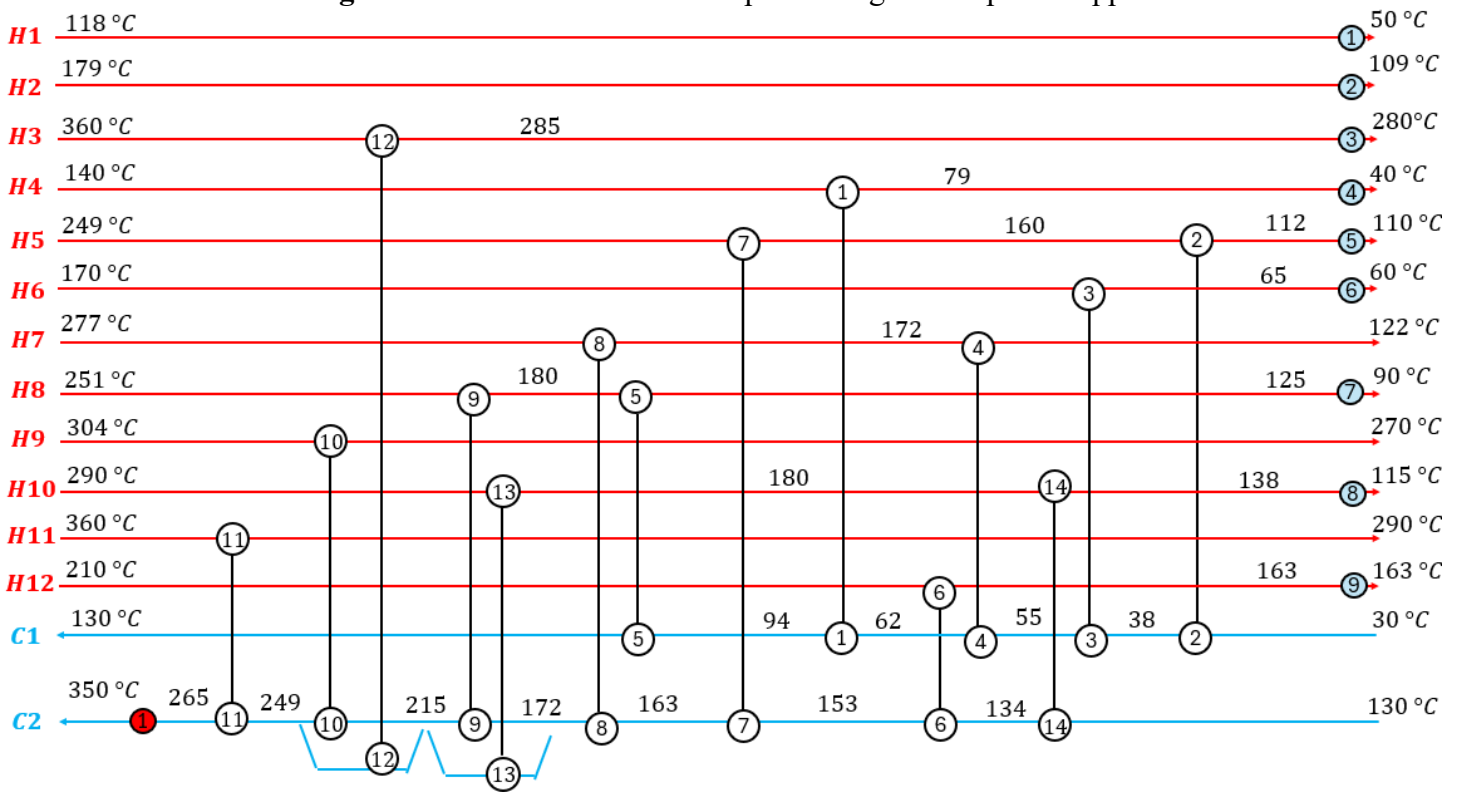
Table 8.14. Coolers details of Example 3

Cooler	1	2	3	4	5
Area (m ²)	246.2	54.9	28.5	296.4	22.7
Number of shells	1	1	1	1	1
<i>dte (m)</i>	0.0127	0.01905	0.0254	0.009525	0.009525
<i>L (m)</i>	3.0488	2.439	2.439	4.8768	1.2195
<i>Ds (m)</i>	0.8382	0.5906	0.3874	0.5906	0.3048
<i>lay</i>	Triangular	Triangular	Square	Square	Square
<i>N_{pt}</i>	1	2	2	1	1
<i>rp</i>	1.25	1.33	1.3	1.25	1.5
<i>N_b</i>	11	14	18	8	4
<i>N_{tt}</i>	2024	376	195	2031	348
Tube stream	Cold stream	Cold stream	Cold stream	Cold stream	Cold stream
HEX	6	7	8	9	
Area (m ²)	48.8	98.1	56.9	27.5	
Number of shells	1	1	1	1	
<i>dte (m)</i>	0.0127	0.01905	0.0254	0.01905	
<i>L (m)</i>	3.0488	2.439	3.0488	1.8293	
<i>Ds (m)</i>	0.3874	0.6858	0.5906	0.489	
<i>lay</i>	Triangular	Square	Triangular	Triangular	
<i>N_{pt}</i>	4	1	1	2	
<i>rp</i>	1.25	1.25	1.25	1.33	
<i>N_b</i>	13	3	11	5	
<i>N_{tt}</i>	401	672	234	251	
<i>Tube stream</i>	Cold stream	Cold stream	Cold stream	Cold stream	

Source: Author's own work, 2024.

Figure 8.2 and Tables 8.19, 8.20 and 8.21 are associated with the results obtained through the HEN retrofit using the simplified approach usually considered in the literature. Table 8.19 are the HEX information, 8.20 with the HEX details retrofit solutions and 8.21 with the details of the new matches in the HEN.

Figure 8.2. HEN retrofit of Example 3 using the simplified approach.



Source: Author's own work, 2024.

Table 8.15. HEX information of the HEN retrofit solution of Example 3

HEX	1	2	3	4	5	6
Q (kW)	6474.9	1538.0	3556.2	1258.0	7172.9	5482.5
Thi (°C)	140.0	160.2	170.1	172.0	179.6	210.0
Tho (°C)	79.0	112.2	64.9	121.9	124.8	163.3
Tci (°C)	61.8	30.0	37.7	55.5	94.1	134.1
Tco (°C)	94.1	37.7	55.5	61.8	130.0	153.2
LMTD (°C)	29.3	101.0	60.8	86.5	39.4	41.5
HEX	7	8	9	10	11	12
Q (kW)	2833.9	2635.0	9288.2	7815.6	4641	1815.2
Thi (°C)	248.8	277.0	250.6	303.8	360.0	359.6
Tho (°C)	160.2	172.0	179.6	270.2	290.0	284.6
Tci (°C)	153.2	163.0	172.1	215.2	248.6	215.2
Tco (°C)	163.0	172.1	215.2	248.6	264.7	248.6
LMTD (°C)	31.5	39.0	17.9	55.0	64.6	88.6
HEX	13	14				
Q (kW)	3099.0	1190.3				
Thi (°C)	290.0	180.1				
Tho (°C)	180.1	137.9				
Tci (°C)	172.1	130.0				
Tco (°C)	215.2	134.1				
LMTD (°C)	29.8	21.6				

Source: Author's own work, 2024.

Table 8.16. HEX details of the HEN retrofit solution of Example 3

HEX	1	5	6	7	8	9	10	11
Retrofit alternative	STHE series	Replace for a new STHE	STHE series	STHE series				
Added area (m ²)	604.6	440.8	457.2	448.	135.8	3790.8	288.4	121.1
U (W/m ² K)	134.9	230.0	236.6	153.8	111.3	176.4	246.8	254.6
Number of shells added	1	1	1	1	1	4	1	1
Additional Δ Pt (kPa)	127.5	100.5	47.8	78.2	85.6	96.5	44.5	33.1
Additional Δ Ps (kPa)	36.4	12.4	32.7	45..8	39.5	75.9	32.0	24.5
dte (m)	0.03175	0.0381	0.01905	0.01905	0.01905	0.01905	0.01905	0.03175
L (m)	6.0976	6.0976	6.0976	4.8768	3.6568	6.0976	4.8768	4.8767
Ds (m)	1.524	1.524	1.143	1.3716	0.6858	1.3716	0.889	0.889
lay	Triangular	Triangular	Square	Triangular	Square	Square	Square	Square
N _{pt}	6	6	4	4	2	6	2	6
rp	1.25	1.33	1.5	1.25	1.25	1.25	1.33	1.5
N _b	16	13	8	16	16	8	6	6
N _{tt}	994	604	1253	1573	648	2597	988	249

Source: Author's own work, 2024.

Table 8.17. HEX details of new matches of HEN retrofit solution of Example 3

HEX	12	13	14
Area (m ²)	192.7	596.4	265.0
U (W/m ² K)	121.0	219.1	262.5
Number of shells	1	3	1
Tube stream	Cold stream	Cold stream	Cold stream
ΔPt (kPa)	76.7	53.7	23.8
ΔPs (kPa)	34.4	42.2	20.8
dte (m)	0.0254	0.01905	0.01905
L (m)	6.0976	3.6585	4.8768
Ds (m)	0.5906	0.889	0.889
lay	Square	Square	Square
Npt	6	6	6
rp	1.33	1.33	1.33
Nb	16	13	7
Ntt	473	908	908

Source: Author's own work, 2024.

Example 4

Tables 8.18 present the complete description of each hot and cold streams

Table 8.18. Streams Data of Example 4

Example	H1	H2	H3	H4	C1	C2	C3	C4	C5
\hat{m} (kg/s)	34.53	47.76	63.94	74.11	38.01	35.86	44.13	78.89	68.52
Inlet \hat{T} (°C)	160	249	227	199	60	116	38	82	93
Outlet \hat{T} (°C)	93	148	126	66	160	212	221	177	205
ρ (kg/m ³)	815	876	872	850	877	908	860	865	850
$\hat{\mu}$ (mPa·s)	0.86	2.8	7.6	0.66	4.2	9.1	2.2	2.5	1.5
\hat{c}_p (J/kg·K)	2670	2317	2433	2512	2105	1780	2008	2300	2130
\hat{k} (W/m·K)	0.10	0.11	0.15	0.13	0.13	0.12	0.14	0.11	0.09
\hat{R}_f (m ² K/KW)	0.275	0.275	0.275	0.275	0.275	0.275	0.275	0.275	0.275

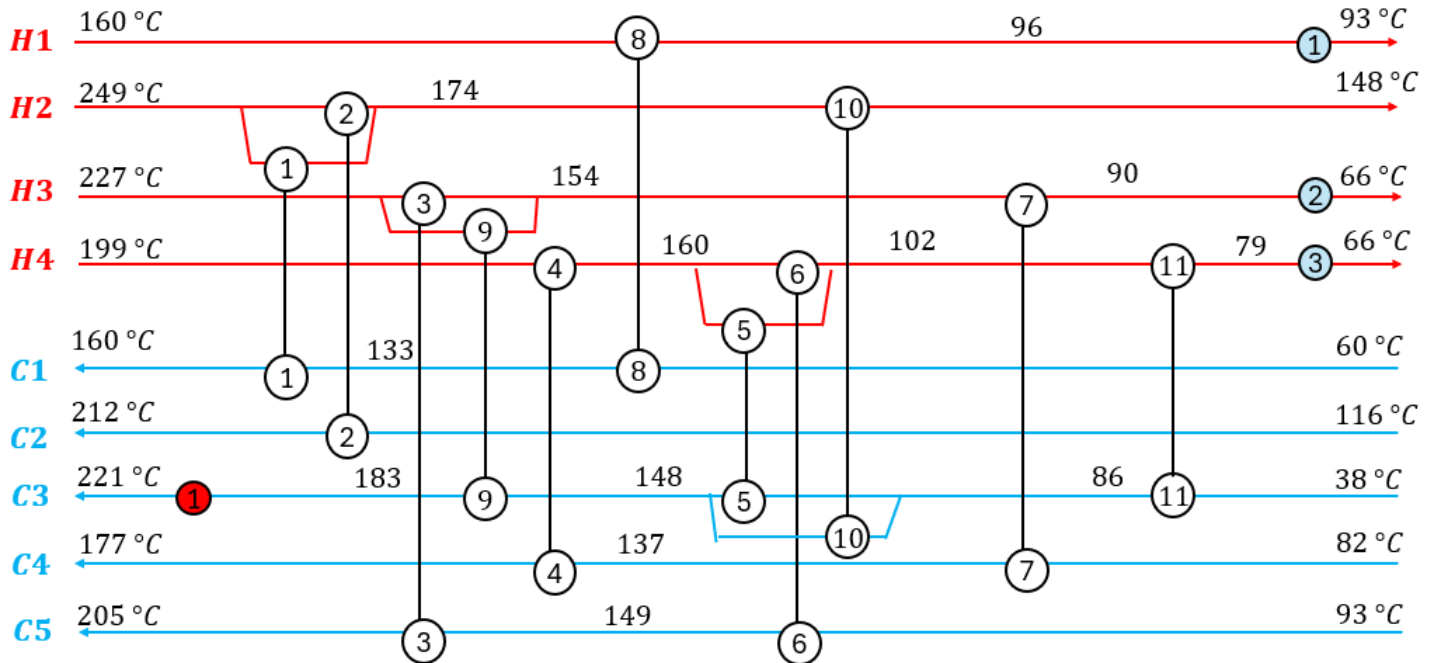
Source: Author's own work, 2024.

Table 8.19 presents the geometry details of the coolers in the HEN.

Table 8.19. Coolers details of Example 4			
Cooler	1	2	3
Area (m ²)	66.1	175.0	259.7
Number of shells	1	1	1
<i>dte (m)</i>	0.0127	0.009525	0.0127
<i>L (m)</i>	2.439	2.439	3.6585
<i>Ds (m)</i>	0.5906	0.6858	0.7874
<i>lay</i>	Triangular	Triangular	Square
<i>N_{pt}</i>	1	2	2
<i>rp</i>	1.5	1.25	1.25
<i>N_b</i>	11	6	6
<i>N_{tt}</i>	679	2398	1779
Tube stream	Cold stream	Cold stream	Cold stream

Source: Author's own work, 2024.

Figure 8.3 and Tables 8.24, 8.25, 8.26 and 8.27 are associated with the results obtained through the HEN retrofit using the simplified approach usually considered in the literature. Table 8.24 are the HEX information, 8.25 with the HEX details retrofit solutions involving STHE, 8.26 associated with GPHE and 8.27 with the details of the new matches in the HEN.

Figure 8.3 HEN retrofit of Example 4 using the simplified approach.

Source: Author's own work, 2024.

Table 8.20. HEX information of the HEN retrofit solution of Example 4

HEX	1	2	3	4	5	6
Q (kW)	2134.8	6128.6	8136.3	7267.0	2541.7	8210.1
Thi (°C)	249.0	249.0	227.0	199.0	159.9	159.9
Tho (°C)	174.3	174.3	154.3	159.9	102.2	102.2
Tci (°C)	133.3	116.0	149.2	136.9	86.4	93.0
Tco (°C)	160.0	212.0	205.0	177.0	148.0	149.2
LMTD (°C)	61.9	46.8	11.6	22.5	13.8	9.9
HEX	7	8	9	10	11	
Q (kW)	9969.9	5866	3130.2	2914.2	4292.0	
Thi (°C)	154.3	160.0	227.0	174.3	102.2	
Tho (°C)	90.1	96.4	154.3	148.0	79.1	
Tci (°C)	82.0	60.0	148.0	86.4	38.0	
Tco (°C)	136.9	133.3	183.3	148.0	86.4	
LMTD (°C)	12.1	31.3	19.4	41.5	26.5	

Source: Author's own work, 2024.

Table 8.21. HEX details of the HEN retrofit solution involving STHE of Example 4

HEX	3	5	6	7
Retrofit alternative	STHE series	Replace for a new STHE	STHE series	STHE series
Added area (m ²)	1343.1	723.8	2175.3	2215.8
U (W/m ² K)	305.9	337.1	306.4	304.6
Number of shells added	3	5	3	3
Additional ΔPt	188.5	224.9	246.3	255.3
Additional ΔPs	96.1	45.1	96.1	118.8
dte (m)	0.01905	0.01905	0.01905	0.01905
L (m)	4.8768	4.8768	6.0976	6.0976
Ds (m)	1.143	0.6858	1.3716	1.2192
lay	Triangular	Triangular	Triangular	Square
Npt	6	6	6	6
rp	1.25	1.25	1.33	1.25
Nb	10	18	16	8
Ntt	1534	496	1987	2024

Source: Author's own work, 2024.

Table 8.22. HEX details of the HEN retrofit solution involving GPHE of Example 4

HEX	8
Retrofit alignment	GPHE series
Added area (m ²)	398.8
U (W/m ² K)	472.5
Additional ΔPh	38.9
Additional ΔPc	59.4
Lp (m)	1.835
Lw (m)	0.945
Dp (m)	0.3
Nph	2
Npc	2
Chevron angle (°C)	45
Np	200

Source: Author's own work, 2024.

Table 8.23. HEX details of new matches associated with the HEN retrofit solution of Example 4

HEX	9	10	11
Area (m ²)	627.3	307.5	624.7
U (W/m ² K)	338.1	269.2	315.2
Number of shells	3	2	2
Tube stream	Cold stream	Hot stream	Cold stream
ΔP_t (kPa)	110.7	90.8	21.6
ΔP_s (kPa)	56.9	34.4	35.1
dte (m)	0.01905	0.0254	0.01905
L (m)	6.0976	6.0976	6.0976
Ds (m)	0.6858	0.6858	0.889
lay	Square	Square	Triangular
N _{pt}	6	6	2
r _p	1.25	1.25	1.33
N _b	10	10	16
N _{tt}	573	316	856

Source: Author's own work, 2024.

APPENDIX D - Articles published during the thesis development

Chemical Engineering Science 280 (2023) 119067



ELSEVIER

Contents lists available at [ScienceDirect](https://www.sciencedirect.com)

Chemical Engineering Science

journal homepage: www.elsevier.com/locate/ces



A new approach for the globally optimal design of gasketed plate heat exchangers with variable properties

André L.M. Nahes^a, André L.H. Costa^a, Miguel J. Bagajewicz^{b,c,*}

^a Institute of Chemistry, Rio de Janeiro State University (UERJ), Rua São Francisco Xavier, 524, Maracanã, Rio de Janeiro, RJ CEP 20550-900, Brazil

^b School of Chemical, Biological and Materials Engineering, University of Oklahoma, 100 E. Boyd St, T331, Norman, Oklahoma 73019, United States

^c Federal University of Rio de Janeiro (UFRJ), Escola de Química CT, Bloco E, Ilha do Fundão, CEP 21949-900, Rio de Janeiro, RJ, Brazil

Chemical Engineering Science 271 (2023) 118524



ELSEVIER

Contents lists available at [ScienceDirect](https://www.sciencedirect.com)

Chemical Engineering Science

journal homepage: www.elsevier.com/locate/ces



A novel method for the globally optimal design of fixed bed catalytic reactors

André L.M. Nahes^a, Miguel J. Bagajewicz^{b,c}, André L.H. Costa^{a,*}

^a Institute of Chemistry, Rio de Janeiro State University (UERJ), Rua São Francisco Xavier, 524, Maracanã, Rio de Janeiro, RJ CEP 20550-900, Brazil

^b School of Chemical, Biological and Materials Engineering, University of Oklahoma, Norman Oklahoma 73019, United States

^c Federal University of Rio de Janeiro (UFRJ), Escola de Química CT, Bloco E, Ilha do Fundão, CEP 21949-900 Rio de Janeiro, RJ, Brazil

Received: 4 November 2023 | Revised: 28 February 2024 | Accepted: 12 March 2024

DOI: 10.1002/aic.18450

RESEARCH ARTICLE

Process Systems Engineering

AICHE
JOURNAL

Globally optimal simultaneous heat exchanger network synthesis and basic heat exchanger design

Diego G. Oliva¹ | Andre L. M. Nahes² | Julia C. Lemos² | André L. H. Costa² | Miguel J. Bagajewicz^{3,4}